LEHNERT • A REVISED ELECTROMAGNETIC THEORY

BO LEHNERT

A REVISED ELECTROMAGNETIC THEORY WITH FUNDAMENTAL APPLICATIONS

EN REVIDERAD ELEKTROMAGNETISK TEORI MED FUNDAMENTALA TILLÄMPNINGAR

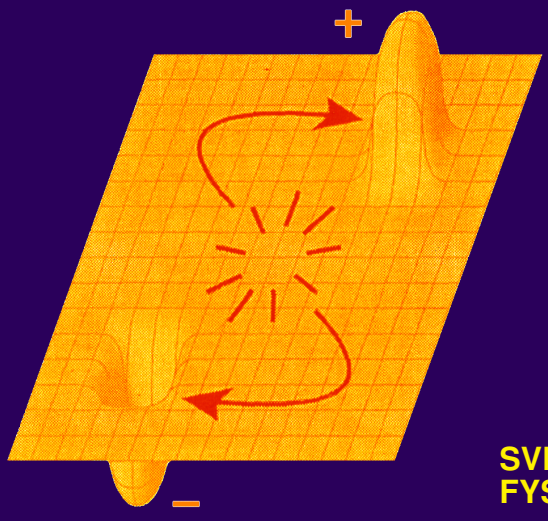

SVENSKA FYSIKARKIVET

Bo Lehnert

Royal Institute of Technology
Stockholm, Sweden

A Revised Electromagnetic Theory with Fundamental Applications

En reviderad elektromagnetisk teori
med fundamentala tillämpningar

2008

Svenska fysikarkivet
Swedish physics archive

Svenska fysikarkivet (that means the *Swedish physics archive*) is a publisher registered with *The National Library of Sweden*, Stockholm. This book was typeset using teTEX typesetting system and Kile, a TEX/LATEX editor for the KDE desktop. Powered by Ubuntu Linux.

Edited by Dmitri Rabounski

Please send all comments on the book, requests for hardcopies, or requests to reprint to the Author or the Publisher.
E-mail: Bo.Lehnert@ee.kth.se
E-mail: admin@ptep-online.com

Svenska fysikarkivet är ett förlagstryckeri registrerat hos *Kungliga biblioteket*. Denna bok är typsatt med typsättningssystemet teTEX och Kile, en TEX/LATEX-redaktion för KDE-skrivbordsmiljön. Utförd genom Ubuntu Linux.

Redaktör: Dmitri Rabounski

Vänligen skicka eventuella kommentarer till boken, efterfrågan av tryckt kopia, eller förfrågan om nytryck till författaren eller förlaget.
E-post: Bo.Lehnert@ee.kth.se
E-post: admin@ptep-online.com

ISBN: 978-91-85917-00-6

Printed in Indonesia
Tryckt i Indonesien

Contents

To my wife
ANN-MARIE

Preface

Maxwell's equations in the vacuum state have served as a guideline and basis in the development of quantum electrodynamics (QED). As pointed out by Feynman, however, there are important areas within which conventional electromagnetic theory and its combination with quantum mechanics does not provide fully adequate descriptions of physical reality. These difficulties are not removed by and are not directly associated with quantum mechanics. Instead electromagnetic field theory is a far from completed area of research, and QED will also become subject to the typical shortcomings of such a theory in its conventional form. As a consequence, modified theories leading beyond Maxwell's equations have been elaborated by several authors. Among these there is one approach which becomes the main subject of this treatise, as well as of its relation to other concepts. The underlying ideas originate from some speculations in the late 1960s, and a revised theory has then been gradually developed. An effort is made here to collect the various parts of the theory into one systematic entity.

The present approach is based on a vacuum state which can become electrically polarized, such as to give rise to a local electric space charge and a related nonzero electric field divergence. The latter can as well be taken as a starting point of such a field theory. The condition of Lorentz invariance then leads to an additional space-charge current which appears along with the conventional displacement current. Maxwell's equations thus become a special case of the theory. Relevant quantum conditions are imposed on the general solutions of the field equations, to result in a first formulation of an extended quantum electrodynamical ("EQED") approach. The nonzero electric field divergence introduces an additional degree of freedom, thereby giving rise to new features which are illustrated by several fundamental applications, such as those to steady electromagnetic states and additional types of wave modes. These are represented by models of the electron, neutrino and photon. They include solutions of so far not understood problems, as represented by the radial force balance of the electron under the influence of its self-charge, the point-charge-like character of the electron and the requirement of its finite self-energy, the nonzero angular momentum of the individual photon, and the wave-particle duality and needle-radiation property of the latter.

The author expresses his sincere thanks to Dr. Jan Scheffel for a fruitful collaboration on a developed electron model. The author is further indebted to to Prof. Kai Siegbahn for his shown interest and encouragement concerning the present theory, and for many valuable considerations, among these on the particle-wave dualism and the photoelectric effect. Also a number of interesting discussions with Prof. Nils Abramson on photon physics and with Prof. Hans Wilhelmsson on the concepts of field theory are gratefully acknowledged. The author is finally indebted to M. Sc. Anna Forsell and M. Sc. Kerstin Holmström for valuable help with the manuscript of this treatise.

Stockholm, Sweden, 2007 *Bo Lehnert*

Chapter 1

INTRODUCTION

§ 1.1 Background

Conventional electromagnetic theory based on Maxwell's equations and quantum mechanics has been very successful in its applications to numerous problems in physics, and has sometimes manifested itself in an extremely good agreement with experiments. Nevertheless there exist areas within which these joint theories do not provide fully adequate descriptions of physical reality. As already stated by Feynman[1], there are thus unsolved problems leading to difficulties with Maxwell's equations that are not removed by and not directly associated with quantum mechanics.

Because of these circumstances, a number of modified and new approaches have been elaborated in electromagnetic field theory since the late twentieth century. Their purpose can be considered as twofold:

- To contribute to the understanding of so far unsolved problems;
- To predict new features of the electromagnetic field.

The corresponding advancement of research has been described in a number of books, reviews, and conference proceedings among which more recent contributions are mentioned here, such as those by Lakhtakia[2], Sachs[3], Evans and Vigier[4], Barrett and Grimes[5], Evans et al.[6,7], Hunter et al.[8], Lehnert and Roy[9], Dvoeglazov[10], Evans, Prigogine and Rice[11], and Amoroso et al.[12] among others.

With this development as a general background, the present treatise will mainly be devoted to an extended approach by the author[9,13–20], as being based on a Lorentz and gauge invariant theory which includes a nonzero electric field divergence in the vacuum state. The latter divergence, with its associated space-charge current density, introduces an extra degree of freedom that leads to new states of the electromagnetic field. The description which is presented here is to be conceived as a first step where the theory is limited to orthogonal coordinate systems, and where relevant quantum conditions are imposed on the general solutions of the field equations. Further steps would include more advanced tensor representations, as well as a quantization of the field equations already from the outset.

§1.2 Some unsolved problems in conventional theory

The failure of standard electromagnetic theory based on Maxwell's equations appears in several important cases, such as those illustrated by the following examples:

- The absence of a steady electromagnetic equilibrium would cause the electron to "explode" under the action of its electric eigencharge;
- The electron behaves like a point charge, i.e. with an extremely small radius, and it carries the smallest free elementary charge, "e". Standard theory is confronted with the infinite self-energy of such a charge. A quantum electrodynamical treatment based on a renormalization procedure has been applied to yield a finite result, as deduced from the difference between two infinite forms. Notwithstanding the success of this normalization, a physically more satisfactory procedure is nevertheless needed concerning the self-energy, as stated by Ryder[21];
- There also arises a so far unanswered question why the elementary electronic charge has just the discrete experimentally determined minimum value "e", and how this becomes related to a possible quantization process;
- Light appears to be made of waves and simultaneously of particles. In conventional theory the individual photon is on one hand conceived to be a massless particle, still having an angular momentum (spin), and is on the other hand regarded as a wave having the frequency ν and the energy $h\nu$, whereas the angular momentum is independent of the frequency. This dualism of the wave and particle concepts is so far not fully understandable in terms of conventional theory[4];
- Concerning the plane wave photon concept, which has no derivatives along its wave front, the energy becomes spread all over an infinite volume. Such a concept cannot account for the needle-like photon configuration with spatially concentrated energy which is required for knocking out an atomic electron in the photoelectric effect. Nor can a plane wave produce the dot-shaped marks which occur on the screen in double-slit experiments on individual photon impacts[22];
- As shown by Heitler[23] among others, the plane wave has no angular momentum and can therefore not represent the photon as a boson particle. As a plane wave an individual photon of nonzero

total energy $h\nu$ would further result in zero local energy density. Contrary to the plane wave geometry, a nonzero angular momentum thus requires derivatives to exist in the directions being transverse to that of the propagation. In addition to this, a spatially limited propagating disturbance of conserved shape cannot be represented by a superposition of plane waves with normals that are oriented in different directions, because such a configuration would disintegrate after some time, as found by Stratton[24]. Further, due to Jackson[25] the plane wave would have to be modified to possess derivatives along its front. As seen from a recent analysis[19], however, this leads to divergent solutions in space which become physically unacceptable;

- To attain photon configurations with transverse derivatives and a nonzero spin, one could in an alternative attempt consider axially symmetric geometry. But then the solutions of Maxwell's equations become divergent in the radial direction and are again physically unacceptable. This divergence was already realized by Thomson[26] and later by Hunter and Wadlinger[27]. There is, in fact, a general feature of the same equations which prevents the solutions from being simultaneously limited in all three directions of space. Also Donev[28] has in a clear way called attention to this crucial shortcoming, in a non-linear extended theory which includes photon-like soliton solutions in the vacuum. In addition, an even more serious problem faces conventional electromagnetic theory in the axisymmetric case. The vanishing axial electric and magnetic field components namely lead to a Poynting vector being directed along the axis of propagation only, and this results in a non-existing angular momentum(spin);
- The process of total reflection of plane waves can in some special cases not be rigorously treated in terms of conventional theory. The Fresnel laws of reflection and refraction of light in non-dissipative media have been known for over 180 years. However, as stressed by Hütt[29], these laws and the underlying conventional theory do not apply to the total reflection of an incident wave which propagates in a dissipative medium being bounded by a vacuum region;
- During total reflection at the vacuum boundary of a dissipation-free medium, the reflected beam has been observed to become subject to a parallel displacement with respect to the incident beam. For this so called Goos-Hänchen effect, the displacement

has a maximum for parallel polarization. At an arbitrary polarization angle the displacement does not acquire an intermediate value, but splits into the two values of parallel and perpendicular polarization[30]. According to de Broglie and Vigier[31] this behaviour cannot be explained by conventional theory;

- In a rotating interferometer fringe shifts have been observed between light beams that propagate parallel and antiparallel with the direction of rotation. Also this Sagnac effect requires an unconventional explanation according to Vigier[32];
- Electromagnetic wave phenomena and the related photon concept remain somewhat of an enigma in more than one respect. The latter concept should in principle apply to wavelengths ranging from about 10^{-15} m of gamma radiation to about 10^{5} m of long radio waves. This includes the yet not fully understandable transition from a low-density beam of individual photons to a nearly plane electromagnetic wave of high photon density.

§ 1.3 The contents of the present treatise

In the following Chapter 2 a short review will be given on a number of modified theories which can serve as a further background to the present approach. The basis of the latter is then presented in Chapter 3, and a review of its new aspects and applications in Chapter 4. A treatment of the resulting electromagnetic steady states then follows, with a presentation of their general features in the axisymmetric geometry of Chapter 5, followed by models of the electron and the neutrino in Chapters 6 to 7. There is further a description of the dynamic states of wave phenomena, including plane waves in Chapter 8 and axisymmetric and screw-shaped modes in Chapter 9. To the analysis on the dynamic states are added some aspects on two somewhat speculative fields which partly are at an early stage of investigation, namely superluminosity in Chapter 10, and nonlocality effects in Chapter 11. Finally, a general summary is given on the main results of the present approach in Chapter 12.

Chapter 2

SHORT REVIEW OF SOME MODIFIED THEORIES

Before turning to the details of the present theory, a further background will be provided here by a short review on some modified theories aiming beyond the scope of Maxwell's equations.

§ 2.1 Theories based on additional vacuum currents

The vacuum is not merely an empty space. There is a nonzero level of its ground state, the zero-point energy, which derives from the quantum mechanical energy states of the harmonic oscillator[33]. A dramatic example of the related electromagnetic vacuum fluctuations was given by Casimir[34] who predicted that two metal plates will attract each other when being brought sufficiently close together. The Casimir effect is due to the fact that only small wavelengths of the fluctuations are permitted to exist in the spacing between the plates, whereas the full spectrum of fluctuations exerts a net force on the outsides of the plates and tends to push them together. This force has been demonstrated experimentally by Lamoreaux[35], in using a sensitive torsion pendulum.

The observed electron-positron pair formation[36] from an energetic photon further indicates that positive and negative electric charges can be created out of an electrically neutral state. Also this supports the idea that the vacuum is not an empty space, and that it can be treated as an electrically polarizable medium.

In addition to the displacement current by Maxwell, electric space charges and related current densities can therefore arise in the vacuum. This feature provides the basis for a number of extended electromagnetic theories. In a four-dimensional form these can here be represented by the Proca-type field equation

$$\Box A_\mu \equiv \left(\frac{1}{c^2} \frac{\partial^2}{\partial t^2} - \nabla^2 \right) A_\mu = \mu_0 J_\mu \,, \qquad \mu = 1, 2, 3, 4 \,, \tag{2.1}$$

given in SI units. In this equation

$$A_\mu = \left(\mathbf{A}, \frac{i\phi}{c} \right), \tag{2.2}$$

where $\mathbf{A}$ and ϕ are the magnetic vector potential and the electrostatic potential in three-space, and

$$J_\mu = (\mathbf{j}, ic\bar{\rho}) \tag{2.3}$$

is the additional four-current density which includes the corresponding three-space current density $\mathbf{j}$ and the electric charge density $\bar{\rho}$. The form (2.1) derives from the original set of field equations, through a gauge transformation in which the Lorentz condition

$$L = \operatorname{div} \mathbf{A} + \frac{1}{c^2}\frac{\partial \phi}{\partial t} = 0 \tag{2.4}$$

is imposed. In fact, the same form is obtained[18] for an arbitrary but constant value of L since only the derivatives of L appear in this deduction.

Maxwell's equations in the vacuum are recovered as a special case in which the current density J_μ disappears, and Eq. (2.1) reduces to the d'Alembert equation.

There are a number of wave equations with a nonzero right-hand member of Eq. (2.1) which explicitly include a particle mass and are not gauge invariant[21]. Here we limit ourselves to some examples having a nonzero current density J_μ.

§ 2.1.1 Quantum mechanical theory of the electron

In the theory of the electron by Dirac[37] the relativistic wave function ψ has four components in spin space. The three-space charge and current densities become[38]

$$\bar{\rho} = e\bar{\psi}\psi \tag{2.5}$$

and

$$\mathbf{j} = ce(\bar{\psi}\alpha_i\psi), \qquad i = 1, 2, 3, \tag{2.6}$$

where α_i are the Dirac matrices of the three spatial directions, and the expression for $\bar{\psi}$ is obtained from that of ψ by replacing the included unit vectors and functions by their complex conjugate values. There is more that one set of choices of the Dirac matrices[39]. Expressions (2.5) and (2.6) can be interpreted as the result of an electronic charge which is "smeared out" over a finite volume of the electron configuration.

§ 2.1.2 Theory of the photon with a rest mass

At an early stage Einstein[40] as well as Bass and Schrödinger[41] have considered the possibility for the photon to possess a very small but nonzero rest mass m_0. Later de Broglie and Vigier[31] and Evans and

Vigier[4] proposed a corresponding form of the four-current in the Proca-type equation (2.1), as given by

$$J_\mu = \left(\frac{1}{\mu_0}\right)\left(\frac{2\pi m_0 c}{h}\right)^2 \left(\mathbf{A}, \frac{i\phi}{c}\right). \tag{2.7}$$

The corresponding solution of the field equations was found to include longitudinal electric and magnetic field components, in addition to the transverse ones. Thereby Evans[42] used cyclically symmetric relations to derive a longitudinal magnetic field part, B(3), in the direction of propagation.

§ 2.1.3 Nonzero electric field divergence theory

In an approach by the author[9,13–20] an additional degree of freedom is introduced, as defined by a nonzero electric field divergence. This leads to a corresponding space-charge density $\bar{\rho}$ and an associated "space-charge current density". In combination with a preserved Lorentz invariance, the resulting four-current density becomes

$$J_\mu = \bar{\rho}\,(\mathbf{C}, ic)\,, \qquad \mathbf{C}^2 = c^2, \tag{2.8}$$

as shown later in detail in Chapter 3. This extra degree of freedom gives rise to new electromagnetic features such as "bound" electromagnetic equilibria and "free" dynamic states in the form of additional wave phenomena. The velocity vector $\mathbf{C}$ in Eq. (2.8) constitutes an important and unique part of the theory. Due to the Lorentz invariance, its modulus is always equal to the velocity of light, but it can possess different components in space depending on the particular geometry in question. It thus becomes associated with the two spin directions in axisymmetric configurations, as well as with the phase and group velocities of a propagating wave, as shown later in this context. There is a certain analogy between the currents (2.6), (2.7), and (2.8), but in the theory of the latter the total electric charge and mass will first come out from the integrated solutions of the field equations.

§ 2.1.4 Nonzero electric conductivity theory

Maxwell's equations in the vacuum were already proposed by Bartlett and Corle[43] to become modified by assigning a small nonzero electric conductivity to the basic equations. As pointed out by Harmuth[44], there was never a satisfactory concept for the velocity of propagating signals within the framework of Maxwell's theory. Thus the equations of the latter fail for waves with a non-negligible relative frequency bandwidth, when propagating in a dissipative medium. To meet this problem, a

nonzero electric conductivity σ and a corresponding three-space current density

$$\mathbf{j} = \sigma \mathbf{E} \tag{2.9}$$

was introduced.

The concept of such a conductivity in the pure vacuum state was later considered by Vigier[45] who showed that the introduction of a current density (2.9) is equivalent to adding a nonzero photon rest mass to the system. The underlying dissipative "tired light" mechanism can be related to a nonzero energy of the vacuum ground state[4,46]. That the current density (2.9) is connected with the four-current (2.7) can be understood from the conventional field equations for homogeneous conducting media[24]. The effect of the nonzero conductivity was further investigated by Roy et al.[47–49] They have shown that there is a resulting dispersion relation having phase and group velocities which are related to a photon rest mass.

The tired light effect possibly provides an additional mechanism for the explanation of the Hubble redshift, being an alternative to a geometrical expansion effect of the universe according to the Big Bang model. The latter is commonly accepted on account of its successful interpretation of a manifold of observed properties. Nevertheless the tired light effect may not be ruled out for certain, as a simultaneously acting mechanism of a moderately large influence.

§ 2.1.5 Single charge theory

A set of first-order field equations was at an early stage proposed by Hertz[50–52] in which the partial time derivatives in Maxwell's equations were substituted by total time derivatives, with respect to the velocity of an "ether". This theory was discarded at its time because it spoiled the spacetime symmetry.

Recently Chubykalo and Smirnov-Rueda[53,54] have presented a renovated version of Hertz' theory, being in accordance with Einstein's relativity principle. For a single point-shaped charged particle which moves at the velocity $\mathbf{v}$, the displacement current in Maxwell's equations is then modified into a "convection displacement current"

$$\mathbf{j} = \varepsilon_0 \left(\frac{\partial}{\partial t} + \mathbf{v} \cdot \nabla \right) \mathbf{E} \tag{2.10}$$

in three-space. This approach includes longitudinal modes which do not exist in Maxwellian theory. The same authors thereby conclude that the Lienard-Wiechert potentials are incomplete, by not being able to describe long-range instantaneous Coulomb interaction.

§ 2.1.6 Related critical questions

Two general objections may at a first glance be raised against the approaches which lead to a nonzero rest mass of the photon. The first concerns the gauge invariance. A positive answer to this point has recently been given by an analysis in terms of covariant derivatives[56]. This is consistent with an earlier conclusion that gauge invariance does not require the photon rest mass to be zero[57]. Concerning the present theory by the author, the deductions in the following Chapter 3 also show that the field equations are gauge invariant, even when they lead to a nonzero photon rest mass. This invariance applies to all systems where the electric and magnetic fields are unaffected by changes in the corresponding potentials, when these are subjected to a gauge transformation.

The second objection concerns the supposition that a nonzero rest mass provides a photon gas with three degrees of freedom, i.e. two transverse and one longitudinal. This would alter Planck's radiation law by a factor of $\frac{3}{2}$, in contradiction with experience[4,9]. There are, however, arguments which resolve also this problem. A detailed analysis by Evans and Vigier[4] shows that the longitudinal magnetic field component, which is associated with the spin and the rest mass, cannot be involved in the process of light absorption. A further argument is due to the fact that transverse photons are not able to penetrate the walls of a cavity, whereas this is the case for longitudinal photons which would then not contribute to the thermal equilibrium[41].

In this connection it should finally be mentioned that the equations of state of a photon gas have been treated by Mézáros[58] and Molnár[59] who find that Planck's distribution cannot be invariant to adiabatic changes occurring in an ensemble of photons. This dilemma is due to the fact that imposed changes cannot become adiabatic and isothermal at the same time. Probably this contradiction may be resolved by including a longitudinal part into the magnetic flux, but further analysis appears to become necessary.

§ 2.2 Theories based on further generalizations

There also exist approaches of a more general character than those based only on additional vacuum currents, as given by the following two concepts.

§ 2.2.1 Magnetic monopoles

From symmetry considerations on the basic field equations, one may raise the question why only the divergence of the electric field should

be permitted to become nonzero, and not also that of the magnetic field. In fact there are a number of investigators who have included the latter divergence and the associated magnetic monopoles in their theories, such as Imeda[60], Omura[61], Harmuth[44], and Múnera[62] among others. According to Dirac[63], the magnetic monopole concept can be considered as an open question. It also leads to a quantization condition on the electric charge for which a similar result has been derived from the 't Hooft-Polyakov monopole[21]. In the present theory we will shortly return to this concept in §3.2.

§2.2.2 Unification of electromagnetism and gravitation

In attempts to proceed in the direction of further generalization, the analysis becomes faced with the profound difference between the theories by Maxwell and those being based on the geometrical features of spacetime. It has thereby been stated by Ryder[21] that in electrodynamics the field is only an "actor" on the spacetime "stage", whereas in gravity the "actor" becomes the "stage" itself. There are several reviews on the theories which aim at a unification of electromagnetism and gravitation, as presented by Evans et al.[7], Roy[9] and Amoroso et al.[12] among others.

From the quantum theoretical point of view the Dirac magnetic monopole has been discussed in connection with the massive photon[64–66]. An attempt has been made by Israelit[66] to generalize the Weyl-Dirac geometry by constructing a framework which includes both a massive photon and a Dirac monopole, thereby offering a basis for deriving both electromagnetism and gravitation from geometry. General unified equations have further been elaborated by Sachs[67,68] where a factorization of Einsten's tensor field equations yields the gravitational and electromagnetic manifestations of matter in a unified field theory. A proposal for unification is also due to Evans[7] who has considered electromagnetism and gravitation as different interlinked parts of the Riemann tensor, where electromagnetism can be considered as a "twisting" and gravitation as a "warping" of spacetime. A number of considerations on the progress in post-quantum physics and classical unified field theory have recently also been presented by Sarfatti[69].

Another way of tackling the unification problem has been elaborated in terms of string theory, which is shortly described later in §5.3.3. The effort to unify electromagnetism and gravitation is in itself an interesting and fundamental task, being so far at a stage of partly controversial discussions.

Chapter 3

BASIS OF PRESENT THEORY

The present treatise mainly consists of an extended form of Maxwell's equations being based on two mutually independent hypotheses:

- A nonzero electric space-charge density and a corresponding electric polarization are assumed to exist in the vacuum state, as being supported by the vacuum fluctuations and the pair formation process mentioned at the beginning of §2.1. Then the resulting concepts of a nonzero electric field divergence and an associated space-charge current density should not become less conceivable than the conventional concepts of a nonzero curl of the magnetic field strength and an associated displacement current. All these concepts can be regarded as intrinsic properties of the electromagnetic field in the vacuum;
- The resulting extended form of the field equations should remain Lorentz invariant. Physical experience supports such a statement, as long as there are no observations getting into conflict with it.

§3.1 Deduction of the space-charge current density

The current density (2.3) appearing in the right-hand side of the Proca-type equation (2.1) is here required to transform as a four-vector. This implies that the square of J_μ should become invariant to a transition from one inertial frame K to another such frame K'. Then Eq. (2.3) yields

$$\mathbf{j}^2 - c^2\bar{\rho}^2 = \mathbf{j}'^2 - c^2\bar{\rho}'^2 = const. \tag{3.1}$$

In addition, the corresponding three-space current density $\mathbf{j}$ is required to exist only when there is also an electric charge density $\bar{\rho}$ associated with the nonzero electric field divergence. This implies that the constant in Eq. (3.1) vanishes. Since J_μ has to become a four-vector, $\mathbf{j}$ and $\bar{\rho}$ must behave as space and time parts of the same vector. Therefore the choice of a vanishing constant in Eq. (3.1) becomes analogous to the choice of the origin at $x = y = z = t = 0$ in the Lorentz invariant relation

$$x^2 + y^2 + z^2 - c^2t^2 = 0 \tag{3.2}$$

between the rectangular coordinates (x, y, z) and time t for a propagating light wave. Consequently the three-space current density becomes

$$\mathbf{j} = \bar{\rho}\mathbf{C} = \varepsilon_0(\mathrm{div}\,\mathbf{E})\mathbf{C}\,, \qquad \mathbf{C}^2 = c^2, \tag{3.3}$$

where $\mathbf{C}$ is a velocity vector having a modulus equal to the velocity c of light. The final form of the four-current density is then given by

$$J_\mu = (\mathbf{j}, ic\bar{\rho}) = \varepsilon_0(\mathrm{div}\,\mathbf{E})(\mathbf{C}, ic)\,. \tag{3.4}$$

Here it is obvious that the charge density $\bar{\rho}$ as well as the velocity vector $\mathbf{C}$ will vary from one inertial frame to another and do not become Lorentz invariant, whereas this is the case of the current density (3.4).

In analogy with the direction to be determined for the current density in conventional theory, the unit vector $\mathbf{C}/c$ will depend on the geometry of the particular configuration to be considered. This unit vector can in principle have components which vary from point to point in space, whereas the modulus of $\mathbf{C}$ remains constant according to the invariance condition (3.3). We also include the relation

$$\mathrm{div}\,\mathbf{C} = 0 \tag{3.5}$$

and have a time-independent velocity vector $\mathbf{C}$.

§ 3.2 The extended field equations

In the four-dimensional representation the present field equations have the form of a Proca-type equation (2.1), with the four-current density (3.4) in the right-hand member. In its character the extension of Maxwell's equations then becomes two-fold. First, there is a change from the homogeneous d'Alembert equation to an inhomogeneous Proca-type equation. Second, the electric field divergence introduces an additional degree of freedom.

In the three-dimensional representation the extended equations of the vacuum state now become

$$\frac{\mathrm{curl}\,\mathbf{B}}{\mu_0} = \varepsilon_0(\mathrm{div}\,\mathbf{E})\mathbf{C} + \frac{\varepsilon_0\partial\mathbf{E}}{\partial t}\,, \tag{3.6}$$

$$\mathrm{curl}\,\mathbf{E} = -\frac{\partial\mathbf{B}}{\partial t}\,, \tag{3.7}$$

$$\mathbf{B} = \mathrm{curl}\,\mathbf{A}\,, \qquad \mathrm{div}\,\mathbf{B} = 0\,, \tag{3.8}$$

$$\mathbf{E} = -\nabla\phi - \frac{\partial\mathbf{A}}{\partial t}\,, \tag{3.9}$$

$$\mathrm{div}\,\mathbf{E} = \frac{\bar{\rho}}{\varepsilon_0}\,, \tag{3.10}$$

where the first term of the right-hand member of Eq. (3.6) and Eq. (3.10) are the new parts being introduced by the present theory. The nonzero electric field divergence introduces an asymmetry in the way which the electric and magnetic fields appear in these equations.

The presence in Eqs. (3.10) and (3.6) of the dielectric constant ε_0 and the magnetic permeability μ_0 of the conventional vacuum state may require further explanation. Liquid and solid matter consist of atoms and molecules which often behave as electric and magnetic dipoles. Such matter can thus become electrically polarized and magnetized when external electric and magnetic fields are being imposed. Then the constants ε_0 and μ_0 have to be replaced by modified values ε and μ, which take these polarization effects into account. One consequence of this is that a conventional plane electromagnetic wave would propagate in such matter at a velocity $\left(\frac{1}{\varepsilon\mu}\right)^{1/2}$ being smaller than the velocity $c=\left(\frac{1}{\varepsilon_0\mu_0}\right)^{1/2}$ in empty vacuum space. In the present extended theory on the vacuum state, however, no electrically polarized and magnetized atoms or molecules are present. There are only electromagnetic fluctuations due to the zero point field as revealed by the Casimir effect, and there can also arise electric space charges out of the vacuum, such as in the case of positron-electron pair formation. In other words, the vacuum state is here conceived as a background of empty space upon which are superimposed zero point electromagnetic wave-like fluctuations, as well as phenomena of a more regular character which could take the form of the wave phenomena and field configurations to be treated in the present theory. In this respect Eq. (3.10) becomes identical with that used in the conventional theory on hot plasmas which contain freely moving charged particles of both polarities, in a background of empty vacuum space and where electric charge separation and a resulting electric field can arise, such as in the case of plasma oscillations. There may exist an interaction between the zero point field and regular modes, not being treated here at this stage.

As mentioned earlier in § 2.2.1, the question may also be raised why only $\mathrm{div}\,\mathbf{E}$ and not $\mathrm{div}\,\mathbf{B}$ should be permitted to become nonzero in an extended approach. It has then to be noticed that the nonzero electric field divergence has its support in the observed pair formation and the vacuum fluctuations, whereas a nonzero magnetic field divergence is so far a possible but not proved theoretical supposition. With Dirac[63] we shall therefore leave the magnetic monopole concept as an open question, but not include it at the present stage in the theory.

As shown later, this theory will lead to a small but nonzero photon rest mass. This raises a further question about the gauge invariance al-

ready being touched upon in §2.1.6. According to earlier investigations it was then concluded that the gauge invariance does not require the photon rest mass to be zero[56,57]. In fact, the field equations (3.6)–(3.7) can easily be seen to become gauge invariant. A new gauge with a magnetic vector potential $\mathbf{A}'$ and an electrostatic potential ϕ' is defined by

$$\mathbf{A}' = \mathbf{A} + \bigtriangledown\psi\,, \qquad \phi' = \phi - \frac{\partial\psi}{\partial t}\,. \tag{3.11}$$

When being inserted into Eqs. (3.8) and (3.9), these gauge relations lead to field strengths $\mathbf{E}' = \mathbf{E}$ and $\mathbf{B}' = \mathbf{B}$ which thus become invariant. The field equations (3.6) and (3.7) only contain the field strengths and therefore become gauge invariant.

As discussed later in §11.4, it has during later years been realized that the electromagnetic four-potential (2.2) does not only serve the purpose of a mathematical intermediary, but also can have a physical meaning of its own. To the discussion on the gauge invariance it has therefore to be added that there are situations where the choice of gauge has indeed a physical influence, such as in the case of a curl-free magnetic vector potential. We return to this question in Chapter 11.

The basic equations (3.3)–(3.10) can as well be derived from the more condensed form of a Lagrangian density

$$\mathcal{L} = \frac{1}{2}\,\varepsilon_0(\mathbf{E}^2 - c^2\mathbf{B}^2) - \bar{\rho}\,\phi + \mathbf{j}\cdot\mathbf{A} \tag{3.12}$$

given e.g. by Goldstein[70]. This constitutes a formally more elegant representation, but it does not lead to more physical information than what is already contained in the original basic equations.

The comparatively simple formalism of the present theory relates it in a surveyable way to a number of physical concepts and applications. This can be taken as an advantage, in particular as there are examples to be shown later where the obtained results seem to agree rather well with experimental experience.

§3.3 Comparison with the Dirac theory

A four-current density in the vacuum state was first introduced in the electron theory by Dirac[37] as described at the beginning of §2.1.1. Here further attention can be called to the analysis by Horwitz and collaborators[71,72], and by Gersten[73,74] combined with a generalization due to Dvoeglazov[75,76]. The corresponding field equations have been put into the Dirac form as demonstrated by Bruce[77] and Dvoeglazov[78].

In Eqs. (2.5) and (2.6) for the charge and current densities of the Dirac theory, $|\alpha_i| = 1$ for the Dirac matrices. These equations are then

seen to be similar to the corresponding relation (3.3) for the current density in the present theory where $|\mathbf{C}| = c$. The angular momentum in the Dirac theory emerges from the spin matrices α_i, whereas the relation $\mathbf{C}^2 = c^2$ leads to the two spin directions of the same momentum when the present theory is applied to an axially symmetric configuration such as that in a model of the electron.

It should further be observed that the electromagnetic field of Eqs. (3.6)–(3.10) forms the basis in an analysis of concrete geometrical configurations, both for "bound" steady states and for "free" states of propagating wave phenomena. Therefore the theory does not have to include the concepts of a particle rest mass and a net electric charge from the beginning. Such concepts will first come out from a spatial integration of the electromagnetic energy density and the electric charge density. When relating the present approach to the Dirac theory, wave functions have thus to be considered which only represent states without an initially included rest mass. One form of this special class is given by[79]

$$\psi = u(x, y, z) \begin{bmatrix} U \\ 0 \\ \pm U \\ 0 \end{bmatrix}, \tag{3.13}$$

where u is an arbitrary function and U a constant. This yields a charge density

$$\bar{\rho} = 2e\bar{U}U\bar{u}u \tag{3.14}$$

and the corresponding current density components

$$j_z = \pm c\bar{\rho}\,, \quad j_x = 0\,, \quad \text{and} \quad j_y = 0\,, \tag{3.15}$$

where a bar over U and u indicates the complex conjugate value. Other analogous forms can be chosen where instead $j_y = \pm c\bar{\rho}$ or $j_x = \pm c\bar{\rho}$.

This result and expressions (2.5) and (2.6) indicate that there is a connection between the present theory and that by Dirac. But the former theory sometimes applies to a larger class of phenomena, in the capacity of both "bound" and of "free" states. Thereby the elementary charge is a given quantity in Dirac's theory, whereas the total net charge of the present approach is deduced from the field equations in a steady axisymmetric state, as shown in the following Chapters 5 and 6.

§ 3.4 The quantum conditions

The relevant quantum conditions to be imposed are those on the angular momentum, the magnetic moment, and on the magnetic flux of the

steady or time-dependent configuration to be analyzed. The rigorous and most complete way to proceed is then to quantize the field equations already from the outset.

As a first step, however, a simplification will instead be made here, by first determining the general solutions of the basic field equations, and then imposing the quantum conditions afterwards. This is at least justified by the fact that the quantized electrodynamic equations become equivalent to the field equations (2.1) in which the potentials A_μ and currents J_μ are replaced by their expectation values, as shown by Heitler[23]. In this connection Gersten[73,74] states that Maxwell's equations should be used as a guideline for proper interpretations of quantum theories. This should also apply to the inhomogeneous and extended equations (2.1) being used here. The present theory may therefore not be too far from the truth, by representing the most probable states in a first approximation to a rigorous quantum-theoretical approach, in the form of a kind of extended quantum electrodynamical (EQED) approach.

§ 3.5 The momentum and energy

The momentum and energy equations of the electromagnetic field are obtained in analogy with conventional deductions. Multiplying Eq. (3.6) vectorially by $\mathbf{B}$ and Eq. (3.7) by $\varepsilon_0\mathbf{E}$, the sum of the resulting expressions can be rearranged into the local momentum equation

$$\mathrm{div}\,{}^2\mathbf{S} = \bar{\rho}\,(\mathbf{E} + \mathbf{C}\times\mathbf{B}) + \varepsilon_0\,\frac{\partial}{\partial t}(\mathbf{E}\times\mathbf{B})\,, \tag{3.16}$$

where ${}^2\mathbf{S}$ is the electromagnetic stress tensor[24]. The corresponding integral form becomes

$$\int {}^2\mathbf{S}\cdot\mathbf{n}\;dS = \mathbf{F}_e + \mathbf{F}_m + \frac{\partial}{\partial t}\int \mathbf{g}\;dV\,. \tag{3.17}$$

Here dS and dV are surface and volume elements, $\mathbf{n}$ is the surface normal,

$$\mathbf{F}_e = \int \bar{\rho}\,\mathbf{E}\;dV \qquad \mathbf{F}_m = \int \bar{\rho}\,\mathbf{C}\times\mathbf{B}\;dV \tag{3.18}$$

are the integrated electric and magnetic volume forces, and

$$\mathbf{g} = \varepsilon_0\mathbf{E}\times\mathbf{B} = \frac{1}{c^2}\,\mathbf{S} \tag{3.19}$$

can be interpreted as an electromagnetic momentum density, with $\mathbf{S}$ denoting the Poynting vector. The latter can be conceived to represent

the magnitude and direction of the energy flow in space. The component S_{jk} of the stress tensor is the momentum that in unit time crosses a unit element of surface in the j direction, and the normal of which is oriented along the k axis. This implies that Eq. (3.17) represents Newton's third law of the electromagnetic field, where the right-hand member stands for the rate of change of the total momentum. The latter consists of one contribution due to the mechanical volume force (3.18), and one due to the momentum (3.19) of the electromagnetic field. The results (3.16) and (3.17) differ from the conventional ones in the appearance of terms which include a nonzero charge density $\bar{\rho}$, and that there is both an electric and a magnetic volume force in the vacuum state.

Scalar multiplication of Eq. (3.6) by $\mathbf{E}$ and Eq. (3.7) by $\frac{\mathbf{B}}{\mu_0}$, and a subtraction of the resulting expressions, yields the local energy equation

$$-\operatorname{div}\mathbf{S} = -\left(\frac{1}{\mu_0}\right)\operatorname{div}(\mathbf{E}\times\mathbf{B}) = \bar{\rho}\,\mathbf{E}\cdot\mathbf{C} + \frac{1}{2}\,\varepsilon_0\,\frac{\partial}{\partial t}\,(\mathbf{E}^2 + c^2\mathbf{B}^2)\,. \quad (3.20)$$

This equation differs from the conventional Poynting theorem through the appearance of the term $\bar{\rho}\,\mathbf{E}\cdot\mathbf{C}$. That such a difference arises in some of the modified theories has also been emphasized by Evans et al.[6] and by Chubykalo and Smirnov-Rueda[53]. These investigators note that the Poynting vector in the vacuum is only defined in terms of transverse plane waves, that the case of a longitudinal magnetic field component leads to a new form of the Poynting theorem, and that the Poynting vector can be associated with the free electromagnetic field only. We shall later return to this question when considering axisymmetric wave packets.

The integral form of expression (3.20) becomes

$$\int \mathbf{S}\cdot\mathbf{n}\;dS + \int \bar{\rho}\,\mathbf{E}\cdot\mathbf{C}\;dV = -\frac{1}{2}\,\varepsilon_0\int\frac{\partial}{\partial t}\,(\mathbf{E}^2 + c^2\mathbf{B}^2)\,dV. \quad (3.21)$$

The customary interpretation of this relation is as follows[24]. It is assumed that the formal expression for the energy density stored in the electromagnetic field is the same as in a stationary state. Then the right-hand side of (3.21) represents the rate of decrease of the electromagnetic energy. This loss is accounted for by an input of energy due to $\bar{\rho}\,\mathbf{E}\cdot\mathbf{C}$, plus an energy outflow in the direction of the Poynting vector $\mathbf{S}$.

This interpretation of Poynting's theorem is, however, open to some criticism[24]. First, from a volume integral representing the total energy of the field no rigorous conclusion can be drawn with regard to its local distribution. Second, the question may be raised as to the propriety of assuming that the energy density and its rate of change remain the

same for rapid as well as for quasi-steady changes. Third, even though the total flow of energy through a closed surface may be represented correctly by the Poynting vector, one cannot conclude definitely that the local intensity of energy flow at a local point is given by the same vector. The classical interpretation of Poynting's theorem thus appears to rest to a considerable degree of hypothesis. It should therefore not be considered as an absolute truth, but as a self-consistent and useful analytical formulation[24].

It has to be remembered that relations (3.16) and (3.20) have merely been obtained from a rearrangement of the basic equations. They therefore have the form of identities by which equivalent expressions are obtained for the momentum and energy from the stress tensor.

§3.6 The energy density

In this connection the concept of the electromagnetic energy density has to be further discussed, both in the case of steady and of time-dependent states. First consider the vector identities

$$\mathrm{div}\,(\mathbf{A}\times\mathrm{curl}\,\mathbf{A}) = (\mathrm{curl}\,\mathbf{A})^2 - \mathbf{A}\cdot\mathrm{curl}\,\mathrm{curl}\,\mathbf{A}\,, \tag{3.22}$$

$$\mathrm{div}\left[\phi\left(\nabla\phi+\frac{\partial\mathbf{A}}{\partial t}\right)\right] = \phi\left(\nabla^2\phi+\frac{\partial}{\partial t}\,\mathrm{div}\,\mathbf{A}\right)+\nabla\phi\cdot\left(\nabla\phi+\frac{\partial\mathbf{A}}{\partial t}\right). \tag{3.23}$$

Using Eqs. (2.1)–(2.4) and (3.3)–(3.10), the sum of expression (3.23) and expression (3.22) multiplied by c^2 leads after some deductions to

$$w_f - w_s = w_{fs} + \mathrm{div}\,\mathbf{F}\,, \tag{3.24}$$

where

$$w_f = \frac{1}{2}\left(\varepsilon_0\mathbf{E}^2+\frac{\mathbf{B}^2}{\mu_0}\right), \tag{3.25}$$

$$w_s = \frac{1}{2}\,(\bar{\rho}\,\phi+\mathbf{j}\cdot\mathbf{A}) = \frac{1}{2}\,\bar{\rho}\,(\phi+\mathbf{C}\cdot\mathbf{A})\,, \tag{3.26}$$

$$w_{fs} = \frac{1}{2}\,\varepsilon_0\left[\frac{\partial\mathbf{A}}{\partial t}\cdot\nabla\phi-\mathbf{A}\cdot\nabla\,\frac{\partial\phi}{\partial t}+\left(\frac{\partial\mathbf{A}}{\partial t}\right)^2-\mathbf{A}\cdot\frac{\partial^2\mathbf{A}}{\partial t^2}\right], \tag{3.27}$$

$$\frac{2}{\varepsilon_0}\,\mathbf{F} = \phi\left(\nabla\phi+\frac{\partial\mathbf{A}}{\partial t}\right)+c^2\mathbf{A}\times\mathrm{curl}\,\mathbf{A} = -\phi\mathbf{E}+c^2\mathbf{A}\times\mathbf{B}\,. \tag{3.28}$$

Here w_f can be interpreted as a "field energy density" being associated with the field strengths $\mathbf{E}$ and $\mathbf{B}$, and w_s as a "source energy

density" being associated with the sources $\bar{\rho}$ and $\mathbf{j}$ of the electromagnetic field. The integral form of Eq. (3.24) becomes

$$\int (w_f - w_s)\ dV = \int w_{fs}\ dV + \int \mathbf{F} \cdot \mathbf{n}\ dS\,. \tag{3.29}$$

In a steady state, and when $\mathbf{F}$ or its normal component vanish at the surface S, the right-hand member of Eq. (3.29) also vanishes. Then the total energy derived from the field energy density becomes the same as that obtained from the source energy density. The local distributions of w_f and w_s are on the other hand entirely different.

§ 3.6.1 Steady states

In a time-independent state where $w_{fs} = 0$ the electrostatic and magnetostatic energy densities have been deduced in an unquestionable way from the work exerted on the charges and currents[24]. This leads to the expression (3.26) for the source energy density. When applying this result care is necessary to secure a physically correct choice of the reference (zero) levels of the potentials $\mathbf{A}$ and ϕ. It has also to be observed that the relation

$$\int w_f\ dV = \int w_s\ dV \tag{3.30}$$

only holds when the surface integral of Eq. (3.29) vanishes, and this is not always the case.

Here $w_f > 0$ according to its quadratic form (3.25), whereas w_s can consist both of positive and of negative local contributions. This implies that even negative energy states cannot be excluded for certain when $\mathrm{div}\,\mathbf{F}$ in Eq. (3.24) differs from zero.

Since w_f and w_s represent different spatial distributions of energy, we also have the inequality

$$\int f \cdot w_f\ dV \neq \int f \cdot w_s\ dV \tag{3.31}$$

for the moment of the energy density being formed with any spatial function $f \neq const.$

In a steady state, and in absence of surface charges and currents, it is incontrovertible that the density (3.26) represents the local work done on the charges and currents, as obtained from the primary deductions of the energy density[24]. This holds also when the electromagnetic field becomes divergent at a particular point, such as at the origin of the spherical coordinates in an axially symmetric configuration. It is then

only necessary to choose a physically correct zero level of the electrostatic potential ϕ. Here we consider the corresponding total energy

$$W = \int w_s \, dV \tag{3.32}$$

which is finite and applies to configurations generated by charges and currents that are restricted to a limited region of space. For the boundaries of the integral (3.32) there are two possibilities to be taken into account:

- When the density w_s is convergent everywhere and vanishes rapidly at large distances from the origin, the integral (3.32) can be extended throughout space;
- When the density w_s still vanishes at large distances, but becomes divergent at the origin, an inner surface S_i is defined which encloses the origin and forms a lower limit of the integral (3.32). The divergence of the energy density can then be handled in terms of the integral as it stands, and by applying a special analytic procedure based on a smallness parameter which defines a shrinking radius of the inner surface S_i. This scheme will be demonstrated later in Chapters 5 to 7.

Here one may ask the question if it would become convenient to divide the electromagnetic field into one "source part" $(\mathbf{A}_s, \phi_s)$ where $\mathrm{curl}\,\mathrm{curl}\,\mathbf{A}_s \neq 0$ and $\nabla^2\phi_s \neq 0$, and one "sourceless part" $(\mathbf{A}_v, \phi_v)$ where $\mathrm{curl}\,\mathrm{curl}\,\mathbf{A}_v = 0$ and $\nabla^2\phi_v = 0$. This does, however, not seem to simplify the analysis which includes all features of the field. The following points have namely to be observed:

- For any given form of the electromagnetic potentials $\mathbf{A}$ and ϕ the field strengths $\mathbf{E}$ and $\mathbf{B}$ as well as the source energy density w_s become uniquely determined;
- In an axially symmetric geometry with a space charge density being mainly concentrated to a region near the origin of a spherical frame of reference, these potentials can in principle be chosen such as to approach the limit determined by the "sourceless part" at large radial distances;
- In such a geometry where the dominating contributions to the source energy density originate from regions near the origin, the integrated total energy (3.32) will become independent of the special asymptotic forms of $\mathbf{A}$ and ϕ at large radial distances. Examples of this will be given by the electron and neutrino models of Chapters 6 and 7.

§ 3.6.2 Time-dependent states

In a time-dependent state the integrals of the energy densities (3.25) and (3.26) are unequal, even when the surface term in Eq. (3.29) vanishes. These two integrals can only become approximately equal when the integral of the density (3.27) becomes small as compared to those of the densities (3.25) and (3.26).

An alternative way of treating the time-dependent case is to take the standpoint due to Stratton[24]. This implies that one considers the Poynting theorem and the momentum and energy balance equations (3.17) and (3.21) as a self-consistent analytical formulation, in terms of the densities $\mathbf{g}$ and w_f of momentum and energy given by Eqs. (3.19) and (3.25).

A special but important question concerns the momentum of the pure radiation field. In conventional QED this momentum is derived from a plane-wave representation and the Poynting vector[23,33]. In the present theory the Poynting vector and the momentum density (3.19) have an analogous rôle, in cases where the volume force in Eq. (3.16) vanishes or can be neglected.

§ 3.7 The volume forces

In the momentum equation (3.16) there is a total local volume force

$$\mathbf{f} = \bar{\rho}\,(\mathbf{E} + \mathbf{C} \times \mathbf{B})\,. \tag{3.33}$$

This force would generally come out to be nonzero in the vacuum when there is an extra degree of freedom in the form of a nonzero electric field divergence.

In analogy with an approach by Donev[28], one might here consider the possibility of a locally "force-free" field defined by $\mathbf{f} = 0$. In the present theory, however, this leads to the extra equation

$$\mathbf{E} + \mathbf{C} \times \mathbf{B} = 0 \tag{3.34}$$

in addition to the basic equations (3.6) and (3.7). The result is then an overdetermined and unacceptable system of nine equations for the six components of $\mathbf{E}$ and $\mathbf{B}$.

With respect to the volume forces, the present method of proceeding has therefore been based on an analysis of the resulting integrated force balance in every particular case. This will later be demonstrated in § 6.8 for an electron model, in § 7.4 for a neutrino model, and in § 9.3.3 for a photon model.

§3.8 Characteristic features of present theory

This chapter is ended in summarizing the characteristic features of the present theory:

- The theory is based on the pure radiation field in the vacuum state;
- The theory is both Lorentz and gauge invariant;
- The nonzero electric field divergence introduces an additional degree of freedom which changes the character of the field equations substantially, and leads to new physical phenomena;
- The velocity of light is no longer a scalar c but a vector $\mathbf{C}$ which has the modulus c;
- Being based on the pure radiation field, the theory includes no ad hoc assumption of particle mass at its outset;
- A possible arising mass and particle behaviour comes out of the "bound" states which result from a type of vortex-like "self-confinement" of the radiation;
- The wave nature results from the "free" states of propagating wave phenomena;
- These "bound" and "free" states can become integrating parts of the same system.

Chapter 4

A REVIEW OF NEW ASPECTS AND APPLICATIONS

The introduction of an additional degree of freedom in the form of a nonzero electric field divergence, and the resulting transition from a homogeneous d'Alembert equation to an inhomogeneous Proca-type equation, lead to a number of new aspects and applications. These include the new class of steady states, and an extended class of time-dependent states with new wave phenomena, as demonstrated by Fig. 4.1.

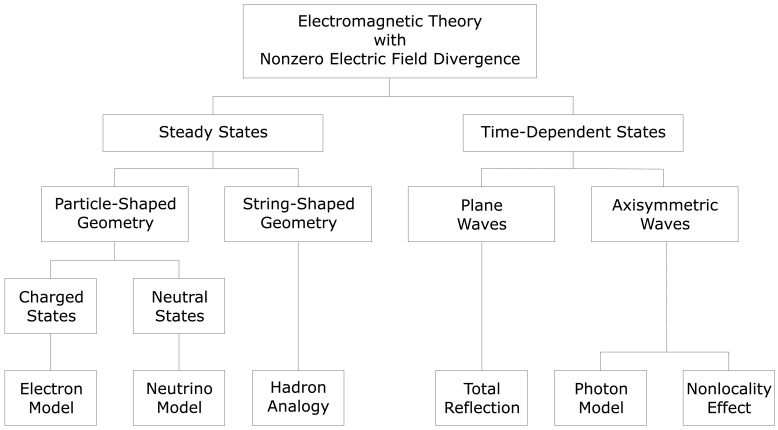

Figure 4.1: New features introduced by the present theory. The lowest row represents possible areas of application.

The theory being described in this book will mainly be applied to "microscopic" configurations such as the individual electrically charged and neutral leptons, and the photon. A transition to the "macroscopic" behaviour of many-particle systems has to some extent been discussed elsewhere[18,80], but will here only be shortly touched upon in §9 as far as light beams are concerned.

§4.1 Steady phenomena

In a time-independent case the space-charge current density makes possible the existence of steady electromagnetic states which are absent

within the frame of Maxwell's equations. From relations (3.5)–(3.10) the steady-state equations

$$c^2 \,\mathrm{curl}\,\mathrm{curl}\,\mathbf{A} = -\,\mathbf{C}\,(\nabla^2\phi) = \frac{\bar{\rho}}{\epsilon_0}\,\mathbf{C} \tag{4.1}$$

are then obtained. On the basis of the electromagnetic forces given by Eqs. (3.16) and (3.18), the corresponding steady electromagnetic equilibrium of the electron will later be discussed in §6.8.

Axisymmetric states will be treated in detail in the following Chapters 5–7. These states can roughly be pictured as a result of "self-confined" circulating electromagnetic radiation, on which relevant quantum conditions are being imposed. Among these "bound" states two subclasses are of special interest:

- Particle-shaped states where the geometrical configuration is bounded both in the axial and in the radial directions. There are states both with a nonzero as well as with a zero net electric charge to be investigated. The corresponding solutions and models may have some bearing on and contribute to the understanding of such truly elementary particles as the leptons;
- String-shaped states where the geometrical configuration is uniform in the axial direction and becomes piled up near the axis of symmetry. These equilibria can in an analogous manner reproduce several desirable features of the earlier proposed hadron string model.

§4.2 Time-dependent phenomena

The basic equations for time-dependent states combine to

$$\left(\frac{\partial^2}{\partial t^2} - c^2\,\nabla^2\right)\mathbf{E} + \left(c^2\,\nabla + \mathbf{C}\,\frac{\partial}{\partial t}\right)(\mathrm{div}\,\mathbf{E}) = 0 \tag{4.2}$$

for the electric field. From the corresponding solution the magnetic field $\mathbf{B}$ can be obtained by means of Eq. (3.7). For the magnetic field $\mathbf{B}$ a general differential equation is on the other hand not available from the basic equations, as long as $\mathrm{div}\,\mathbf{E}$ remains nonzero. A divergence operation on Eq. (3.6) further yields

$$\left(\frac{\partial}{\partial t} + \mathbf{C}\cdot\nabla\right)(\mathrm{div}\,\mathbf{E}) = 0 \tag{4.3}$$

in combination with Eq. (3.5). In some cases this equation becomes useful to the analysis, but it does not introduce more information than

that already contained in Eq. (4.2). The result (4.3) is directly related to the condition of charge conservation

$$\operatorname{div}\mathbf{j} = -\frac{\partial\bar{\rho}}{\partial t} \tag{4.4}$$

as obtained from Eqs. (3.3), (3.5) and (3.10).

Three limiting cases can be identified on the basis of Eq. (4.2):

- When $\operatorname{div}\mathbf{E} = 0$ and $\operatorname{curl}\mathbf{E} \neq 0$ the result is a conventional *transverse* electromagnetic wave, henceforth denoted as an "EM wave";
- When $\operatorname{div}\mathbf{E} \neq 0$ and $\operatorname{curl}\mathbf{E} = 0$ a purely *longitudinal* electric space-charge wave arises, here being denoted as an "S wave";
- When both $\operatorname{div}\mathbf{E} \neq 0$ and $\operatorname{curl}\mathbf{E} \neq 0$ a hybrid *nontransverse* electromagnetic space-charge wave appears, here denoted as an "EMS wave".

In a general case these various modes can become superimposed, also the EMS modes with different velocity vectors $\mathbf{C}$. That the basic equations can give rise both to modes with a nonvanishing and a vanishing electric field divergence is not less conceivable than the analogous property of the conventional basic equations governing a magnetized plasma. The frame of the latter accommodates both longitudinal electrostatic waves and transverse Alfvén waves. These are, like the EM, S, and EMS waves, separate modes even if they originate from the same basic formalism.

The wave equation (4.2) has several applications leading to new aspects in optics and photon physics, as demonstrated later in Chapters 8 to 12, also including contributions to the discussion on superluminosity and nonlocality effects.

According to the present approach, the zero-point field fluctuations defined at the beginning of § 2.1 should not only consist of conventional electromagnetic EM modes, but could also include the space-charge related EMS and S modes just being identified.

The conditions under which the pure S mode may exist are not clear at this stage. With a vanishing vector potential $\mathbf{A}$ the Lorentz condition (2.4) would thus not apply, but there still results a wave equation for this mode in some cases. We will return to this question later in § 11.4.

Chapter 5

GENERAL FEATURES OF STEADY AXISYMMETRIC STATES

The general features of steady axisymmetric electromagnetic states are now investigated in the cases of electrically charged and neutral particle-shaped states, and of string-shaped configurations.

For particle-shaped states a frame (r, θ, φ) of spherical coordinates is introduced where all relevant quantities are independent of the angle φ. The analysis is further restricted to a current density $\mathbf{j} = (0, 0, C\bar{\rho})$ and a magnetic vector potential $\mathbf{A} = (0, 0, A)$. Here $C = \pm c$ represents the two possible spin directions. The basic equations (4.1) then take the form

$$\frac{(r_0\,\rho)^2\,\bar{\rho}}{\varepsilon_0} = D\phi = \left[D + (\sin\theta)^{-2}\right](CA)\,, \tag{5.1}$$

where the dimensionless radial coordinate

$$\rho = \frac{r}{r_0} \tag{5.2}$$

has been introduced, r_0 is a characteristic radial dimension, and the operator D is given by

$$D = D_\rho + D_\theta\,, \quad D_\rho = -\frac{\partial}{\partial\rho}\left(\rho^2\frac{\partial}{\partial\rho}\right)\,, \quad D_\theta = -\frac{\partial^2}{\partial\theta^2} - \frac{\cos\theta}{\sin\theta}\frac{\partial}{\partial\theta}\,. \tag{5.3}$$

For string-shaped states a frame (r, φ, z) of cylindrical coordinates is instead adopted, with both φ and z as ignorable quantities, and with z directed along the axis of the configuration. Then Eqs. (4.1) reduce to

$$\frac{(r_0\,\rho)^2\,\bar{\rho}}{\varepsilon_0} = D\,\phi = \left[D + \frac{1}{\rho^2}\right](CA) \tag{5.4}$$

with the operator

$$D = -\frac{1}{\rho}\frac{d}{d\rho}\left(\rho\,\frac{d}{d\rho}\right). \tag{5.5}$$

§5.1 The generating function

The general solution of Eqs. (5.1) in particle-shaped geometry can now be obtained in terms of a *generating function*

$$F(r, \theta) = CA - \phi = G_0 \cdot G(\rho, \theta)\,, \tag{5.6}$$

where G_0 stands for a characteristic amplitude and G for a normalized dimensionless part. This yields the solution

$$CA = -(\sin^2\theta)\, DF\,, \tag{5.7}$$

$$\phi = -\big[1 + (\sin^2\theta)\, D\big] F\,, \tag{5.8}$$

$$\bar{\rho} = -\frac{\varepsilon_0}{r_0^2\,\rho^2}\, D\,\big[1 + (\sin^2\theta)\, D\big] F\,, \tag{5.9}$$

which is easily seen by direct insertion to satisfy Eqs. (5.1). Starting from an arbitrary function F, the corresponding spatial distributions of the potentials CA and ϕ and of the space-charge density $\bar{\rho}$ are thus generated, i.e. those which simultaneously satisfy the set (5.1) of equations. If one would instead start from a given distribution of only one of the field quantities CA, ϕ, or $\bar{\rho}$, this would not provide a simple solution such as that obtained from the set (5.6)–(5.9).

The extra degree of freedom which is introduced by the nonzero electric field divergence and the inhomogeneity of the Proca-type equation (2.1) is underlying this general result by which the quantities (5.7)–(5.9) become coupled and determined by the function (5.6).

In string-shaped geometry a similar generating function

$$F(r) = CA - \phi = G_0 \cdot G(\rho) \tag{5.10}$$

results in

$$CA = -\rho^2\, DF\,, \tag{5.11}$$

$$\phi = -\big(1 + \rho^2\, D\big)\, F\,, \tag{5.12}$$

$$\bar{\rho} = -\frac{\varepsilon_0}{r_0^2\,\rho^2}\, D\,\big(1 + \rho^2\, D\big)\, F\,. \tag{5.13}$$

The quantities (5.7)–(5.9) and (5.11)–(5.13) are uniquely determined by the generating function. The latter can be chosen such that all field quantities decrease rapidly to zero at large radial distances from the origin. In this way the charge and current density, as well as all associated features of an electromagnetic field configuration, can be confined to a limited region of space.

§ 5.2 Particle-shaped states

In the analysis of particle-shaped states the functions

$$f(\rho,\theta) = -(\sin\theta)\, D\,\big[1 + (\sin^2\theta)\, D\big]\, G\,, \tag{5.14}$$

$$g(\rho,\theta) = -\big[1 + 2(\sin^2\theta)\, D\big]\, G \tag{5.15}$$

will now be introduced. Using expressions (5.7)–(5.9), (3.26), (3.30), and (5.10)–(5.15), integrated field quantities can be obtained which represent a net electric charge q_0, magnetic moment M_0, mass m_0, and angular momentum s_0. The magnetic moment is obtained from the local contributions provided by the current density (3.3). The mass and the angular momentum are deduced from the local contributions of $\frac{w_s}{c^2}$ being given by the source energy density (3.26) and the energy relation by Einstein. The current density (3.3) then behaves as a convection current being common to all contributions from the charge density. The corresponding mass flow originates from the velocity vector $\mathbf{C}$ which has the same direction for positive as for negative charge elements. The integrated field quantities finally become

$$q_0 = 2\pi\varepsilon_0 r_0 G_0 J_q\,, \qquad I_q = f\,, \tag{5.16}$$

$$M_0 = \pi\varepsilon_0 C r_0^2 G_0 J_M\,, \quad I_M = \rho(\sin\theta) f\,, \tag{5.17}$$

$$m_0 = \frac{\pi\varepsilon_0}{c^2}\, r_0 G_0^2 J_m\,, \qquad I_m = fg\,, \tag{5.18}$$

$$s_0 = \frac{\pi\varepsilon_0 C}{c^2}\, r_0^2 G_0^2 J_s\,, \qquad I_s = \rho(\sin\theta) fg\,. \tag{5.19}$$

These relations include normalized integrals defined by

$$J_k = \int_{\rho_k}^{\infty}\int_0^{\pi} I_k\; d\rho\, d\theta\,, \qquad k = q, M, m, s, \tag{5.20}$$

where ρ_k are small radii of circles centered around the origin $\rho = 0$ when G is divergent there, and $\rho_k = 0$ when G is convergent at $\rho = 0$. The case $\rho_k \neq 0$ will later be treated in detail. Expressions (5.16)–(5.20) have been obtained from integration of the local contributions dq_0, dM_0, dm_0, and ds_0 to the total charge, magnetic moment, mass, and angular momentum. With the volume element $dV = 2\pi\rho^2(\sin\theta)d\rho\, d\theta$ these contributions become $dq_0 = \bar{\rho}\, dV$, $dM_0 = \frac{1}{2}(\sin\theta) C\rho\, dq_0$, $dm_0 = \frac{w}{c^2}\, dV$, and $ds_0 = C\rho\,(\sin\theta) dm_0$. So far the integrals (5.16)–(5.20) are not uniquely determined but depend on the distribution of the function G in space. They will first become fully determined when further conditions are being imposed, such as those of a quantization. The general forms (5.16)–(5.20) thus provide the integrated quantities with a certain degree of flexibility.

Also in a particle-shaped steady state where the net charge (5.16) becomes nonzero, such as in the model of the electron developed later in Chapter 6, there is a steady momentum balance as based on Eqs. (5.1)

and (3.16) and investigated later in detail in §6.8. This leads under certain conditions to a self-confined balance between the electromagnetic forces. The electron can then be prevented from "exploding" under the action of its electric eigencharge, as otherwise being predicted by conventional theory[24,25].

At this point a further step is taken by imposing the restriction of a separable generating function

$$G(\rho,\theta) = R(\rho)\cdot T(\theta)\,. \tag{5.21}$$

The integrands of the normalized form (5.20) then become

$$I_q = \tau_0 R + \tau_1(D_\rho R) + \tau_2 D_\rho(D_\rho R)\,, \tag{5.22}$$

$$I_M = \rho\,(\sin\theta)\,I_q\,, \tag{5.23}$$

$$I_m = \tau_0\tau_3 R^2 + (\tau_0\tau_4 + \tau_1\tau_3)\,R(D_\rho R) + \tau_1\tau_4(D_\rho R)^2 + \\ + \tau_2\tau_3 R D_\rho(D_\rho R) + \tau_2\tau_4(D_\rho R)[D_\rho(D_\rho R)]\,, \tag{5.24}$$

$$I_s = \rho\,(\sin\theta)\,I_m\,, \tag{5.25}$$

where

$$\tau_0 = -\,(\sin\theta)(D_\theta T) - (\sin\theta)D_\theta\big[(\sin^2\theta)(D_\theta T)\big]\,, \tag{5.26}$$

$$\tau_1 = -\,(\sin\theta)T - (\sin\theta)D_\theta\big[(\sin^2\theta)T\big] - \sin^3\theta(D_\theta T)\,, \tag{5.27}$$

$$\tau_2 = -\,(\sin^3\theta)\,T\,, \tag{5.28}$$

$$\tau_3 = -\,T - 2\,(\sin^2\theta)(D_\theta T)\,, \tag{5.29}$$

$$\tau_4 = -\,2\,(\sin^2\theta)\,T\,. \tag{5.30}$$

Among the possible forms to be adopted for the radial function $R(\rho)$ and the polar function $T(\theta)$, we will here consider the following cases:

- The radial part R can become convergent or divergent at the origin $\rho = 0$ but it always goes strongly towards zero at large distances from it;
- The polar part T is always finite and has finite derivatives. It can become symmetric or antisymmetric with respect to the "equatorial plane" (mid-plane) defined by $\theta = \frac{\pi}{2}$.

The restriction (5.21) of separability becomes useful when treating configurations where the sources $\bar{\rho}$ and $\mathbf{j}$ and the corresponding energy density are mainly localized to a region near the origin, such as for a particle of limited extent. Then the far-field properties, at great distances

from the origin, have a negligible influence on the integrated field quantities (5.16)–(5.19). This restriction is also supported indirectly by the results which follow and which in several respects seem to be consistent with experimental facts.

§ 5.2.1 The radial part of the generating function

We first turn to a generating function with a convergent radial part for which $\rho_k = 0$ in Eq. (5.20). For the electric charge (5.16) integration by parts with respect to ρ then results in a normalized integral

$$J_q = \int_0^\infty \int_0^\pi \tau_0 R \; d\rho + \\ + \int_0^\pi \left\{ -\tau_1 \left[\rho^2 \frac{dR}{d\rho} \right]_0^\infty + \tau_2 \left[\rho^2 \frac{d^2}{d\rho^2} \left(\rho^2 \frac{dR}{d\rho} \right) \right]_0^\infty \right\} d\theta \,, \tag{5.31}$$

where R and its derivatives vanish at infinity and are finite at $\rho = 0$. Since the integrals of τ_1 and τ_2 are finite in Eq. (5.31),

$$J_q = \int_0^\infty R \, d\rho \; \cdot \int_0^\pi \tau_0 \, d\theta \equiv J_{q\rho} \cdot J_{q\theta} \,. \tag{5.32}$$

For convergent integrals $J_{q\rho}$ one thus has to analyse the part $J_{q\theta}$ which by partial integration transforms into

$$J_{q\theta} = \left\{ (\sin\theta) \frac{d}{d\theta} \left[(\sin^2\theta)(D_\theta T) \right] + (\sin\theta) \frac{dT}{d\theta} \right\}_0^\pi . \tag{5.33}$$

For all functions T with finite derivatives at $\theta = (0, \pi)$, it is then seen that $J_{q\theta}$ and q_0 vanish in general.

Turning next to the magnetic moment (5.17) and the integral J_M, it is first observed that

$$\int_0^\infty \rho R \, d\rho = -\frac{1}{2} \int_0^\infty \rho (D_\rho R) \, d\rho = \frac{1}{4} \int_0^\infty \rho \, D_\rho (D_\rho R) \, d\rho \tag{5.34}$$

as obtained by partial integration. Using this relation, Eq. (5.23) yields

$$J_M = \int_0^\infty \rho R \, d\rho \int_0^\pi (\sin\theta)(\tau_0 - 2\tau_1 + 4\tau_2) \, d\theta \equiv J_{M\rho} \cdot J_{M\theta} \,. \tag{5.35}$$

Partial integration with respect to θ further results in

$$J_{M\theta} = \left\{ (\sin^3\theta) \frac{d}{d\theta} \left[(\sin\theta)(D_\theta T - 2T) \right] \right\}_0^\pi \tag{5.36}$$

which vanishes for functions T having finite derivatives at $\theta = (0, \pi)$. Then M_0 will also vanish.

Concerning the mass and the angular momentum, the convergent normalized integrals J_m and J_s of Eqs. (5.18)–(5.20) cannot vanish in general. A simple test with $R = e^{-\rho}$ and $T = 1$ can be used to illustrate this.

The conclusions from these deductions are as follows:

- Convergent radial functions R lead to a class of electrically neutral particle states where q_0 and M_0 both vanish, whereas m_0 and s_0 are nonzero;
- For the present particle-shaped geometry to result in electrically charged states, the *divergence* of the radial function becomes a necessary but not sufficient condition. This leads to the subsequent question whether the corresponding integrals (5.20) would then be able to form the basis of a steady state having *finite* and nonzero values of all the integrated field quantities (5.16)–(5.19). This will later in Chapter 6 be shown to become possible.

§ 5.2.2 The polar part of the generating function

The top-bottom symmetry properties of the polar function T are now considered with respect to the equatorial plane. The integrals (5.20) which are evaluated in the interval $0 \leqslant \theta \leqslant \pi$ become nonzero for symmetric integrands I_k, but vanish for antisymmetric ones. These symmetry properties are evident from expressions (5.22)–(5.30). Thus, the product of two symmetric or of two antisymmetric functions becomes symmetric, whereas a product of a symmetric function with an antisymmetric one becomes antisymmetric. The symmetry or antisymmetry of T leads to a corresponding symmetry or antisymmetry of $D_\theta T$, $D_\theta\big[(\sin^2\theta)T\big]$, and $D_\theta\big[(\sin^2\theta)(D_\theta T)\big]$. Therefore all functions (5.26)–(5.30) are either symmetric or antisymmetric in the same way as T. These properties are easily tested in the simple cases of $T = \sin\theta$ and $T = \cos\theta$. As a consequence, the polar part T of the generating function obeys the following rules:

- The integrands I_q and I_M of Eqs. (5.22) and (5.23) have the same symmetry properties as T.
- The integrands I_m and I_s of Eqs. (5.24) and (5.25) are always symmetric, irrespective of the symmetry properties of T.

These rules further lead to two general conclusions about the integrated field quantities (5.16)–(5.19):

- The charge and the magnetic moment vanish for antisymmetric forms of T, irrespective of the form of R.
- The mass and the angular momentum generally differ from zero, both when T is symmetric and when it is antisymmetric.

§ 5.2.3 Summary of related properties

The discussion on the convergence and on the top-bottom symmetry properties of the generating function, and the resulting consequences for the integrated charge and magnetic moment, have been summarized in Table 5.1. Thereby it is understood that the integrated mass and angular momentum are nonzero in all cases listed in the table. Possible applications to models of the electron and the neutrino are given within brackets.

$T(\theta)$ / $R(\rho)$	**a. Top-bottom symmetry**	**b. Top-bottom antisymmetry**
A. Convergence at origin (model)	Aa. $q_0 = 0 \quad M_0 = 0$ (neutrino)	Ab. $q_0 = 0 \quad M_0 = 0$ (neutrino)
B. Divergence at origin (model)	Ba. $q_0 \neq 0 \quad M_0 \neq 0$ (electron)	Bb. $q_0 = 0 \quad M_0 = 0$ (neutrino)

Table 5.1: Convergence and symmetry properties of the generating function $G = R(\rho) \cdot T(\theta)$, and resulting consequences for the integrated charge q_0 and magnetic moment M_0 of particle-shaped axisymmetric states. The integrated mass m_0 and angular momentum s_0 are nonzero in all cases.

§ 5.2.4 Particle-shaped matter and antimatter models

With $C = \pm c$ and $G_0 = \pm |G_0|$ it is seen from Eqs. (5.16)–(5.30) that there are pairs of solutions having the same geometry of their local distributions, but having opposite signs of the corresponding integrated field quantities in places where G_0 and C appear linearly. This could become the basis for models of charged and neutral particles of matter as well as of antimatter. A minor difference between matter and antimatter will then not be included in or come out of the models.

With such geometrical configurations, annihilation reactions can be imagined to become "explosive" on account of the mutual forces which remain attractive at any separation distance of two particles consisting

of matter and antimatter. When the particles tend to overlap at a vanishing such distance, the local charge distributions would then cancel each other completely at any local point.

§ 5.3 String-shaped states

For string-shaped configurations expressions (5.4), (5.5) and (5.10)–(5.13) can be used to study states determined by the generating function

$$G = e^{-\rho} \cdot H(\rho)\,. \tag{5.37}$$

Here the exponential factor secures the convergence at large distances from the axis of symmetry where $H(\rho)$ is finite.

§ 5.3.1 The net electric charge

In analogy with Eq. (5.16) the net electric charge per unit length becomes

$$\frac{q_0}{L_s} = 2\pi\varepsilon_0 G_0 J_q\,, \qquad J_q = \int_0^\infty f_q\, d\rho\,, \tag{5.38}$$

where L_s is the length of the string and

$$f_q = -\rho D(1+\rho^2 D)G = \frac{r_0^2}{\varepsilon_0 G_0}\,\rho\bar{\rho} \tag{5.39}$$

according to Eq. (5.13). With the operator (5.5) the integral (5.38) becomes

$$J_q = \left\{\rho\,\frac{d}{d\rho}\left[G - \rho\,\frac{d}{d\rho}\left(\rho\,\frac{dG}{d\rho}\right)\right]\right\}_0^\infty . \tag{5.40}$$

The generating function (5.37) then yields

$$\begin{aligned} J_q = \Big\{\rho^2 e^{-\rho}[(3-\rho)(H'-H) + (3-2\rho)(H''-H') + \\ + \rho\,(H'''-H'')]\Big\}_0^\infty , \end{aligned} \tag{5.41}$$

where a prime denotes derivation with respect to ρ. When H and all its derivatives are finite at $\rho = 0$ and at infinity , we thus obtain $J_q = 0$ and a vanishing total charge q_0.

§ 5.3.2 The magnetic field

There is an axial magnetic field obtained from the circulating current $\mathbf{j} = \bar{\rho}\,\mathbf{C}$, and being given by

$$B(\rho) = G_0\left(\frac{C}{c^2 r_0}\right) b(\rho)\,, \qquad b(\rho) = \int_0^\infty \frac{f_q}{\rho}\, d\rho\,. \tag{5.42}$$

As a simple example, a choice of $H = 1$ yields

$$b(\rho) = e^{-\rho}\left(-\rho^2 + 4\rho - 2\right). \tag{5.43}$$

This field is in the negative axial direction at the axis $\rho = 0$, changes sign at the points $\rho = 2 \pm \sqrt{2}$, and vanishes at large ρ. The total magnetic flux

$$\mathbf{\Phi} = 2\pi \int_0^\infty \rho\, b\, d\rho = 0 \tag{5.44}$$

also vanishes.

§ 5.3.3 Comparison with quantum mechanical string model

In quantum electrodynamics a string model of the hadron structure has been proposed as described by Nambu[81]. Even if the hadron colour field and the present electromagnetic field are different concepts, they still become somewhat analogous in a number of respects. The results (5.41), (5.43) and (5.44) may therefore be of some general interest to the former concept, because of the following desirable features of the present Proca-type field equations:

- There is a constant longitudinal stress which tends to pull the ends of the configuration towards each other;
- The magnetic field and its stress are localized to a narrow channel defined by the string;
- The system has no net electric charge;
- No artificial model is needed which is based on magnetic poles at the ends of the string.

§ 5.4 Quantum conditions of particle-shaped states

As already has been pointed out in §3.4, a simplified road is chosen in this analysis, by imposing relevant quantum conditions on the obtained general solutions of the field equations. Here charged and neutral particle-shaped states are treated in terms of such a procedure.

§ 5.4.1 The angular momentum

The angular momentum (spin) condition to be imposed on the models of the electron in the capacity of a fermion particle, as well as of the neutrino, is combined with Eq. (5.19) to result in

$$s_0 = \pi \frac{\varepsilon_0 C}{c^2} r_0^2 G_0^2 J_s = \pm \frac{h}{4\pi}. \tag{5.45}$$

This condition becomes compatible with the two signs of $C = \pm c$, as obtained from relation (2.8) due to the Lorentz invariance.

In particular, for a charged particle such as the electron, muon, tauon or their antiparticles, Eqs. (5.16) and (5.19) combine to

$$q^* \equiv \left|\frac{q_0}{e}\right| = \left(\frac{f_0 J_q^2}{2J_s}\right)^{1/2}, \qquad f_0 = \frac{2\varepsilon_0 ch}{e^2}, \tag{5.46}$$

where q^* is a dimensionless charge being normalized with respect to the experimentally determined electronic charge "e", and $f_0 \approx 137.036$ is the inverted value of the fine-structure constant.

§ 5.4.2 The magnetic moment

According to Schwinger and Feynman[82], and Dirac[37] the quantum condition on the magnetic moment of a charged particle such as the electron becomes

$$\frac{M_0 m_0}{q_0 s_0} = 1 + \delta_M, \qquad \delta_M = \frac{1}{2\pi f_0} \tag{5.47}$$

which shows excellent agreement with experiments. Here the unity term of the right-hand member is due to Dirac who obtained the correct Landé factor by considering the electron to be situated in an imposed external magnetic field. This leads to a magnetic moment being twice as large as that expected from an elementary proportionality relation between the electron spin and the magnetic moment[21]. Further, in Eq. (5.47) the term δ_M is a small quantum mechanical correction due to Schwinger and Feynman, as obtained from an advanced analysis where the electron is considered to emit and absorb a photon during its way from one place to another.

Conditions (5.45) and (5.47) can also be made plausible by elementary physical arguments based on the present picture of a particle-shaped state of "self-confined" radiation. In the latter picture there is a circulation of radiation at the velocity of light around the axis of symmetry. If this circulation takes place at the average characteristic radial distance r_0, the corresponding frequency of revolution would become $\nu \simeq \frac{c}{2\pi r_0}$. In combination with the energy relations $W = m_0 c^2$ and $W = h\nu$ by Einstein and Planck, one then obtains

$$r_0 m_0 \simeq \frac{h}{2\pi c}, \tag{5.48}$$

where r_0 has the same form as the Compton radius. With the total

current $q_0\nu$, the magnetic moment further becomes

$$M_0 = \pi r_0^2 q_0 \nu = \frac{1}{2} q_0 c r_0 = \frac{q_0 h}{4\pi m_0} , \tag{5.49}$$

which agrees with conditions (5.45) and (5.47) when δ_M is neglected. Thereby the angular momentum becomes $|s_0| = \frac{r_0 c m_0}{2} = \frac{h}{4\pi}$ when its inwardly peaked spatial distribution corresponds to an equivalent radius $\frac{r_0}{2}$. This should, however, only be taken as a crude physical indication where the radius in Eq. (5.48) comes out to be far too large as compared to observations. In any case, it is not unimaginable for an imposed external field to rearrange the distributions of charge and energy density which appear in the integrals (5.16)–(5.20). According to the discussion at the beginning of §5.2, the flexibility of the local distributions would support such a point of view. Thereby the unequal integrands of the magnetic moment and the angular momentum in Eqs. (5.17) and (5.19) could also be reconcilable with a proportionality relation between s_0 and M_0 which leads to the correct Landé factor. Another possibility of obtaining a correct value of this factor is to modify Eq. (5.48) to represent the first "subharmonic" given by the path length $4\pi r_0$, but this would become a rather far-fetched proposal in a purely axisymmetric case. The use of condition (5.47) leads in any case to results which are reconcilable with several experimental facts, as will later be demonstrated by the detailed deductions of Chapter 6.

§5.4.3 The magnetic flux

In a charged particle-shaped state with a nonzero magnetic moment, the electric current distribution will generate a total magnetic flux Γ_{tot} and a corresponding total magnetic energy. In such a state the quantized value of the angular momentum further depends on the type of configuration being considered. It thus becomes $|s_0| = \frac{h}{4\pi}$ for a fermion, but $|s_0| = \frac{h}{2\pi}$ for a boson. We now consider the electron to be a system also having a quantized charge q_0. As in a number of other physical systems, the flux should then become quantized as well, and be given by the two quantized concepts s_0 and q_0, in a relation having the dimension of magnetic flux. This leads to the quantum condition[18,83]

$$\Gamma_{tot} = \left| \frac{s_0}{q_0} \right| . \tag{5.50}$$

Chapter 6

A MODEL OF THE ELECTRON

In this chapter a model of the electron will be elaborated which in principle also applies to the muon, tauon and to corresponding antiparticles[84]. According to § 5.2.1 and case Ba in Table 5.1, a charged particle-shaped state only becomes possible by means of a generating function having a radial part R which is divergent at the origin, and a polar part T with top-bottom symmetry. In its turn, the divergence of R leads to the question how to obtain finite and nonzero integrated field quantities (5.16)–(5.20). The following analysis will show this to become possible, by shrinking the characteristic radius r_0 to the very small values of a "point-charge-like" state. It does on the other hand not imply that r_0 has to become strictly equal to zero, which would end up into the unphysical situation of a structureless point.

§ 6.1 The form of the generating function

The generating function to be considered has the parts

$$R = \rho^{-\gamma} e^{-\rho}\,, \qquad \gamma > 0\,, \tag{6.1}$$

$$T = 1 + \sum_{\nu=1}^{n} \{a_{2\,\nu-1} \sin[(2\,\nu - 1)\,\theta] + a_{2\nu} \cos(2\,\nu\theta)\} = \\ = 1 + a_1 \sin\theta + a_2 \cos 2\theta + a_3 \sin 3\theta + \ldots \tag{6.2}$$

Concerning the radial part (6.1), it may at a first glance appear to be somewhat special and artificial. Under general conditions one could thus have introduced a negative power series of ρ instead of the single term $\rho^{-\gamma}$. However, for a limited number of terms in such a series, that with the largest negative power will in any case dominate near the origin. Moreover, due to the following analysis the same series has to contain one term only, with a locked special value of the radial parameter γ. The exponential factor in expression (6.1) has been included to secure the convergence of any moment with R at large distances from the origin. This factor will not appear in the end results of the analysis.

The polar part (6.2) represents a general form of axisymmetric geometry having top-bottom symmetry with respect to the equatorial plane. Here it should be noticed that all sine and cosine terms can be rewritten

into a corresponding power series of $\sin\theta$, as well as the entire resulting series. Thus[38]

$$\sin n\theta = n\sin\theta\cos^{n-1}\theta - \binom{n}{3}\sin^3\theta\cos^{n-3}\theta + \\ + \binom{n}{5}\sin^5\theta\cos^{n-5}\theta - \dots \quad (6.3)$$

$$\cos n\theta = \cos^n\theta - \binom{n}{2}\sin^2\theta\cos^{n-2}\theta + \binom{n}{4}\sin^4\theta\cos^{n-4}\theta - \dots \quad (6.4)$$

A separable generating function (5.21) is used in this analysis which in the first place aims at the region near the origin where the charge density is mainly being concentrated. As will be shown later, and pointed out in §3.6.1, the dominating contributions to the source energy density then originate from this region. The final result obtained from the corresponding integrals is independent of the special asymptotic forms of the electromagnetic potentials at large radial distances. To achieve the correct asymptotic forms $A_v = \frac{\mu_0 M_0 \sin\theta}{4\pi c^2 r_0^2 \rho^2}$ and $\phi_v = \frac{q_0}{4\pi\varepsilon_0 r_0 \rho}$ one would instead have to pass over to a nonseparable generating function

$$F = G_0 G(\rho,\theta) = G_0 R(\rho)\cdot T(\theta) + (CA_v - \phi_v)\, e^{(-1/\rho)}. \quad (6.5)$$

This would, however, much complicate the analysis, without changing the final results which are of main importance to this investigation.

§6.2 Integrated field quantities

The radial form given by Eq. (6.1) can now be inserted into the integrands (5.22)–(5.25). The expressions for $D_\rho R$ and $D_\rho(D_\rho R)$ give rise to sets of terms with different negative powers of ρ. Since the radial integrals (5.20) are extended to very low limits ρ_k, they become dominated by contributions from terms of the strongest negative power. Keeping these contributions only, the integrands reduce to

$$I_k = I_{k\rho} I_{k\theta}\,, \qquad k = q, M, m, s, \quad (6.6)$$

where

$$I_{q\rho} = R\,, \quad I_{M\rho} = \rho R\,, \quad I_{m\rho} = R^2\,, \quad I_{s\rho} = \rho R^2\,, \quad (6.7)$$

and

$$I_{q\theta} = \tau_0 - \gamma(\gamma-1)\tau_1 + \gamma^2(\gamma-1)^2\tau_2\,, \quad (6.8)$$

$$I_{M\theta} = (\sin\theta)\, I_{q\theta}\,, \quad (6.9)$$

$$I_{m\theta} = \tau_0\tau_3 - \gamma(\gamma-1)(\tau_0\tau_4 + \tau_1\tau_3) + \\ + \gamma^2(\gamma-1)^2(\tau_1\tau_4 + \tau_2\tau_3) - \gamma^3(\gamma-1)^3\tau_2\tau_4\,, \quad (6.10)$$

$$I_{s\theta} = (\sin\theta)\, I_{m\theta}\,. \quad (6.11)$$

The corresponding integrals (5.20) then become

$$J_k = J_{k\rho}\, J_{k\theta}\,, \tag{6.12}$$

where

$$J_{q\rho} = \frac{1}{\gamma-1}\,\rho_q^{-(\gamma-1)}\,, \qquad J_{M\rho} = \frac{1}{\gamma-2}\,\rho_M^{-(\gamma-2)}, \tag{6.13}$$

$$J_{m\rho} = \frac{1}{2\gamma-1}\,\rho_m^{-(2\gamma-1)}\,, \qquad J_{s\rho} = \frac{1}{2(\gamma-1)}\,\rho_s^{-2(\gamma-1)}\,, \tag{6.14}$$

and

$$J_{k\theta} = \int_0^\pi I_{k\theta}\; d\theta\,. \tag{6.15}$$

In expression (6.13) for the magnetic moment a point-charge-like behaviour excludes the range $\gamma < 2$.

The divergences of the so far undetermined radial expressions (6.13)–(6.14) appear in the integrals of Eqs. (5.16)–(5.20) when the lower limits ρ_k approach zero. To outbalance these, one has to introduce a shrinking characteristic radius defined by

$$r_0 = c_0\,\varepsilon\,, \qquad c_0 > 0\,, \qquad 0 < \varepsilon \ll 1\,. \tag{6.16}$$

Here c_0 is a positive constant having the dimension of length, and ε is a dimensionless characteristic radius which has the role of a decreasing smallness parameter. Replacing ε by any power of ε would not lead to more generality. Combination of Eqs. (6.13), (6.14), and (6.16) with Eqs. (5.16)–(5.20) gives the result

$$q_0 = 2\pi\varepsilon_0 c_0 G_0\,\frac{J_{q\theta}}{(\gamma-1)}\,\frac{\varepsilon}{\rho_q^{\gamma-1}}\,, \tag{6.17}$$

$$M_0 m_0 = \pi^2\,\frac{\varepsilon_0^2 C}{c^2}\,c_0^3 G_0^3\,\frac{J_{M\theta}J_{m\theta}}{(\gamma-2)(2\gamma-1)}\,\frac{\varepsilon^3}{\rho_M^{\gamma-2}\rho_m^{2\gamma-1}}\,, \tag{6.18}$$

$$s_0 = \pi\frac{\varepsilon_0 C}{c^2}\,c_0^2 G_0^2\,\frac{J_{s\theta}}{2(\gamma-1)}\left(\frac{\varepsilon}{\rho_s^{\gamma-1}}\right)^2. \tag{6.19}$$

The reason for introducing the compound quantity $M_0 m_0$ in Eq. (6.18) is that this quantity appears as a single entity of all finally obtained relations in the present theory. So far it has not become possible to separate the magnetic moment from the mass in the analysis. In itself, this would become an interesting and probably difficult future task.

The outbalance of the divergence of the generating function by a shrinking characteristic radius, and the resulting finite values (6.17)–(6.19) of the integrated field quantities in a point-charge-like state, is a specific feature which has no counterpart in conventional theory.

We further require the configuration and its integrated quantities (6.17)–(6.19) to scale in such a way that the geometry is preserved by becoming independent of ρ_k and ε within the range of small ε. Such a uniform scaling implies that

$$\rho_q = \rho_M = \rho_m = \rho_s = \varepsilon \tag{6.20}$$

and that the radial parameter γ has to approach the value 2 from above, i.e.

$$\gamma(\gamma-1) = 2+\tilde{\delta}\,, \qquad 0 \leqslant \tilde{\delta} \ll 1\,, \qquad \gamma \approx 2+\frac{\tilde{\delta}}{3}\,. \tag{6.21}$$

For the quantities M_0 and m_0 to become finite separately when ε approaches zero, the corresponding conditions become less straightforward[14], but $M_0 m_0$ can be made to follow the scaling of Eq. (6.20) also in such a case.

From the earlier obtained results (5.33) and (5.36) it is further seen that the contribution from τ_0 in Eq. (6.8) vanishes as well as $J_{M\theta}$ when $\gamma = 2$. In the limit (6.21) the integrands (6.8)–(6.11) can then be replaced by

$$I_{q\theta} = -2\tau_1 + 4\tau_2\,, \tag{6.22}$$

$$\frac{I_{M\theta}}{\tilde{\delta}} = (\sin\theta)(-\tau_1+4\tau_2)\,, \tag{6.23}$$

$$I_{m\theta} = \tau_0\tau_3 - 2(\tau_0\tau_4+\tau_1\tau_3) + 4(\tau_1\tau_4+\tau_2\tau_3) - 8\,\tau_2\tau_4\,, \tag{6.24}$$

$$I_{s\theta} = (\sin\theta)\, I_{m\theta}\,. \tag{6.25}$$

With the integrals (6.15) and the definitions

$$A_q \equiv J_{q\theta}\,, \qquad A_M \equiv \frac{J_{M\theta}}{\tilde{\delta}}\,, \qquad A_m \equiv J_{m\theta}\,, \qquad A_s \equiv J_{s\theta} \tag{6.26}$$

the integrated quantities (6.17)–(6.19) take the final form

$$q_0 = 2\pi\varepsilon_0 c_0 G_0 A_q \varepsilon^{-\tilde{\delta}/3}\,, \tag{6.27}$$

$$M_0 m_0 = \pi^2\,\frac{\varepsilon_0^2 C}{c^2}\, c_0^3 G_0^3 A_M A_m \varepsilon^{-\tilde{\delta}}\,, \tag{6.28}$$

$$s_0 = \frac{1}{2}\,\pi\,\frac{\varepsilon_0 C}{c^2}\, c_0^2 G_0^2 A_s \varepsilon^{-2\tilde{\delta}/3} \tag{6.29}$$

for small $\tilde{\delta}$. These relations can be considered to include an undetermined but finite equivalent amplitude $G_0\varepsilon^{-\tilde{\delta}/3}$. Since we are free to choose the magnitude of G_0, this holds whether or not δ approaches zero more strongly than ε.

Through combination of expressions (5.18), (5.20), (5.49), (6.6), (6.14), (6.16), (6.26), and (6.29), and due to the fact that the ratio $\frac{A_m}{A_s}$ is close to unity, it is readily seen that the radial constant c_0 becomes nearly equal to the Compton wavelength $\frac{h}{m_0 c}$ divided by 6π.

§6.3 Magnetic flux

According to Eq. (5.7) the magnetic flux function becomes

$$\Gamma = 2\pi r\,(\sin\theta)A = -2\pi r_0\,\frac{G_0}{c}\,\rho\,(\sin^3\theta)\,DG \tag{6.30}$$

which vanishes at $\theta = (0, \pi)$. Making use of Eqs. (5.3), (6.1), and (6.16) the flux becomes

$$\Gamma = 2\pi\,\frac{c_0 G_0}{C}\,\sin^3\theta\big\{\big[\gamma(\gamma-1) + 2(\gamma-1)\rho + \rho^2\big]\,T - \\ - D_\theta T\big\}\,\frac{\varepsilon}{\rho^{\gamma-1}}\,e^{-\rho}. \tag{6.31}$$

This relation shows that the flux increases strongly as ρ decreases towards small values, in accordance with a point-charge-like behaviour. To obtain a nonzero and finite magnetic flux when γ approaches the value 2 from above, one has to choose a corresponding dimensionless lower radius limit $\rho_\Gamma = \varepsilon$, in analogy with expressions (6.16) and (6.20). There is then a magnetic flux which intersects the equatorial plane. It is counted from the point $\rho = \rho_\Gamma = \varepsilon$ and outwards, as given by

$$\Gamma_0 = -\Gamma\left(\rho = \varepsilon,\ \theta = \frac{\pi}{2}\right) = 2\pi\,\frac{c_0 G_0 \varepsilon^{-\tilde{\delta}/3}}{C}\,A_\Gamma\,, \tag{6.32}$$

where

$$A_\Gamma = \big[D_\theta T - 2T\big]_{\theta=\frac{\pi}{2}} \tag{6.33}$$

for $\gamma = 2$. Also here the result can be considered to include the amplitude $G_0\varepsilon^{-\tilde{\delta}/3}$. The flux (6.32) can be regarded as being generated by a configuration of thin current loops. These have almost all their currents located to a spherical surface with the radius $\rho = \varepsilon$, and the corresponding magnetic field lines cut the equatorial plane at right angles. For $C < 0$ and $q_0 < 0$ there is then an "upward" flux $-\Gamma_0$ within the inner region $0 < \rho < \varepsilon$ of the equatorial plane, being equal to a "downward" flux Γ_0 within the outer region $\rho > \varepsilon$ of the same plane.

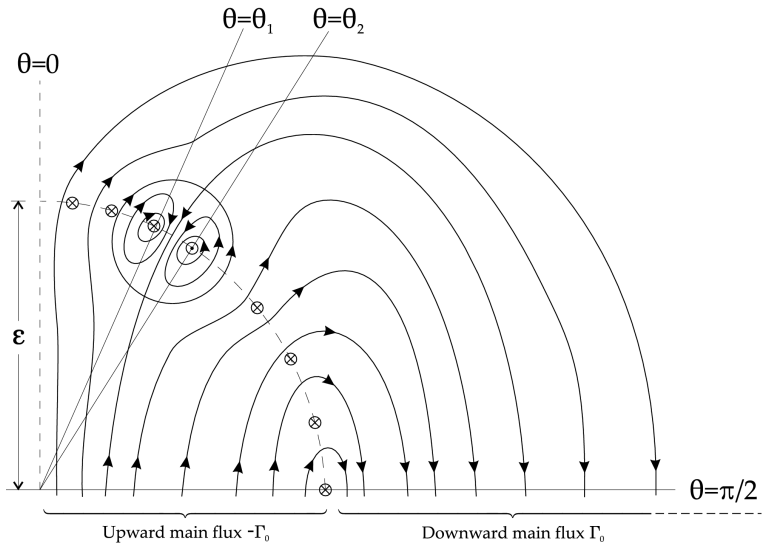

Figure 6.1: Crude outline of a magnetic field configuration in the case of one magnetic island situated above and one below the equatorial plane $\theta = \frac{\pi}{2}$. Only the upper half-plane is shown, and the figure is axially (rotationally) symmetric around the vertical axis $\theta = 0$. In the interval $\theta_1 \leqslant \theta \leqslant \theta_2$ there is a magnetic flux into the spherical surface $\rho = \epsilon$ (dashed circular line) being equal to the inward magnetic island flux only. The outward flux parts in the intervals $0 \leqslant \theta \leqslant \theta_1$ and $\theta_2 \leqslant \theta \leqslant \frac{\pi}{2}$ consist of the outward main flux, plus an outward island flux.

It has to be observed that the flux (6.32) is not necessarily the total flux which is generated by the current system as a whole. There are cases in which magnetic islands are formed above and below the equatorial plane, and where these islands possess an isolated circulating extra flux which does not intersect the same plane. The total flux Γ_{tot} then consists of the "main flux" $-\Gamma_0$ of Eq. (6.32), plus the extra "island flux" Γ_i, which can be deduced from the function (6.31), as will be shown later. This type of field geometry turns out to prevail in the analysis which follows, and it leads to a magnetic configuration being similar to that outlined in Fig. 6.1.

In the analysis of the contribution from the magnetic islands we introduce the normalized flux function defined by Eq. (6.31) in the upper half-plane of the sphere $\rho = \varepsilon \ll 1$. It becomes

$$\Psi \equiv \frac{\Gamma\,(\rho = \varepsilon,\, \theta)}{2\pi} \left| \frac{C\,\varepsilon^{\tilde{\delta}/3}}{c_0 G_0} \right| = (\sin^3\theta)(D_\theta T - 2T)\,. \tag{6.34}$$

Within the region near this spherical surface the function (6.31) and the corresponding vector potential both consist of the product of two separate functions of ρ and θ. This also applies to the components of the magnetic field given by Eq. (3.8). The polar component B_θ is then seen to be proportional to the function Ψ of Eq. (6.34), whereas the radial component B_ρ becomes proportional to $\frac{d\Psi}{d\theta}$. In all cases to be treated here the situation outlined in Fig. 6.1 is then represented by a magnetic near-field configuration being demonstrated in Fig. 6.2.

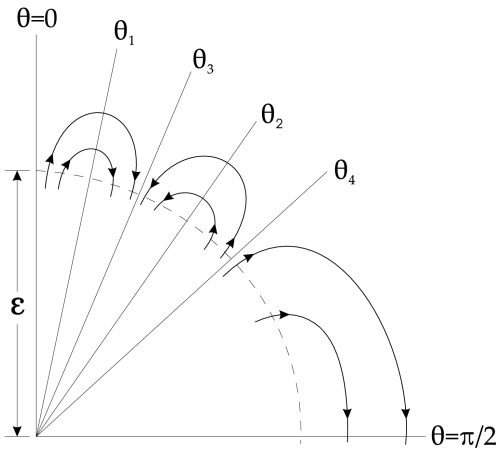

Figure 6.2: Outline of the magnetic field configuration corresponding to the present detailed deductions. The figure shows the field in the region near the spherical surface $\rho = \epsilon$. The radial magnetic field component B_ρ vanishes along the lines $\theta = \theta_1$ and $\theta = \theta_2$, whereas the polar component B_θ vanishes along the lines $\theta = \theta_3$ and $\theta = \theta_4$.

In the range of increasing θ, the component B_ρ then vanishes along the lines $\theta = \theta_1$ and $\theta = \theta_2$, whereas the component B_θ vanishes along the lines $\theta = \theta_3$ and $\theta = \theta_4$. Consequently, the increase of θ from the axis at $\theta = 0$ first leads to an increasing flux Ψ up to a maximum at the angle $\theta = \theta_1$. Then there follows an interval $\theta_1 < \theta < \theta_2$ of decreasing flux, down to a minimum at $\theta = \theta_2$. In the range $\theta_2 \leqslant \theta \leqslant \frac{\pi}{2}$ there is again an increasing flux, up to the value

$$\Psi_0 = \Psi\left(\frac{\pi}{2}\right) = A_\Gamma\,, \tag{6.35}$$

which is equal to the main flux.

We further introduce the parts of the integrated magnetic flux defined by

$$\Psi_1 = \Psi(\theta_1) - \Psi(0) = \Psi(\theta_1)\,, \qquad \Psi_2 = \Psi\left(\frac{\pi}{2}\right) - \Psi(\theta_2)\,, \tag{6.36}$$

and associated with the ranges $0 < \theta < \theta_1$ and $\theta_2 < \theta < \frac{\pi}{2}$ of Figs.6.1 and 6.2. The sum of these parts includes the main flux Ψ_0, plus an outward directed flux from one magnetic island. The contribution from

the latter becomes $\Psi_1 + \Psi_2 - \Psi_0$. The total flux which includes the main flux and that from two islands is then given by

$$\Psi_{tot} = 2\,(\Psi_1 + \Psi_2 - \Psi_0) + \Psi_0 \tag{6.37}$$

which also can be written as

$$\Psi_{tot} = f_{\Gamma f}\Psi_0 \qquad f_{\Gamma f} = \frac{2(\Psi_1 + \Psi_2) - \Psi_0}{\Psi_0}\,, \tag{6.38}$$

where $f_{\Gamma f} > 1$ is a corresponding flux factor.

§6.4 Quantum conditions

The analysis is now at a stage where the relevant quantum conditions of §5.4 can be imposed. For the angular momentum (5.45) and its associated charge relation (5.46) the result becomes

$$q^* = \left(\frac{f_0 A_q^2}{A_s}\right)^{1/2} \tag{6.39}$$

according to Eqs. (6.12)–(6.15), (6.20) and (6.26) in the limit $\gamma = 2$.

For the magnetic moment condition (5.47) reduces to

$$\frac{A_M\,A_m}{A_q\,A_s} = 1 + \delta_M \tag{6.40}$$

when applying Eqs. (6.27)–(6.29). The condition (6.40), and its counterpart of Eq. (5.47), has earlier been made plausible by the simple physical arguments of §5.4.2. This also seems to be supported by the forms of the integrands (6.8)–(6.11) according to which the local relation $I_{M\theta}I_{m\theta} = I_{q\theta}I_{s\theta}$ is obtained. However, as has become obvious from the present analysis and Eqs. (6.21)–(6.23), the detailed deductions of the electron model do not become quite as simple.

Magnetic flux quantization is expressed by condition (5.50). Combination of Eqs. (6.35), (6.17), (6.19) and (6.26) then yields

$$8\pi f_{\Gamma q} A_\Gamma A_q = A_s\,, \tag{6.41}$$

where $f_{\Gamma q}$ is the flux factor being *required* by the corresponding quantum condition. This factor should not be confused with the factor $f_{\Gamma f}$ of Eq. (6.38) which *results* from the magnetic field geometry. Only when one arrives at a self-consistent solution will these two factors become equal to the common flux factor

$$f_\Gamma = f_{\Gamma f} = f_{\Gamma q}\,. \tag{6.42}$$

§6.5 Comparison with conventional renormalization

The previous analysis has shown that well-defined convergent and nonzero integrated physical quantities can be obtained in a point-charge-like steady state, thereby avoiding the problem of an infinite self-energy. Attention may here be called to Ryder[21] who has stressed that, despite the success of the conventional renormalization procedure, a more physically satisfactory way is needed concerning the infinite self-energy problem. Possibly the present theory could provide such an alternative, by tackling this problem in a more surveyable manner. The finite result due to a difference between two "infinities" in renormalization theory, i.e. by adding extra counter-terms to the Lagrangian, is then replaced by a finite result obtained from the product of an "infinity" with a "zero", as determined by the combination of the present divergent integrands with a shrinking characteristic radius.

As expressed by Eq. (6.16), the latter concept also has an impact on the question of Lorentz invariance of the electron radius. In the limit $\varepsilon = 0$ of a vanishing radius r_0 corresponding to a structureless mass point, the deductions of this chapter will thus in a formal way satisfy the requirement of such an invariance. At the same time the obtained solutions can also be applied to the physically relevant case of a very small but nonzero radius of a configuration having an internal structure.

§6.6 Variational analysis of the integrated charge

The elementary electronic charge has so far been considered as an independent and fundamental physical constant of nature, being determined by measurements only[84]. However, since it appears to represent the smallest quantum of free electric charge, the question can be raised whether there is a more profound reason for such a minimum charge to exist, possibly in terms of a quantized variational analysis.

The present theory can provide the basis for such an analysis. In a first attempt one would use a conventional procedure including Lagrange multipliers in searching for an extremum of the normalized charge q^* of Eq. (6.39), under the subsidiary quantum conditions (6.40)–(6.42) and (6.38). The available variables are then the amplitudes $a_{2\nu-1}$ and $a_{2\nu}$ of the polar function (6.2). Such an analysis has unfortunately been found to become quite complicated[83], partly due to its nonlinear character and a high degree of the resulting equations. But there is even a more serious difficulty which upsets such a conventional procedure. The latter namely applies only when there are well-defined and localized points of an extremum, in the form of a maximum or minimum or a saddle-point

in parameter space, but not when such single points are replaced by a flat plateau which has the effect of an infinite number of extremum points being distributed over the same space.

A plateau-like behaviour is in fact what occurs here[83], and an alternative approach therefore has to be elaborated. The analysis then proceeds by successively including an increasing number of amplitudes $(a_1, a_2, a_3, \ldots)$ which are being "swept" (scanned) across their entire range of variation. The flux factor (6.42) has at the same time to be determined in a self-consistent way through an iteration process. For each iteration the lowest occurring value of q^* can then be determined. Thereby both conditions (6.40) and (6.41) and the flux factors of Eqs. (6.38) and (6.41) include variable parameters. Thus the flux factor $f_{\Gamma f}$ of Eq. (6.41) does not become constant but varies with the amplitudes of the polar function (6.2) when there are magnetic islands which contribute to the magnetic flux. At a first sight this appears also to result in a complicated and work-consuming process. However, as demonstrated later in §6.6.2 and §6.6.3 on a flat plateau behaviour, this simplifies the corresponding iteration scheme and the physical interpretation of its results.

In the numerical analysis which follows, solutions with two real roots have always been found. Of these roots only that resulting in the lowest value of q^* will be treated in detail in the following parts of this chapter.

§6.6.1 General numerical results

As a first step the solutions for only two nonzero amplitudes, a_1 and a_2, are considered as obtained from conditions (6.40)–(6.42). Matching of the two flux factors of Eqs. (6.38) and (6.47) is then illustrated by Fig. 6.3 where the self-consistent value of the normalized charge becomes $q^* \simeq 1.01$. This value will, however, not turn out to be the lowest one obtained by means of the present variational analysis on a larger number of nonzero amplitudes.

In the next step four amplitudes (a_1, a_2, a_3, a_4) are included in the polar function (6.2). The normalized charge q^* can then be plotted as a function of the two amplitudes a_3 and a_4 which are swept across their entire range of variation, but for a fixed flux factor $f_\Gamma = f_{\Gamma q} = 1.82$. The result is shown in Fig. 6.4 for the lowest of the two roots obtained for q^*. In fact, the corresponding result of a self-consistent analysis which takes Eq. (6.42) into account, leads only to small modifications which hardly become visible on the scale of Fig. 6.4. From the figure is seen that there is a steep barrier in its upper part, from which q^* drops

down to a flat plateau being close to the level $q^* = 1$. The corresponding derivative of the magnetic flux (6.34) is plotted in Fig. 6.5 as a function of the polar angle θ, where positive values stand for a magnetic outflux through the spherical surface $\rho = \varepsilon$ indicated in Figs. 6.1 and 6.2. A similar behaviour is also found for the second root which yields a minimum plateau level at $q^* = 4.9$, thus being much higher than that obtained for the first root.

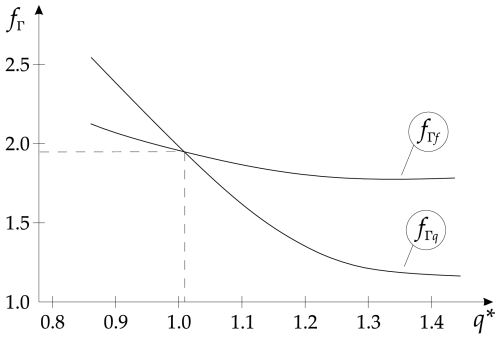

Figure 6.3: The self-consistent solution of the normalized charge q^* obtained through matching of the flux factors $f_{\Gamma q}$ and $f_{\Gamma f}$ in the case of only two nonzero amplitudes a_1 and a_2 of the polar function.

When further increasing the number of amplitudes, the results were still found to become plateau-like. The details of these deductions will be discussed in the coming subsections 6.6.2 and 6.6.3.

The multistep iteration process which leads to a self-consistent flux factor for the two independent relations (6.38) and (6.41) requires a rather high degree of accuracy, also being related to a determination of the zero points θ_1 and θ_2 of the derivative $\frac{d\Psi}{d\theta}$ in Figs. 6.2 and 6.5. This problem can be tackled more efficiently in terms of a special analysis restricted to the plateau regime, as shown in the next subsection.

§6.6.2 Asymptotic theory on the plateau regime

The plateau behaviour demonstrated by Fig. 6.4 and obtained from the numerical analysis can be taken as a basis for an asymptotic theory, being adapted to the limit of large moduli of the amplitudes in the polar function (6.2), i.e. for the behaviour at large distances from the origin $a_3 = a_4 = 0$ in Fig. 6.4. To include all points of large amplitudes which are contained within the plateau region far from the origin, we now restrict the range of the amplitudes through the condition

$$\frac{a_i}{k_i} = a_\infty \longrightarrow +\infty \qquad i = 3, 4, \ldots \tag{6.43}$$

Here k_i are scaling factors associated with each amplitude, and which in principle could become functions of the parameters which define the plateau region. Since the amplitudes a_1 and a_2 cannot vanish in this

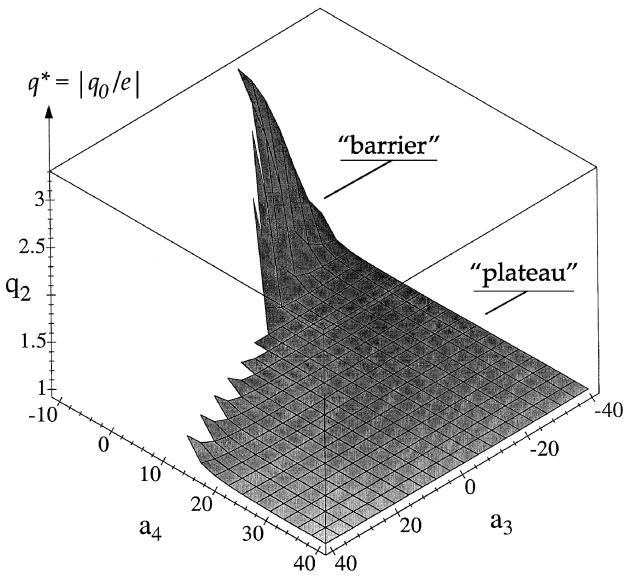

Figure 6.4: The normalized electron charge $q^* \equiv |q_0/e|$ as a function of the two amplitudes a_3 and a_4, for solutions satisfying the subsidiary quantum conditions for a fixed flux factor $f_\Gamma = f_{\Gamma q} = 1.82$, and being based on a polar function T having four amplitudes (a_1, a_2, a_3, a_4). The profile of q^* consists of a steep "barrier" in the upper part of the figure, and a flat "plateau" in the lower part. The plateau is close to the level $q^* = 1$. The figure only demonstrates the ranges of the real solutions of the first (lowest) root. The deviations of this profile from that obtained for the self-consistent solutions which obey condition (6.42) are hardly visible on the scale of the figure.

asymptotic limit, we introduce the new variables

$$x = \frac{a_1}{a_\infty}\,, \qquad y = \frac{a_2}{a_\infty}\,. \tag{6.44}$$

In the plateau region expression (6.2) can then be used to define a normalized asymptotic polar function

$$\bar{T} = \frac{T}{a_\infty} = x \sin\theta + y \cos 2\theta + \bar{T}_n\,, \tag{6.45}$$

where

$$\bar{T}_n = \sum_{\nu=3}^{n} \left\{ k_{2\nu-1} \sin\left[(2\nu-1)\,\theta\right] + k_{2\nu} \cos(2\nu\theta) \right\}. \tag{6.46}$$

Of particular interest to the following analysis is the case where the factors k_i are constants of order unity. In the four-amplitude geometry

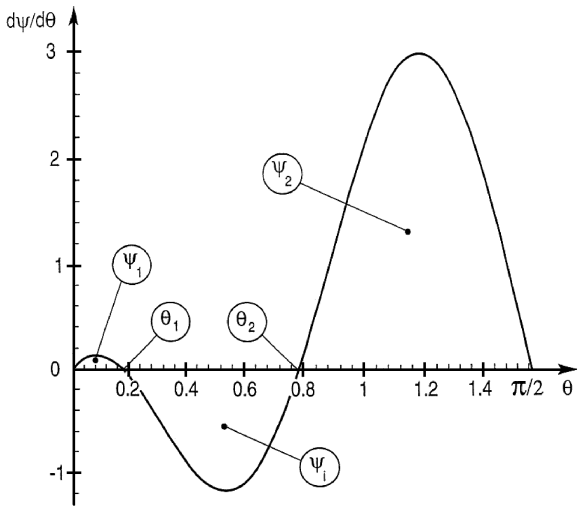

Figure 6.5: The normalized magnetic flux $d\Psi/d\theta$ per unit angle θ at the spherical surface $\rho = \varepsilon$. The sum of the areas Ψ_1 and Ψ_2 represents the total outflux, and the area $\Psi_i = \Psi_1 + \Psi_2 - \Psi_0$ is the counter-directed flux due to one magnetic island.

of Fig. 6.4 the analysis is then performed along lines within the plateau which at different angles originate from the point $a_3 = a_4 = 0$. With the asymptotic forms (6.43)–(6.46) inserted into expressions (5.26)–(5.30) and (6.34) the corresponding field quantities become

$$\bar{\tau}_\nu = \frac{\tau_\nu}{a_\infty} = \tau_\nu(\bar{T})\,, \tag{6.47}$$

$$\bar{A}_q = \frac{A_q}{a_\infty}\,, \qquad \bar{A}_M = \frac{A_M}{a_\infty}\,, \tag{6.48}$$

$$\bar{A}_m = \frac{A_m}{a_\infty^2}\,, \qquad \bar{A}_s = \frac{A_s}{a_\infty^2}\,, \tag{6.49}$$

$$\bar{A}_\Gamma = \frac{A_\Gamma(T)}{a_\infty} = A_\Gamma(\bar{T})\,, \tag{6.50}$$

$$\bar{\Psi} = \frac{\Psi(T)}{a_\infty} = \Psi(\bar{T})\,, \tag{6.51}$$

and

$$\bar{f}_{\Gamma f} = \frac{\left[2(\bar{\Psi}_1 + \bar{\Psi}_2) - \bar{\Psi}_0\right]}{\bar{\Psi}_0}\,. \tag{6.52}$$

The quantum conditions (6.39)–(6.41) further take the analogous

forms

$$\bar{q}^* = \left(\frac{f_0 \bar{A}_q^2}{\bar{A}_s} \right)^{1/2} = \left(\frac{f_0 \bar{A}_q}{8\pi \bar{f}_{\Gamma q} \bar{A}_\Gamma} \right)^{1/2} , \tag{6.53}$$

$$\frac{\bar{A}_M \bar{A}_m}{\bar{A}_q \bar{A}_s} = 1 + \delta_M \, , \tag{6.54}$$

$$8\pi \bar{f}_{\Gamma q} \bar{A}_\Gamma \bar{A}_q = \bar{A}_s \, , \tag{6.55}$$

where condition (6.42) still applies, with T of Eq. (6.2) being replaced by $\bar{T}$ of Eq. (6.45).

In this asymptotic limit the analysis becomes simplified, from a many-amplitude case to that of only two amplitudes defined by Eqs. (6.44). The reduced equations (6.43)–(6.55) also provide a better understanding of the plateau behaviour. The minimum values of $\bar{q}^*$ which result from these equations are thereby the same as those obtained from the more elaborate general analysis of §6.6.1.

The plateau analysis also suits an accurate numerical iteration process. Starting from the given values of the constants $f_0 \approx 137.036$ and $\delta_M \approx 0.00116$ defined by Eqs. (5.46) and (5.47), the following set of equations is considered. First, the ratio

$$h_0 = \frac{\bar{A}_m}{\bar{A}_s} \tag{6.56}$$

is introduced. The so far performed analysis has revealed this ratio to be of the order of unity, and to become a slow function of the parameters involved. This is understandable from the form of Eq. (6.25). Second, the condition (6.53) can be rewritten as

$$\bar{A}_q^2 = k_q \bar{A}_m \, , \qquad k_q = \frac{(\bar{q}^*)^2}{f_0 \, h_0} \, . \tag{6.57}$$

Third, condition (6.54) becomes

$$\bar{A}_M = k_M \bar{A}_q \, , \qquad k_M = \frac{(1 + \delta_M)}{h_0} \, . \tag{6.58}$$

Fourth, the flux factor has to be determined in a self-consistent way, by satisfying both Eq. (6.55) and Eq. (6.52). This implies that

$$\bar{f}_\Gamma = \frac{\bar{A}_s}{8\pi \bar{A}_\Gamma \bar{A}_q} = \frac{\left[2(\bar{\Psi}_1 + \bar{\Psi}_2) - \bar{\Psi}_0 \right]}{\bar{\Psi}_0} \, . \tag{6.59}$$

Fifth, the flux factor obtained from the last member of this equation

also has to be related to the normalized charge $\bar{q}^*$ when the iteration procedure converges.

With this set of equations the iteration procedure can be performed according to the following scheme:

- One first assumes some plausible initial values of q^* and h_0 which both are of the order of unity;
- With these values Eq. (6.58) becomes a linear relation between x and y;
- Solving for x by means of Eq. (6.58) and substituting the result into Eq. (6.57), a quadratic equation is obtained for y;
- The two roots obtained for y will at the end of the first iteration result in two values for the normalized charge (6.53). The one with the lowest q^* then represents the main line in the proceeding steps of the iteration procedure;
- With x and y thus being determined, all the quantities (6.48)–(6.51) are determined as well. This also applies to the two values of the flux factor which are obtained from the second and third members of Eq. (6.59). These values usually differ from each other, and their ratio converges towards unity first when a self-consistent solution is obtained after several iterations, as required by Eq. (6.59);
- The new values of $\bar{A}_q$ and $\bar{A}_\Gamma$ are further inserted into the last member of Eq. (6.53), but with the flux factor $\bar{f}_{\Gamma q}$ being replaced by $\bar{f}_{\Gamma f}$. This gives a new value of q^* to be inserted into a second step of iteration. The obtained values of $\bar{A}_m$ and $\bar{A}_s$ also define a new value of h_0 through Eq. (6.56), to be used in the second iteration;
- The process is repeated, until the two flux factors of Eq. (6.59) converge towards the same value. This yields the final minimum value q^*_m of the normalized charge for a given number of amplitudes of the polar function (6.2).

§ 6.6.3 Numerical analysis of the plateau region

The simplest case of only two amplitudes a_1 and a_2 has already been treated in § 6.6.1, thereby resulting in the value $q^* \simeq 1.01$. We now proceed to a larger number of nonzero amplitudes as follows:

- A detailed plateau analysis is first performed on the four-amplitude case, with its special sub-case of three amplitudes represented by the line $a_4 = 0$ in Fig. 6.4. The latter clearly demonstrates the

plateau behaviour and supports the theory of §6.6.2. With the definition (6.43) and introducing $k_3 = -\sin\alpha_p$ and $k_4 = \cos\alpha_p$, the angle α_p will describe the positions of a_3 and a_4 at long distances from the origin $a_3 = a_4 = 0$, i.e. along the perimeter of the plateau region in Fig. 6.4. The self-consistent minimum values of q^* have then been found to increase almost linearly from $q^* \simeq 0.969$ for $f_\Gamma \simeq 1.81$ in the three-amplitude case where $\alpha_p = \frac{\pi}{2}$, to $q^* \simeq 1.03$ for $f_\Gamma \simeq 1.69$ when $\alpha_p = -\frac{\pi}{4}$. Consequently, the plateau of Fig. 6.4 becomes slightly "warped", being locally partly below and partly above the level $q^* = 1$ for the self-consistent solutions obeying condition (6.42);

- For an increasing number of amplitudes, i.e. more than four, there is a similar plateau behaviour, and the flux function is also found to have a form being similar to that demonstrated by Fig. 6.5. Sweeping again the amplitude parameters at a fixed value $f_\Gamma = = f_{\Gamma q} = 1.82$ of the flux factor, there was hardly any detectable change in the plateau level[87]. As an example of a corresponding self-consistent analysis one obtains $q_m^* \simeq 1.1$ and $f_\Gamma \simeq 1.51$ for five amplitudes with $k_5 = +1$. Having instead $k_5 = -1$, one ends up into a "barrier" in hyperspace;
- That the minimum level is found to increase when including an extra variable amplitude is not in conflict with the principle of the variational analysis. This is due to the fact that any function q^* of the amplitudes in the hyperspace $(a_3, a_4, a_5, \ldots)$ can have minima in the form of "depressions" or "valleys" at points where some of these amplitudes vanish;
- This analysis thus indicates that the final minimum value of q^* is $q_m^* \simeq 0.969$, being obtained at the plateau in the three-amplitude case.

The flat plateau behaviour of q^* at an increasing number of included amplitudes of the expansion (6.45) can be understood as follows. The last member of Eq. (6.53) includes the ratio $\frac{A_q}{A_\Gamma}$. Inspection of Eqs. (6.27) and (6.32) shows that this ratio can be taken to stand for the ratio between the charge q_0 and the magnetic flux Γ_0. The latter is generated by the circulating current density (3.3) which is directly proportional to the charge density. Therefore the considered ratio does not depend on the total charge, but solely on the profile shape of the charge distribution in space. Consequently q^* is expected to have a plateau-like character, i.e. to become a rather slow function of the higher "multipole" terms in the expansion of Eq. (6.45).

§6.6.4 Proposals for quantum mechanical correction

The reason for the deviation of the deduced minimum charge from the experimentally determined value is not clear at this stage, but a quantum mechanical correction may offer one possibility for its removal. Due to the extremely small dimensions of the present configuration, the quantum conditions are also likely to have an influence in more than one respect. Here two speculative and preliminary proposals are made, possibly also to be combined with each other.

A successful quantum mechanical modification of the magnetic moment has earlier been made by Schwinger and Feynman[82], as given by Eq. (5.47). Without getting into the details of the advanced and work-consuming analysis which leads to this correction, it may here be proposed that also the magnetic flux and its related quantum condition (6.55) would then have to be modified into the form[85]

$$\tilde{f}_{\Gamma q} = \frac{\bar{A}_s}{8\pi \bar{A}_\Gamma \bar{A}_q}(1+\delta_\Gamma)\,, \qquad \delta_\Gamma = \frac{c_\Gamma}{f_0}\,, \tag{6.60}$$

where c_Γ is a so far unspecified constant. For this proposal to lead to an agreement with the experimental value $q^* = 1$, a modified self-consistency relation

$$\tilde{f}_{\Gamma q} = \bar{f}_{\Gamma f} \tag{6.61}$$

would have to be satisfied by $c_\Gamma \simeq (4\pi)^{1/2}$. This value is obtained from the three-amplitude case, within the limits of accuracy of the present numerical analysis.

The second proposal concerns the quantum mechanical fluctuations. It can thus be imagined that, at the scale of the present configuration, the amplitudes $(a_1, a_2, a_3, \ldots)$ would become subject to such fluctuations in time. As a result, the minimum value q_m^* could deviate from its quantum mechanical expectation value $<q_m^*>$. Since it has been found in §6.6.3 that q^* attains values at the plateau which are both below and above the level $q^* = 1$, the expectation value $<q_m^*>$ could be anticipated to come closer to the level $<q_m^*> = 1$, and possibly even be equal to it.

Provided that the deductions of §6.6.2 and 6.6.3 and the present proposals hold true, the elementary electric charge would no longer be an independent constant of nature, but becomes a deduced quantized concept which is determined by the velocity of light, Planck's constant, and the dielectric constant only.

The force balance later described in §6.8 will support these results and conclusions.

§6.7 A possible modification due to General Relativity

In the models of steady equilibria considered so far, one can conceive electromagnetic radiation to be forced to circulate along closed orbits around an axis of symmetry. This leads to the question whether these imagined curved orbits would introduce an additional effect due to General Relativity. The conventional theory by Maxwell, as well as the present extended theory, are based on Lorentz invariance in Euclidian geometry. The attempts to unify electromagnetism and gravity imply, however, that one has to abandon Euclidian geometry and proceed to a curved representation of space-time, in the sense of General Relativity.

In this subchapter a somewhat speculative and simplified approach will be made on a possibly appearing modification, as being caused by the forced circulation around the axis of symmetry in the electron model. The effect of the circulation is then imagined to be "inverted", such that the forced curved orbit gives rise to an equivalent gravitation field which, in its turn, modifies the balance represented by Eq. (5.1). In a first approximation the so far established Lorentz invariant basic equations then also have to be modified by a superimposed correction due to General Relativity. Such a procedure is, of course, not completely rigorous and requires in any case the correction to remain small, but the purpose of the approach is merely to estimate the order of magnitude of the appearing modification. A survey of the analysis will be given here, the details of which are described elsewhere[9].

§6.7.1 The deflection of light and its equivalent force

According to the theory of General Relativity, the deflection of light by a mass m_g becomes determined by the curvature of space being caused by the associated gravitational field. Light rays which are localized to the plane $\theta = \frac{\pi}{2}$ will then be deflected according to the equation[86]

$$\frac{d^2 W_d}{d\varphi^2} + W_d = \frac{3 W_d^2 G_g m_g}{c^2} \,, \tag{6.62}$$

where $W_d = \frac{1}{r}$ and G_g is the constant of gravitation. In the special case of a circular path the first term of this equation vanishes and

$$r_g = \frac{3 G_g m_g}{c^2} \tag{6.63}$$

becomes the radius of the circular geodesic orbit being associated with the equivalent mass m_g.

In the present case the electron mass m_0 of Eq. (5.18) is easily shown to generate a far too small gravitation field to cause a deflection into

the circular path of the electron model[9]. Such a path is instead imposed by the forced circulation around the axis of symmetry. We therefore "reverse" the present effect due to General Relativity by considering m_g to be the equivalent mass which is the cause of the circular motion. The equivalent gravitation force is then estimated as follows.

Combining the radius (6.63) with the mass density $\mu_g = \frac{w_s}{c^2}$ of the electromagnetic field, the equivalent local gravitation force per unit volume in the radial direction becomes

$$f_g \simeq \frac{G_g m_g \mu_g}{r_g^2} = \frac{\mu_g c^2}{3 r_g} \,. \tag{6.64}$$

Apart from the factor $\frac{1}{3}$ this force can as well be interpreted as the result of a centrifugal acceleration which generates a force in the outward radial direction. This is the equivalent extra force to be included into the set of modified field equations.

The force (6.64) is now compared to the radial electrostatic force

$$f_{\scriptscriptstyle E} = \bar{\rho}\, E_r \tag{6.65}$$

at the given radius $r = r_g$. With the profile factors c_g and c_q of the mass and charge density distributions, the latter become

$$\mu_g \simeq \frac{3 c_g m_0}{4\pi r_g^3} \tag{6.66}$$

and

$$\bar{\rho} \simeq \frac{3 c_q q_0}{4\pi r_g^3} = \varepsilon_0 (\mathrm{div}\, \mathbf{E}) \simeq \frac{\varepsilon_0 E_r}{r_g} \,. \tag{6.67}$$

This yields

$$f_{\scriptscriptstyle E} \simeq \frac{9 c_q^2 q_0^2}{16\pi^2 \varepsilon_0 r_g^5} \tag{6.68}$$

and a local force ratio

$$\frac{f_g}{f_{\scriptscriptstyle E}} \simeq \frac{4\pi\varepsilon_0 c_g c^2}{9 c_q^2 q_0^2}\, m_0 r_g \,. \tag{6.69}$$

In a first approximation the ratio $\frac{c_g}{c_q^2}$ of the profile factors can be taken to be of order unity. With r_g approximately equal to the characteristic radius r_0 of the configuration, the average force ratio (6.69) then reduces for $q_0 = e$ to

$$\delta_g \equiv \frac{<f_g>}{<f_{\scriptscriptstyle E}>} \simeq \frac{4\pi\varepsilon_0 c^2}{9e^2}\, m_0 r_0 \simeq 10^{44}\, m_0 r_0 \tag{6.70}$$

which decreases with a decreasing radius r_0.

§6.7.2 Modification of the basic equations

A crude first-order estimate of the effect of the equivalent "centrifugal force" f_g of Eq. (6.64) is now made in replacing the steady-state momentum equation (3.16) by the form

$$f_B \simeq -f_E - f_g + |\mathrm{div}^2 \mathbf{S}| \tag{6.71}$$

with

$$f_B = |\bar{\rho}\,\mathbf{C} \times \mathbf{B}|\,, \qquad f_E = |\bar{\rho}\,\mathbf{E}|\,. \tag{6.72}$$

Here f_E and f_g are directed out of the body of the electron, whereas f_B plays the role of an inward directed "confining" magnetic force, as later being explained in detail in §6.8. This implies that part of the magnetic force now has to balance the force (6.64), and the rest of the same magnetic force should then be in equilibrium with the additional forces in Eq. (6.71). We further assume the terms of the steady-state equation (3.16) to be of the same order of magnitude, as obtained from a simple dimensional analysis. The final result of this crude estimate is then that the effect of the force (6.64) can be represented by a reduced magnetic force $(1-\delta_g)f_B$ in the unmodified analysis of the previous §6.1–6.6. A corresponding modification of the field equations is then obtained in replacing the vector potential $\mathbf{A} = (0, 0, A)$ introduced at the beginning of Chapter 5 by the modified potential

$$\mathbf{A}^* = (0, 0, A^*)\,, \qquad A^* = (1-\delta_g)A \equiv A + \tilde{A}\,. \tag{6.73}$$

The linear dependence on δ_g is due to the restriction to a small modification where $0 < \delta_g \ll 1$, whenever this comes out to be the case. There is then a modified generating function

$$F^* = F + \delta_g \tilde{F} = (1-\delta_g)\,CA - \phi \equiv G_0 G^* \tag{6.74}$$

with the normalized form

$$G^* = G + \delta_g \tilde{G}\,, \qquad \tilde{G} = -\frac{CA}{G_0} = (\sin^2\theta)\,DG \tag{6.75}$$

and modified forms $(A^*, \phi^*, \bar{\rho}^*)$ being obtained from expressions which are analogous to Eqs. (5.7)–(5.9). In its turn, this leads to modified expressions $(q_0^*, M_0^*, m_0^*, s_0^*)$ for the integrated quantities (5.16)–(5.19) where the associated normalized integrals are given by

$$J_k^* = \int_{\rho_k}^{\infty} \int_0^{\pi} I_k^*\, d\rho\, d\theta\,, \qquad I_k^* = I_k + \delta_g \tilde{I}_k\,. \tag{6.76}$$

The modifications $\tilde{I}_k$ of the integrands then become

$$\tilde{I}_q = \tilde{f}\,, \qquad \tilde{I}_M = \rho\, s\,(f + \tilde{f})\,, \tag{6.77}$$

$$\tilde{I}_m = f\,(\tilde{g} + \tilde{h}) + \tilde{f}_g\,, \quad \tilde{I}_s = \rho\, s\,[f(\tilde{g} + \tilde{h}) + \tilde{f}_g]\,, \tag{6.78}$$

where

$$\tilde{f} = -sD(1 + s^2 D)(s^2 DG)\,, \tag{6.79}$$

$$\tilde{g} = -(1 + 2s^2 D)(s^2 DG)\,, \tag{6.80}$$

$$\tilde{h} = -2s^2 DG\,, \tag{6.81}$$

$s \equiv \sin\theta$, and I_k as well as f and g have been defined earlier in Eqs. (5.16)–(5.19), (5.14) and (5.15).

§6.7.3 Estimated magnitude of the modification

In a first estimation of the order of magnitude of the present modification we now refer to an earlier simplified analysis which has been based on the form

$$T = -1 + \bar{N}(\sin\theta)^{\alpha} \tag{6.82}$$

of the polar part of the generating function[9]. Here the parameters $\bar{N}$ and α are chosen such as to satisfy the quantum conditions (5.45)–(5.47) and the condition $q^* = 1$ in the unmodified case. In numerical computations by Scheffel[87,9] the deviations of the normalized charge and of the magnetic moment were studied as functions of the ratio (6.70). It is then found that a modification of the order of that introduced by the correction δ_M in Eq. (5.47) can be caused at a characteristic electron radius of about 10^{-19} meters. For the modification not to interfere with the imposed condition (5.47), the electron radius would thus have to be substantially smaller than this value. Such an estimation should be compared to a statement by Johnson[88] according to which leptons and quarks are thought to be no larger than 10^{-17} meters.

A preliminary proposal can finally be made here for the electron radius to be confined between two limits:

- Its upper limit is somewhat higher that 10^{-19} meters, as being given by the value for which the modification due to the present effect by General Relativity cannot be neglected. Above this limit the solutions deduced in §6.1–6.6 do not apply.
- Its lower limit is defined by the smallest physically relevant linear dimension, as being represented by the Planck length which is equal to about 4×10^{-35} meters.

§6.8 Force balance of the electron model

The fundamental description of a charged particle in conventional theory is deficient in several respects. Thus, an equilibrium cannot be maintained by the classical electrostatic forces, but has been assumed to require forces of a nonelectromagnetic character to be present[23–25]. In other words, the electron would otherwise "explode" under the action of its self-charge.

Here it will be shown that a steady electromagnetic equilibrium can under certain conditions be established by the present extended theory. The underlying physical mechanism will first be demonstrated by some simple examples, and then be followed by its application to the present axisymmetric electron model in the plateau region.

§6.8.1 Simple examples on electromagnetic confinement

First consider two parallel line charges in empty space, both with the charge density $\bar{\rho}$ per unit length and being separated at the distance r. They are then subject to the electrostatic repulsion force

$$f_E = \frac{\bar{\rho}^2}{2\pi\varepsilon_0 r} \tag{6.83}$$

per unit length. But in the case of the present theory, these line charges also become parallel line currents of the strength

$$J = c\,\bar{\rho} \tag{6.84}$$

according to Eq. (3.3) when the velocity vector $\mathbf{C}$ is directed along z of a frame (r, φ, z). Each line current thereby generates a magnetic field of the strength

$$B = \frac{\mu_0 J}{2\pi r} \tag{6.85}$$

at the position of the opposite line current. This results in an attractive force

$$f_B = -JB = -\frac{\mu_0 c^2 \bar{\rho}^2}{2\pi r} = -f_E \tag{6.86}$$

between the line currents. Thus, the net mutual force vanishes, and there is an electromagnetic equilibrium.

As a next example we consider a straight and circularly symmetric configuration where there is a constant charge density $\bar{\rho}$ per unit volume within a region $0 \leqslant r \leqslant a$. Inside this region there is an electrostatic radial force

$$f_E = \frac{\bar{\rho}^2 r}{2\varepsilon_0} \tag{6.87}$$

per unit volume in the outward direction. At the same time there is a current density according to Eq. (3.3), with $\mathbf{C}$ in the axial direction. This generates a magnetic field in the φ direction, and a corresponding magnetostatic force

$$f_{B} = -\frac{\mu_0 c^2 \bar{\rho}^2 r}{2} = -f_{E}\,. \tag{6.88}$$

Also in this example there is thus a steady electromagnetic equilibrium in which the outward directed electrostatic expansion force is balanced by an inward directed magnetostatic "pinch" force.

When proceeding from the straight geometry to a curvilinear configuration, such as that in spherical and axial symmetry, a local balance cannot generally be realized, but only under certain conditions. This is due to the fact that, apart from straight cylindrical geometry, the equipotential surfaces of the electrostatic potential ϕ do not generally coincide with the magnetic field lines determined by the magnetic vector potential $\mathbf{A}$.

§6.8.2 The present electron model

We now turn to the momentum balance of the present axisymmetric electron model in a frame (r, θ, φ) of spherical coordinates. The integral form of the equivalent forces is in a steady state given by Eqs. (3.17) and (3.18), on the form

$$\mathbf{F} = \mathbf{F}_e + \mathbf{F}_m = \int \bar{\rho}\,(\mathbf{E} + \mathbf{C} \times \mathbf{B})\, dV\,. \tag{6.89}$$

When first considering the polar direction represented by the angle θ, it is readily seen that the corresponding integrated force F_θ vanishes due to the axial symmetry.

Turning then to the radial direction, the earlier obtained results of Eqs. (5.1)–(5.9) and (5.21) are applied to obtain the radial force component[83,85]

$$F_r = -2\pi\varepsilon_0 G_0^2 \iint \big[DG + D(s^2 DG)\big] \cdot \left[\frac{\partial G}{\partial \rho} - \frac{1}{\rho}\, s^2 DG\right] \rho^2 s\, d\rho\, d\theta\,, \tag{6.90}$$

where $s = \sin\theta$. For the point-charge-like model of Eqs. (6.1)–(6.2) with $G = RT$, $\gamma \to 2$ and $R \to \frac{1}{\rho^2}$ at small ρ, we then have

$$\rho^2 DG = D_\theta T - 2T \tag{6.91}$$

to be inserted into the integrand of expression (6.90). The latter can then be represented by the form

$$F_r = I_+ - I_-\,, \tag{6.92}$$

where I_+ and I_- are the positive and negative contributions to the radial force F_r.

Consequently, there will arise an integrated radial force balance in the form of electromagnetic confinement when $I_+ = I_-$. This applies to very small but nonzero values of the characteristic radius (6.16), i.e. when not proceeding all the way to the structureless point case where $r_0 = 0$.

The integrals (6.90) and (6.92) are now applied to the plateau region of Fig. 6.4 and its properties being described in §6.6.3. We thus vary the angle α_p related to the positions at the perimeter of the plateau region, and to the associated values of the normalized charge q^*. It is then found that the ratio $\frac{I_+}{I_-}$ decreases from $\frac{I_+}{I_-} = 1.27$ at $q^* = 0.98$ to $\frac{I_+}{I_-} = 0.37$ at $q^* = 1.01$, thus passing the equilibrium point $\frac{I_+}{I_-} = 1$ at $q^* \simeq 0.988$, as shown in Fig. 6.6. The remaining degrees of freedom being available in the parameter ranges of the plateau have then been used up by the condition of a radially balanced equilibrium.

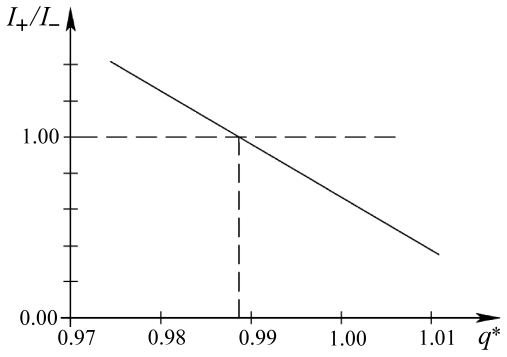

Figure 6.6: The ratio I_+/I_- between the positive and negative contributions to the integrated radial force of the electron model in the plateau region, as a function of the normalized charge q^*. The figure applies to the case of four amplitude factors. The level $I_+/I_- = 1$ represents a fully balanced equilibrium. It occurs at $q^* \simeq 0.988$ where the deduced charge only deviates by about one percent from the experimentally determined elementary charge.

To sum up, the variational analysis of §6.6 has resulted in a plateau region at the perimeter of which the normalized charge q^* varies in the range $0.97 < q^* < 1.03$, and where the lowest possible value $q^* \simeq 0.97$ is obtained in the three-amplitude case. However, this latter value does not satisfy the requirement of a radial force balance. Such a balance is on the other hand realized within the plateau region, but at the value $q^* \simeq 0.99$, i.e. where the deduced charge only deviates by about one percent from the experimental value of the elementary charge. To compensate for this deviation by the proposed quantum mechanical correction given by Eq. (6.60) of §6.6.4, the constant $c_{\rm r}$ would then have to be of the order of unity.

At the extremely small dimensions of the present point-charge-like model, it should become justified to consider the integrated force balance instead of its localized counterpart. The quantum mechanical wave nature is then expected to have a smoothing and overlapping effect on the local variations within the configuration. In addition to this, a requirement of the local electrodynamic force in Eq. (6.89) to vanish identically, would result in the unacceptable situation of an overdetermined system of basic equations.

The obtained deviation of q^* by about one percent only from the value $q^* = 1$ can, in itself, be interpreted as an experimental support of the present theory. This is particularly the case as the deduced result has been obtained from two independent aspects, namely the minimization of the charge by a variational analysis, and the determination of the charge from the requirement of a radial balance of forces.

It has finally to be observed that slightly higher values of q^* have been obtained for the expansion (6.46) of the polar function with more than four amplitude factors[83,85]. However, if there would exist a balance of forces at a higher corresponding value of q^*, then the solution of q^* in the four-amplitude case of Fig. 6.6 still corresponds to the lowest possible q^* for an average radial force balance.

The present considerations of the integrated (total) forces, performed instead of a treatment on their local parts, are in full analogy with the earlier deductions of the integrated charge, angular momentum, magnetic moment, and magnetic flux.

This chapter is terminated in observing that the present deductions, leading to an integrated charge being close to its experimental value, can be taken as an indirect support and deduction of the correct Landé factor of Eqs. (5.47) and (6.40), as well as of the factor involved in the quantum condition (5.50) of the magnetic flux. A change of the order of two in either of these factors would thus lead to a substantial deviation of the deduced charge from the experimental value.

Chapter 7

A MODEL OF THE NEUTRINO

The electrically neutral steady states described in § 5.2 will in this chapter be used as the basis for a model of the neutrino. In principle these states include all the three alternatives Aa, Ab, and Bb of Table 5.1, but since there is little difference in the outcome of cases Aa and Ab, the analysis will be limited to Aa and Bb. The model to be developed here will at least be seen to reproduce some of the basic features of the neutrino. Since the analysis is restricted to the steady state of a particle-shaped configuration, thus being at rest, it includes the concept of a nonzero rest mass. The existence of such a mass appears to be supported by the observed neutrino oscillations. At this stage it can on the other hand not be expected that the present theory should be able to describe the occurrence of more detailed and subtle properties such as the various types of propagating neutrinos, neutrino oscillations, and the question of the missing right-hand neutrino. Such questions have to be postponed to a more advanced treatment based on a fully developed quantum field theory.

The basic theory of electrically neutral particle-shaped states has already been elaborated in Chapter 5, including general expressions for the integrated field quantities and the symmetry properties. This implies that we can now turn to the details of two possible models derived from the corresponding choices of the generating function[89].

§ 7.1 Basic relations with a convergent generating function

In the earlier performed analysis[9] one model has been elaborated which arises from a convergent radial part and a top-bottom symmetrical polar part of the generating function of case Aa in Table 5.1, as given by

$$G = R \cdot T\,, \qquad R = \rho^{\gamma} e^{-\rho}, \qquad T = (\sin\theta)^{\alpha}, \tag{7.1}$$

where $\gamma \gg \alpha \gg 1$. We insert the function (7.1) into the forms (5.22)–(5.30), and combine the obtained result with Eqs. (5.18)–(5.20), the relations

$$C_{2n} = \int_0^{\pi} (\sin\theta)^{2n}\, d\theta = \pi\, \frac{1 \cdot 3 \cdot 5 \cdot \ldots (2n-1)}{2 \cdot 4 \cdot 6 \cdot \ldots 2n}\,, \tag{7.2}$$

$$C_{2n+1} = \int_0^{\pi} (\sin\theta)^{2n+1}\, d\theta = 2 \cdot \frac{2 \cdot 4 \cdot 6 \cdot \ldots 2n}{3 \cdot 5 \cdot 7 \cdot \ldots (2n+1)}\,, \tag{7.3}$$

$$\frac{C_{2n+2}}{C_{2n}} = \frac{(2n+1)}{(2n+2)}\,, \tag{7.4}$$

and the Euler integral

$$J_0 = \int_0^{\infty} \rho^{2\gamma}\, e^{-2\rho}\, d\rho = \left(\frac{1}{2^{2\gamma+1}}\right) \Gamma(2\gamma - 1)\,. \tag{7.5}$$

Expressions are then obtained for the normalized integrals J_m and J_s which include a large number of terms with various powers of γ and α. But in the limit $\gamma \gg \alpha \gg 1$ the ratio $\frac{J_m}{J_s}$ reduces to the simple form[9]

$$\frac{J_m}{J_s} = \frac{15}{38\gamma}\,. \tag{7.6}$$

At increasing values of ρ the radial part R in Eq. (7.1) first increases to a maximum at $\rho = \hat{\rho} = \frac{\hat{r}}{r_0} = \gamma$, after which it drops steeply towards zero at large ρ. Therefore $\hat{r} = \gamma r_0$ can in this case be considered as an effective radius of the configuration. By combining the ratio $\frac{m_0}{|s_0|}$ of expressions (5.18) and (5.19) with Eq. (7.6) and the quantum condition (5.45) of the angular momentum, the final result becomes

$$m_0 \hat{r} = m_0 \gamma r_0 = \frac{15h}{152\pi c} \simeq 7{\times}10^{-44}\ [\mathrm{kg \cdot m}]. \tag{7.7}$$

§ 7.2 Basic relations with a divergent generating function

We now turn to case Ab in Table 5.1 where the generating function has a divergent radial part, and a polar part with top-bottom antisymmetry.

A radial part is adopted here which has the same form (6.1) as that of the electron model in § 6.1. Then the earlier discussion on the included factors also applies here. The forthcoming results in this chapter will be seen not to depend explicitly on the radial parameter γ. When $r = \rho r_0$ increases monotonically from $r = 0$, the radial part of Eq. (6.1) decreases from a high level, down to $R = e^{-1}$ at $r = r_0$, and then further to very small values when $r \gg r_0$. Thus $\hat{r} = r_0$ can here be taken as an effective radius of the configuration.

In an electrically neutral state the expansion (6.2) of the polar part has now to be replaced by one of general top-bottom antisymmetry with respect to the equatorial plane. As already shown in § 5.2, this leads to a state having vanishing charge and magnetic moment, but nonzero mass and angular momentum.

§ 7.2.1 Conditions for a small effective radius

For a divergent radial part (6.1) the contributions to the integrals (5.20) at small lower limits ρ_k originate from the ranges close to these limits, as already pointed out in §6.2. Also here the analysis is analogous to that of the electron model. This implies that $I_{m\rho}$ and $I_{s\rho}$ are still obtained from Eq. (6.7), that Eqs. (6.10), (6.11) and (6.14) will apply, and that Eq. (6.15) refers to $k = m, s$. Insertion of the obtained forms into Eqs. (5.18) and (5.19) then yields

$$m_0 = \pi \frac{\varepsilon_0}{c^2} r_0 G_0^2 \frac{1}{2\gamma - 1} \frac{1}{\rho_m^{2\gamma-1}} J_{m\theta} , \tag{7.8}$$

$$s_0 = \pi \frac{\varepsilon_0 C}{c^2} r_0 G_0^2 \frac{1}{2(\gamma - 1)} \frac{1}{\rho_s^{2(\gamma-1)}} J_{s\theta} . \tag{7.9}$$

To obtain nonzero and finite values of the mass m_0 and the angular momentum s_0 at decreasing radial limits ρ_m and ρ_s we now introduce a shrinking effective radius $\hat{r}$ and a shrinking amplitude factor G_0 as defined by

$$\hat{r} = r_0 = c_r \cdot \varepsilon , \qquad G_0 = c_G \cdot \varepsilon^{\beta}, \tag{7.10}$$

where c_r, c_G, and β are all positive constants and $0 < \varepsilon \ll 1$ with ε as a smallness parameter. Also here a situation is excluded where ε, ρ_m, and ρ_s all become exactly equal to zero in the unphysical case of a point mass with no internal structure. With the introduction of Eqs. (7.10), expressions (7.8) and (7.9) take the forms

$$m_0 = \pi \frac{\varepsilon_0}{c^2} c_r c_G^2 \frac{1}{2\gamma - 1} J_{m\theta} \frac{\varepsilon^{1+2\beta}}{\rho_m^{2\gamma-1}} , \tag{7.11}$$

$$s_0 = \pi \frac{\varepsilon_0 C}{c^2} c_r^2 c_G^2 \frac{1}{2(\gamma - 1)} J_{s\theta} \frac{\varepsilon^{2(1+\beta)}}{\rho_s^{2(\gamma-1)}} . \tag{7.12}$$

For nonzero and finite values of m_0 and s_0 it is then required that

$$\rho_m = \varepsilon^{(1+2\beta)/(2\gamma-1)}, \qquad \rho_s = \varepsilon^{(1+\beta)/(\gamma-1)}. \tag{7.13}$$

§ 7.2.2 Quantization of the angular momentum

With the quantum condition (5.45) on the angular momentum, Eqs. (7.8)–(7.13) combine to

$$\frac{m_0}{|s_0|} = \frac{4\pi m_0}{h} = \frac{2(\gamma - 1) J_{m\theta}}{c c_r (2\gamma - 1) J_{s\theta}} . \tag{7.14}$$

Introducing the effective radius $\hat{r}$ this further yields

$$m_0\,\hat{r} = \frac{h}{2\pi c}\,\frac{\gamma-1}{2\gamma-1}\,\frac{J_{m\theta}}{J_{s\theta}}\,\varepsilon\,. \tag{7.15}$$

The ratio $\frac{J_{m\theta}}{J_{s\theta}}$ is expected to become a slow function of the profile shapes of $T(\theta)$ and $I_{m\theta}$, thereby being of the order of unity. As an example, if $I_{m\theta}$ would become constant in the interval $0\leqslant\theta\leqslant\pi$, this would result in $\frac{J_{m\theta}}{J_{s\theta}}=\frac{\pi}{2}$, whereas a strongly peaked profile at $\theta=\frac{\pi}{2}$ gives $\frac{J_{m\theta}}{J_{s\theta}}=1$. For $I_{m\theta}=const(\sin\theta)$ we would further have $\frac{J_{m\theta}}{J_{s\theta}}=\frac{4}{\pi}$. Somewhat different ratios are expected to arise when $I_{m\theta}$ is both positive and negative within the same interval.

An additional specific example can be given for $\gamma=3$ and $\beta=\frac{3}{2}$ where Eqs. (7.13) result in

$$\rho_m = \varepsilon^{4/5}, \qquad \rho_s = \varepsilon^{5/4}, \tag{7.16}$$

i.e. where ρ_m and ρ_s decrease nearly linearly with ε. Then the simple top-bottom antisymmetric form $T=\cos\theta$ gives rise to the integrands

$$I_{m\theta} = \left[6\cos^2\theta - 21\cos^4\theta + 18\cos^6\theta\right](\sin\theta) = \frac{I_{s\theta}}{\sin\theta}\,, \tag{7.17}$$

which are integrated to $J_{m\theta}\simeq 0.743$, $J_{s\theta}\simeq 0.441$, and $\frac{J_{m\theta}}{J_{s\theta}}\simeq 1.686$. We observe that $I_{m\theta}$ then becomes negative within parts of the interval $0\leqslant\theta\leqslant\pi$.

Consequently, relation (7.15) can in a first approximation be written as

$$m_0\,\hat{r} \simeq 2\times 10^{-43}\,\varepsilon\ [\mathrm{kg\cdot m}]. \tag{7.18}$$

§ 7.3 Mass and effective radius

The present steady-state configurations essentially become confined to a limited region of space near the origin. Thereby the corresponding effective radius $\hat{r}$ can become very small. It is important that no artificial boundaries have to be introduced in space to define such a geometry, and that the integrated solutions become finite and nonzero. This also applies to the angular momentum (5.19) which is related to the integral J_s of Eq. (5.20). Consequently, it is justified to quantize this result according to Eq. (5.45).

If the features of the present model are to be consistent with current experiments, the mass m_0 has to be reconcilable with obtained data. The best ones available at present for the upper bounds of the mass are 3.9 to 5.6 eV for the electron-neutrino, 170 keV for the muon-neutrino,

and 18.2 MeV for the tauon-neutrino[90]. These values correspond to about 8.4×10^{-36}, 3.0×10^{-31}, and 3.2×10^{-29} kg, respectively.

The neutrino can travel as easily through the Earth as a bullet through a bank of fog[91]. In this way it has to penetrate solid matter consisting of nucleons, each with a radius of about $r_N = 6\times10^{-15}$ meters[92]. The models of Sections 7.1 and 7.2 will now be compared to this fact. Then very small as well as very large ratios $\frac{\hat{r}}{r_N}$ are expected to result in a weak interaction between the neutrino and solid matter.

The effective radii which appear in Eqs. (7.7) and (7.18) can be taken as measures of the corresponding cross sections. This holds also for a neutrino propagating at a velocity near that of light, because there is no Lorentz contraction in the direction being perpendicular to the motion.

§ 7.3.1 Radius with a convergent generating function

We first turn to the result (7.7). The ratio $\frac{\hat{r}}{r_N}$ between the effective neutrino radius and the nucleon radius is estimated for the given upper bounds of the neutrino rest mass. This results in ratios of about 10^6, 40, and 0.4 for the electron-neutrino, the muon-neutrino, and the tauon-neutrino.

Concerning the large estimated ratio for the electron-neutrino, the corresponding interaction is then expected to take place between the short-range nucleon field as a whole on one hand, and a very small part of the neutrino field on the other. If this small influence on the neutrino field by a nucleon impact could "heal" itself by a restoring effect or by quantum mechanical tunneling, then the effective interaction would become very weak. This would also apply to impacts with the electrons being present in the matter structure, since these have an extremely small radius. If such an imagined interaction becomes relevant, the neutrino would represent the "fog" and the matter particles the "bullet".

The values of $\frac{\hat{r}}{r_N}$ for the muon-neutrino and the tauon-neutrino are on the other hand of order unity, and the neutrino mean free paths would thus become comparatively short when being based on relation (7.7).

§ 7.3.2 Radius with a divergent generating function

According to relation (7.18) the upper bounds of the rest mass will instead correspond to ratios $\frac{\hat{r}}{r_N}$ of about $4\times10^6\,\varepsilon$, $100\,\varepsilon$, and ε for the electron-neutrino, muon-neutrino and tauon-neutrino. These ratios can then become small for all neutrino types when ε becomes very small. In such a case the neutrino would instead play the role of the "bullet" and the nucleon that of the "fog".

In the interaction with an electron having the effective radius r_e the ratio $\frac{\hat{r}}{r_e}$ could come out either to be much larger or much smaller than unity. In both cases the interaction with the neutrino is expected to become weak, provided that it would only take place in the ways just being imagined for the neutrino interaction with a nucleon.

§ 7.4 The integrated force balance

Even if there does not arise any net electric charge in the present neutrino model, there is still a nonzero local volume force $\bar{\rho}\,(\mathbf{E}+\mathbf{C}\times\mathbf{B})$. To attain the state of an integrated force balance, one can proceed in a way being analogous to that described in § 6.8.2 for the electron model. The polar part $T(\theta)$ of the generating function would then have to include an additional free parameter, to be chosen such as to make the integrated radial volume force vanish. A corresponding detailed analysis will not be present here.

§ 7.5 Conclusions on the neutrino model

The present analysis should be taken as a first approach to a neutrino model. It gives in any case a correct picture of some of the basic features of the neutrino, in having a vanishing total electric charge and magnetic moment, a nonzero angular momentum with two spin directions, and a very small rest mass. The two cases of convergent and divergent radial parts of the generating function can further be combined to provide the possibility of a very weak interaction with solid matter. However, the exact magnitude of this interaction is still an open question.

In analogy with the discussion in Chapter 6 on a modification due to General Relativity, there is also here an equivalent gravitational effect which modifies the electric and magnetic force balance. For the model of § 7.3.2 with a divergent generating function there is then two radial limits being analogous to those proposed at the end of § 6.7.3.

Chapter 8

PLANE WAVES

Because of their relative simplicity, plane waves provide a convenient first demonstration of the wave types defined in § 4.2. In this chapter their features will be studied, without imposing quantum conditions. An application is further given on total reflection at the vacuum interface of a dissipative medium.

§ 8.1 The wave types

Plane waves are now considered having a constant velocity vector $\mathbf{C}$, and where any field component Q has the form

$$Q\,(x,y,z,t) \equiv Q_0\, e^{i\Theta}, \qquad \Theta = -\omega t + \mathbf{k}\cdot\mathbf{r}\,, \tag{8.1}$$

Here ω and $\mathbf{k} = (k_x, k_y, k_z)$ are the frequency and wave number in a rectangular frame with $\mathbf{r} = (x, y, z)$. Eqs. (3.6)–(3.10) then yield

$$c^2\mathbf{k}\times\mathbf{B} = (\mathbf{k}\cdot\mathbf{E})\,\mathbf{C} - \omega\mathbf{E}\,, \tag{8.2}$$

$$\omega\mathbf{B} = \mathbf{k}\times\mathbf{E}\,. \tag{8.3}$$

With $\mathbf{k}$ chosen in the z direction and $\mathbf{C}$ located in the plane perpendicular to $\mathbf{B}$, these types are illustrated as follows:

- When $\mathbf{k}\cdot\mathbf{E} = 0$ and $\mathbf{k}\times\mathbf{E} \neq 0$ there is a conventional electromagnetic (EM) wave with a magnetic field according to Eq. (8.3). The dispersion relation becomes

  $$\omega = \pm kc \tag{8.4}$$

  and the phase and group velocities are

  $$v_p = \pm c\,, \qquad \mathbf{v}_g = \pm\frac{c\mathbf{k}}{k}\,, \qquad k \equiv |\mathbf{k}|\,. \tag{8.5}$$

  All electric and magnetic field components are perpendicular to the direction of propagation which is along the wave normal;

- When $\mathbf{k}\cdot\mathbf{E} \neq 0$ and $\mathbf{k}\times\mathbf{E} = 0$ there is a purely longitudinal electric space-charge (S) wave having no magnetic field. Thus $\mathbf{C}\times\mathbf{E} = 0$ and $\mathbf{k}\times\mathbf{C} = 0$ due to Eqs. (8.2) and (8.3). The dispersion relation and the phase and group velocities are the same as in Eqs. (8.4) and (8.5) for the EM wave;

- When both $\mathbf{k}\cdot\mathbf{E}\neq 0$ and $\mathbf{k}\times\mathbf{E}\neq 0$ there is a nontransverse electromagnetic space-charge (EMS) wave with a magnetic field due to Eq. (8.3). This is the mode of main interest to this context. Here $\mathbf{k}\times\mathbf{C}$ differs from zero, and Eqs. (8.2) and (8.3) combine to

$$(\omega^2-k^2c^2)\,\mathbf{E}+(\mathbf{k}\cdot\mathbf{E})\,\mathbf{F}_k=0\,,\qquad \mathbf{F}_k=c^2\,\mathbf{k}_k-\omega\,\mathbf{C}\,,\tag{8.6}$$

  which corresponds to Eq. (4.2). Scalar multiplication of Eq. (8.6) by $\mathbf{k}$, combined with the condition $\omega\neq 0$, leads to the dispersion relation

$$\omega=\mathbf{k}\cdot\mathbf{C}\,,\qquad (\mathbf{k}\times\mathbf{C}\neq 0)\,.\tag{8.7}$$

  This relation could as well have been obtained directly from Eq. (4.3). Since $\mathbf{k}$ and $\mathbf{C}$ are not parallel in a general case, the phase velocity becomes

$$v_p=\frac{\omega}{k}=\mathbf{k}\cdot\frac{\mathbf{C}}{k}\tag{8.8}$$

  and the group velocity is given by

$$\mathbf{v}_g=\frac{\partial\omega}{\partial\mathbf{k}}=\mathbf{C}\,.\tag{8.9}$$

  Thus these velocities both differ from each other and from those of the EM and S waves. The field vectors $\mathbf{E}$ and $\mathbf{C}$ have components that are both perpendicular and parallel to the wave normal. From Eq. (8.3) we further have $\mathbf{k}\cdot\mathbf{B}=0$ and $\mathbf{E}\cdot\mathbf{B}=0$. Scalar multiplication of $\mathbf{F}_k$ in Eq. (8.6) by $\mathbf{C}$ yields $\mathbf{C}\cdot\mathbf{F}_k=0$ when using relation (8.7). Combination of this result with the scalar product of Eq. (8.6) with $\mathbf{C}$ yields $\mathbf{E}\cdot\mathbf{C}=0$. Finally, the scalar product of Eq. (8.6) with $\mathbf{E}$ results in $\mathbf{E}^2=c^2\mathbf{B}^2$ when combined with Eq. (8.3).

For the EMS wave it is seen that $\mathbf{k}$ and $\mathbf{E}$ are localized to a plane being perpendicular to $\mathbf{B}$, and that $\mathbf{E}$ and $\mathbf{C}$ form a right angle. We can then introduce the general relation

$$\mathbf{k}\cdot\mathbf{E}=kE(\cos\chi)\,,\tag{8.10}$$

where $E=|\mathbf{E}|$. Here the angle χ stands for the extra degree of freedom introduced by the nonzero electric field divergence. There is a set of wave solutions which range for a decreasing χ from the EM mode given by $\chi=\frac{\pi}{2}$, via the EMS mode in the range $\frac{\pi}{2}>\chi>0$, to the S mode where $\chi=0$. The choice of wave type and of the parameters $\mathbf{C}$ and χ depends on the boundary conditions and the geometry of the particular configuration to be considered.

We finally turn to the momentum and energy equations (3.16)–(3.20) of §3.5. Since the charge density is nonzero for the S and EMS modes, these equations differ from those of the conventional EM mode in the vacuum:

- For the S mode both equations contain a contribution from $\bar{\rho}\,\mathbf{E}$ but have no magnetic terms.
- For the EMS mode the momentum equation (3.17) includes the additional forces $\mathbf{F}_e$ and $\mathbf{F}_m$. Because of the result $\mathbf{E}\cdot\mathbf{C}=0$, the energy equation (3.20) will on the other hand be the same as for the EM mode.

Poynting's theorem for the energy flow of plane waves in the vacuum thus applies both to the EM and the EMS modes, but not to the S mode. Vector multiplication of Eq. (8.6) by $\mathbf{k}$, and combination with Eq. (8.3) and the result $\mathbf{E}\cdot\mathbf{C}=0$ is easily shown[9] to result in a Poynting vector that is parallel with the group velocity $\mathbf{C}$ of Eq. (8.9). Later in Chapter 9 we shall return to this theorem in the case of axisymmetric waves.

In general the physical interpretation and relevance of the purely longitudinal electric space-charge S waves is at this stage still an open question. Two points are thus to be made here:

- A spectrum of plane S waves with normals oriented in different directions can in principle be adopted, to form a three-dimensional arbitrary disturbance at a certain initial time. At later times, however, such a disturbance would become disintegrated in a way being similar to that being formed by conventional plane EM waves[24].
- In cylindrical and spherical geometry, there are S wave solutions of the basic equations as discussed later in §11.4. There it is shown that problems arise with the energy conservation of propagating S waves, thus calling the existence of such waves into question in curvilinear geometries.

The plane wave concept provides the analysis with a simple demonstration of various wave modes, but it should be used with care. Thus, a single plane wave with its unlimited spatial extension is a straightforward concept, but it can end up far from physical reality on account of existing boundary conditions.

§8.2 Total reflection at a vacuum interface

The process of total reflection of an incident wave propagating in an optically dense medium in the direction towards a vacuum interface has turned out to be of renewed interest with respect to the concepts of

nontransverse and longitudinal waves. In particular, when a dense medium is dissipative, this leads to questions not being fully understood in terms of classical electromagnetic theory and Fresnel's laws, as pointed out by Hütt[29]. The incident and reflected waves in the dense medium then become inhomogeneous (damped) in their directions of propagation. As a consequence, matching at the interface to a conventional undamped electromagnetic wave in the vacuum becomes impossible.

This problem is now considered in a frame (x, y, z) where $x = 0$ defines the vacuum interface. The orientation of the xy plane is chosen such as to coincide with the plane of wave propagation, and all field quantities are then independent of z. In the dense medium (region I) where $x < 0$ the refractive index is $n_{\text{I}} \equiv n > 1$, and an incident (i) damped EM wave is assumed to give rise to a reflected (r) damped EM wave. The vacuum (region II) corresponds to $x > 0$ and has the refractive index $n_{\text{II}} = 1$. The normal direction of the boundary forms the angle φ with the wave normals of the incident and reflected waves. The wave numbers[24] and phases (8.1) of these weakly damped waves then result in

$$\begin{aligned}\Theta_{i,r} = \Big(\frac{\omega}{c}\Big)\big[-ct \pm n\,(\cos\varphi)\,x + n\,(\sin\varphi)\,y\big] + \\ + i\,\bar{\delta}\Big(\frac{\omega}{c}\Big)\,n\,\big[\pm(\cos\varphi)\,x + (\sin\varphi)\,y\big]\end{aligned} \tag{8.11}$$

with the upper and lower signs corresponding to (i) and (r). Here the damping factor is denoted by $\bar{\delta} = \frac{1}{2\omega\eta\bar{\varepsilon}} \ll 1$, with $\bar{\varepsilon}$ standing for the electric permittivity and η for the electric resistivity in region I. For the phase of a transmitted wave in region II the notation

$$\Theta_t = \frac{\omega}{c}\,(-ct + p_t x + r_t y) + i\Big(\frac{\omega}{c}\Big)(q_t x + s_t y) \tag{8.12}$$

is introduced where all quantities (p_t, r_t, q_t, s_t) are real.

The possibility of matching a transmitted EM wave to the incident and reflected waves is first investigated. This requires the phases (8.11) to be matched to the phase (8.12) of the transmitted wave at every point of the interface. This condition can be written as

$$r_t = n_\varphi > 0\,, \qquad s_t = \bar{\delta}\,n_\varphi > 0\,, \qquad n_\varphi = n(\sin\varphi)\,, \tag{8.13}$$

where total reflection corresponds to $n_\varphi > 1$. For the transmitted EM wave in the vacuum, combination of Eqs. (4.2) and (8.12) results in

$$1 = p_t^2 + r_t^2 - (q_t^2 + s_t^2)\,, \tag{8.14}$$

$$\frac{q_t}{s_t} = -\frac{r_t}{p_t}\,. \tag{8.15}$$

The transmitted wave should further travel in the positive x direction, into region II, and this also applies in the limit where the angle of its normal with the vacuum interface approaches zero during total reflection. Thus, $p_t > 0$. Eqs. (8.15) and (8.13) then combine to the condition

$$q_t = -\frac{n_\varphi^2\,\bar{\delta}}{p_t} < 0\,. \tag{8.16}$$

For total reflection, however, there should be no flow of energy into region II, and the transmitted wave must represent a flow directed parallel to the interface, thereby being limited in amplitude to a narrow layer at the vacuum side of the interface[24]. This excludes the negative value of q_t given by Eq. (8.16), as well as the form (8.12) for an EM wave. Therefore it does not become possible to match the inhomogeneous (damped) EM waves in region I by a homogeneous (undamped) EM wave in region II. This agrees with an earlier result by Hütt[29].

Turning instead to the possibility of matching the incident and reflected EM waves to transmitted EMS waves in the vacuum region, we consider the two cases of parallel and perpendicular polarization of the electric field of the incident wave. The velocity $\mathbf{C}$ of an EMS wave is now given by

$$\mathbf{C} = c\left(\cos\beta\cos\alpha,\ \cos\beta\sin\alpha,\ \sin\beta\right). \tag{8.17}$$

In combination with the definitions (8.1) and (8.12) the dispersion relation (8.7) of this wave type yields

$$\frac{1}{\cos\beta} = p_t\cos\alpha + r_t\sin\alpha\,, \tag{8.18}$$

$$q_t\cos\alpha = -s_t\sin\alpha\,. \tag{8.19}$$

According to Eqs. (8.19) and (8.13) matching of the phase by a transmitted EMS wave becomes possible when

$$q_t = -\,s_t\tan\alpha = -\,n_\varphi\,\bar{\delta}\tan\alpha\,. \tag{8.20}$$

In the case of total reflection the velocity vector $\mathbf{C}$ of Eq. (8.17), and the corresponding current density (3.3), can then be directed almost parallel with the interface $x = 0$, i.e. when $|\cos\alpha| \ll 1$, $|\sin\alpha| \simeq 1$ and $\tan\alpha < 0$. The EMS wave in region II is then matched to the amplitudes of the EM waves in region I which slightly decrease in the y direction. This also implies that q_t in Eq. (8.20) can be made positive and large for weakly damped EM waves in region I, i.e. when the resistivity is small and the damping factor large. Even a moderately large $q_t > 0$ provides the possibility of a transmitted energy flow along the interface, within

a narrow boundary layer and for an EMS wave amplitude that drops steeply with an increasing distance from the interface.

As a next step the electric and magnetic fields have to be matched at the interface. This raises three questions being in common with those of conventional theory[24]. The first issue is due to the expectation that the transmitted and reflected waves are no longer in phase at the surface $x = 0$ with the incident wave. The second question concerns the amplitude ratio of the reflected and incident waves which must have a modulus equal to unity. This is due to the expectation that no energy can be lost during the instantaneous reflection process. This question also leads to the third issue that concerns the energy flow of the transmitted wave. As already being pointed out, this flow has to be directed along the interface and be localized to a narrow boundary layer.

To meet these requirements we observe that the wave number and the phase are coupled through the angles of the velocity form (8.17). In this way the angle of any transmitted EMS wave in region II can be expressed in terms of the angles α and β.

The details of the deductions to follow are given elsewhere[9,17], and are summarized as follows:

- For inhomogeneous (damped) incident EM waves the necessary matching of the phases at the interface can be provided by non-transverse EMS waves in the vacuum region;
- The transmitted EMS waves are confined to a narrow layer at the vacuum side of the interface, and no energy is extracted from the reflection process;
- A far from simple question concerns the magnitude of the damping factor $\bar{\delta}$ which in physical reality forms a limit between the analysis of damped and undamped incident waves. In most experimental situations the ratio $\frac{1}{\bar{\delta}}$ between the damping length and the wave length is very large, and this makes it difficult to decide when the present analysis on inhomogeneous incident waves becomes relevant. It should first become applicable at large damping factors, but this requires large initial amplitudes to give rise to a detectable reflected wave.

Chapter 9

CYLINDRICAL WAVE MODES

During several decades a number of investigators have discussed the nature of light and photon physics, not only in relation to the propagation of plane wave fronts but also to axisymmetric wave packets, the concept of a photon rest mass, the existence of a magnetic field component in the direction of propagation, and to an associated angular momentum (spin) of the photon in the capacity of a boson particle.

The analysis of plane waves is relatively simple. As soon as one begins to consider waves varying in more than one spatial dimension, however, new features arise which complicate the analysis. This also applies to the superposition of elementary modes to form wave packets. In this chapter dissipation-free axially symmetric modes are investigated on the basis of the present theory. A corresponding wave packet configuration then results in a photon model, being one of the possible representations of an individual photon concept.

In analogy with the previous analysis on axisymmetric equilibria, we will also here search for a model where the entire vacuum space is treated as one single entity, without introducing internal boundaries and boundary conditions.

The aim is here to elaborate a model of the individual photon in the capacity of a boson particle with an angular momentum(spin), propagating with preserved geometry and limited extensions in a defined direction of space. This leads to the concept of cylindrical waves and wave packets.

The first parts of this chapter will deal with axisymmetric wave modes, whereas screw-shaped modes are treated to some extent in its later parts.

§ 9.1 Elementary normal axisymmetric modes

A cylindrical frame (r, φ, z) is introduced where φ is an ignorable coordinate. In this frame the velocity vector is assumed to have the form

$$\mathbf{C} = c\,(0,\ \cos\alpha,\ \sin\alpha) \tag{9.1}$$

with either sign of $\cos\alpha$ and $\sin\alpha$, and a constant angle α. We further define the operators

$$D_1 = \frac{\partial^2}{\partial r^2} + \frac{1}{r}\frac{\partial}{\partial r} + \frac{\partial^2}{\partial z^2} - \frac{1}{c^2}\frac{\partial^2}{\partial t^2}\,, \tag{9.2}$$

$$D_2 = \frac{\partial}{\partial t} + c\,(\sin\alpha)\,\frac{\partial}{\partial z}\,. \tag{9.3}$$

The basic equations (4.2) and (4.3) are then represented by the system

$$\left(D_1 - \frac{1}{r^2}\right)E_r = \frac{\partial}{\partial r}\,(\operatorname{div}\mathbf{E})\,, \tag{9.4}$$

$$\left(D_1 - \frac{1}{r^2}\right)E_\varphi = \frac{1}{c}\,(\cos\alpha)\,\frac{\partial}{\partial t}\,(\operatorname{div}\mathbf{E})\,, \tag{9.5}$$

$$D_1 E_z = \left[\frac{\partial}{\partial z} + \frac{1}{c}\,(\sin\alpha)\,\frac{\partial}{\partial t}\right](\operatorname{div}\mathbf{E})\,, \tag{9.6}$$

and

$$D_2(\operatorname{div}\mathbf{E}) = 0\,. \tag{9.7}$$

Thereby Eq. (9.7) originates from Eq. (4.3) and does not introduce more information than that already contained in Eqs. (9.4)–(9.6). By further defining the operator

$$D_3 = \frac{\partial^2}{\partial z^2} - \frac{1}{c^2}\frac{\partial^2}{\partial t^2} \tag{9.8}$$

Eq. (9.4) reduces to

$$D_3 E_r = \frac{\partial^2 E_z}{\partial r\,\partial z}\,. \tag{9.9}$$

Combination with Eq. (9.5) then yields

$$D_3\Big(D_1 - \frac{1}{r^2}\Big)E_\varphi = \frac{1}{c}\,(\cos\alpha)\,\frac{\partial^2}{\partial z\,\partial t}\,D_1 E_z\,. \tag{9.10}$$

Normal modes depending on z and t as $\exp\big[i\,(-\omega t + kz)\big]$ are now considered, first in the conventional case where $\operatorname{div}\mathbf{E} = 0$, and then for the EMS mode where $\operatorname{div}\mathbf{E} \neq 0$. In fact, there are a number of choices with respect to the form (9.1) as represented by $\pm\cos\alpha$ and $\pm\sin\alpha$ which satisfy the condition of Eq. (3.3), thereby corresponding to the two directions along and around the axis of symmetry.

We shall later in §9.6 shortly discuss modes which are not strictly axisymmetric but also have a periodic dependence on the angle φ of the direction around the z axis.

At this stage it also has to be noticed that there is no solution for an axisymmetric S wave propagating along the z axis and having two components of $\mathbf{C}$, as shown by Eqs. (3.6) and (3.9) in the case of a vanishing magnetic field. This would namely result in two non-identical equations for the same electrostatic potential.

§ 9.1.1 Conventional normal modes

In the case of a vanishing electric field divergence, Eqs. (9.4)–(9.6) reduce to those of an axisymmetric EM mode. The separation constant of the z- and t-dependence is

$$\bar{\theta}^2 = k^2 - \left(\frac{\omega}{c}\right)^2 . \tag{9.11}$$

Then the phase and group velocities v_p and v_g become

$$v_p = \frac{\omega}{k} = \pm\, c\, \sqrt{1 - \frac{\theta^2}{k^2}}\ , \tag{9.12}$$

$$v_g = \frac{\partial\omega}{\partial k} = \pm \frac{c}{\sqrt{1 - \frac{\theta^2}{k^2}}}\, . \tag{9.13}$$

Here $\bar{\theta}^2 > 0$ results in $v_g^2 < c^2$ with solutions including Bessel functions of the first and second kinds[24].

As a next step we assume $\bar{\theta}^2$ to vanish which corresponds to a phase and group velocity equal to c. Then Eqs. (9.4)–(9.6) reduce to

$$\left(\bar{D}_\rho - \frac{1}{\rho^2}\right)(E_r, E_\varphi) = 0\,, \qquad \bar{D}_\rho\, E_z = 0\,, \tag{9.14}$$

where

$$\bar{D}_\rho = \frac{\partial^2}{\partial\rho^2} + \frac{1}{\rho}\frac{\partial}{\partial\rho}\,. \tag{9.15}$$

The solutions $E_\nu = \hat{E}_\nu(\rho)\exp\big[\,i\,(-\omega t + kz)\big]$ with $\nu = (r, \varphi, z)$ become

$$\hat{E}_r = k_{r1}\rho + \frac{k_{r2}}{\rho}\,, \quad \hat{E}_\varphi = k_{\varphi1}\rho + \frac{k_{\varphi2}}{\rho}\,, \quad \hat{E}_z = k_{z1}\ln\rho + k_{z2}\,, \tag{9.16}$$

where k_{r1}, k_{r2}, $k_{\varphi1}$, $k_{\varphi2}$, k_{z1} and k_{z2} are constants. The magnetic field is obtained from Eq. (3.7).

A similar divergence of the field at the axis $\rho = 0$ and at large ρ was already realized by Thomson[26] and further discussed by Heitler[23], as well as by Hunter and Wadlinger[27]. It leaves the problem with the radial dependence unresolved. Thus the field does not converge within the entire vacuum space, and cannot be made to vanish at large radial distances as long as k_{r1}, $k_{\varphi1}$ and k_{z1} differ from zero. All parts of the

solutions (9.16) further result in integrals of the energy density which become divergent when being extended all over the vacuum space. This also applies to the solutions with Bessel functions being related to the case $\bar{\theta}^2 \neq 0$. An additional point of concern is due to the vanishing electric field divergence of Eq. (9.16) which becomes

$$2k_{r1} + i\,k\,(k_{z1}\ln\rho + k_{z2}) \equiv 0 \tag{9.17}$$

and has to vanish identically for all (ρ, k) in the case of conventional electromagnetic waves. Thereby the last part of Eq. (9.17) requires the parallel electric field component E_z to vanish identically, but then it also becomes necessary for the constant k_{r1} in Eq. (9.17) to disappear. There are further analogous solutions for the magnetic field, by which also the axial component B_z vanishes in the conventional case. In its turn, this results in a Poynting vector (3.19) having only a component in the direction of propagation, thus leading to a vanishing angular momentum with respect to the axial direction. Here we observe that Eqs. (9.14) and (9.17) are differential equations of second and first order, respectively.

In this connection we may as well consider a corresponding case in a rectangular frame (x, y, z), with propagation along z of the form $f(x,y)\exp\big[i\,(-\omega t + kz)\big]$ and where $\omega^2 = k^2c^2$. Assuming then, as in an example given by Jackson[25], that there are derivatives with respect to x and y along the wave front, Eq. (4.2) reduces to

$$\left(\frac{\partial^2}{\partial x^2} + \frac{\partial^2}{\partial y^2}\right)\mathbf{E} = 0\,. \tag{9.18}$$

With separable solutions of the form $f = X(x)\cdot Y(y)$ this yields

$$X = c_{x1}\,e^{k_x x} + c_{x2}\,e^{-k_x x}, \tag{9.19}$$

$$Y = c_{y1}\,e^{k_y y} + c_{y2}\,e^{-k_y y}, \tag{9.20}$$

and

$$k_x^2 + k_y^2 = 0\,, \tag{9.21}$$

which solution becomes divergent, either in the x or in the y direction, and cannot satisfy the condition $\operatorname{div}\mathbf{E} = 0$.

For a physically relevant photon model with no spatial limitations, the integrated field energy has to be finite. It is thus seen that photon models based on Maxwell's equations either lead to plane waves with no derivatives along the wave front and no angular momentum, or to solutions with such derivatives which could in principle generate an angular momentum but then become both physically unacceptable due to their divergence in space and incompatible with the condition $\operatorname{div}\mathbf{E} \equiv 0$.

§9.1.2 Normal electromagnetic space-charge modes

Returning to the axisymmetric EMS mode of Eqs. (9.1)–(9.10), a dispersion relation

$$\omega = k\,v\,, \qquad v = c\,(\sin\alpha) \tag{9.22}$$

is obtained from Eq. (9.7), having the phase and group velocities v. Here we limit ourselves to positive values of $\cos\alpha$ and $\sin\alpha$. With the dispersion relation (9.22), Eq. (9.10) takes the form

$$\left[\frac{\partial^2}{\partial r^2} + \frac{1}{r}\frac{\partial}{\partial r} - \frac{1}{r^2} - k^2(\cos\alpha)^2\right]E_\varphi = \\ = -(\tan\alpha)\left[\frac{\partial^2}{\partial r^2} + \frac{1}{r}\frac{\partial}{\partial r} - k^2(\cos\alpha)^2\right]E_z\,. \tag{9.23}$$

We can now introduce a *generating function*

$$G_0 \cdot G = E_z + (\cot\alpha)\,E_\varphi\,, \qquad G = R(\rho)\,e^{i(-\omega t + kz)}, \tag{9.24}$$

where G_0 stands for the amplitude, G for a normalized form, $\rho = \frac{r}{r_0}$ is again a normalized coordinate with respect to the characteristic radius r_0 of the configuration, and $R(\rho)$ is a dimensionless function of ρ. The function (9.24) is based on the electric field components and differs in its character from the steady-state generating function (5.6) which is based on the electromagnetic potentials. With the operator of Eq. (9.15), the definition

$$D = \bar{D}_\rho - \theta^2(\cos\alpha)^2, \qquad \theta = k\,r_0\,, \tag{9.25}$$

and using Eqs. (9.22), (9.9), and (3.7), insertion into Eq. (9.23) results in

$$E_r = -i\,G_0\,\frac{1}{\theta(\cos\alpha)^2}\,\frac{\partial}{\partial\rho}\big[(1-\rho^2 D)\,G\big] = -\frac{1}{r_0}\frac{\partial\phi}{\partial\rho} + i\omega A_r\,, \tag{9.26}$$

$$E_\varphi = G_0(\tan\alpha)\rho^2 DG = i\,\omega A_\varphi\,, \tag{9.27}$$

$$E_z = G_0(1-\rho^2 D)\,G = -ik\phi + i\omega A_z \tag{9.28}$$

and

$$B_r = -G_0\,\frac{1}{c\,(\cos\alpha)}\,\rho^2 DG = -ikA_\varphi\,, \tag{9.29}$$

$$B_\varphi = -i\,G_0(\sin\alpha)\frac{1}{\theta\,c\,(\cos\alpha)^2}\,\frac{\partial}{\partial\rho}\big[(1-\rho^2 D)\,G\big] = ikA_r - \frac{1}{r_0}\frac{\partial A_z}{\partial\rho}\,, \tag{9.30}$$

$$B_z = -i\,G_0\,\frac{1}{\theta\,c\,(\cos\alpha)}\Big(\frac{\partial}{\partial\rho} + \frac{1}{\rho}\Big)(\rho^2 DG) = \frac{1}{r_0\,\rho}\frac{\partial}{\partial\rho}\,(\rho\,A_\varphi)\,. \tag{9.31}$$

Here the parameter θ should not be confused with the polar angle in the spherical frame of coordinates applied in Chapters 5 and 6. These expressions are reconfirmed by insertion into the basic equations. The obtained result demonstrates that the electromagnetic field of the normal mode is determined by one single generating function (9.24), in analogy with the function (5.6) of the steady state, and that the three equations (9.4)–(9.6) are not strictly independent of each other. This is a special feature of the present theory. It makes possible a choice of generating functions and corresponding modes which are physically relevant within the entire vacuum space, and which become consistent with the imposed quantum conditions.

Due to the dispersion relation (9.22) the EMS mode propagates at phase and group velocities which are smaller than c. Not to get into conflict with the experimental observations by Michelson and Moreley, we limit ourselves for a positive $\cos\alpha$ to the condition

$$0 < \cos\alpha \ll 1\,, \tag{9.32}$$

which then has to be taken into account. Since the velocity v of Eq. (9.22) becomes slightly less than c, the condition (9.32) will be related to a very small but nonzero rest mass of the photon, as shown later in more detail. Such a rest mass has also been considered earlier by Einstein[40], Bass and Schrödinger[41], de Broglie and Vigier[31], and Evans and Vigier[4].

With the condition (9.32) the present mode has a dominant radially polarized electric field component (9.26), and an associated magnetic field component (9.30). The field configuration of Eqs. (9.26)–(9.31) thus differs in several respects from elliptically, circularly and linearly polarized plane waves.

The components (9.26)–(9.31) are reconcilable with the field configuration by Evans and Vigier[4,6,7], in the sense that all components are nonzero and form a helical structure which also includes an axial magnetic field component in the direction of propagation. The present result is, however, not identical with that by Evans and Vigier, because it originates from a Proca-type relation (2.1) of the form (2.8) being different from Eq. (2.7) which is the basis of the analysis by de Broglie, Vigier and Evans.

So far the deductions have been performed with respect to the laboratory frame K. In the present case where the phase and group velocities $v < c$, a physically relevant rest frame K' can be defined, but not in the conventional case where there is no rest mass, $\cos\alpha = 0$, and $v = c$. Here it is justified to make a transformation from K to K', in terms of

the small parameter

$$\delta \equiv \sqrt{1-\frac{v^2}{c^2}} = \cos\alpha\,, \qquad v = \left[0,0,c\,(\sin\alpha)\right]. \tag{9.33}$$

The Lorentz transformation then leads to the result

$$r' = r\,, \qquad z' = \frac{z - c\,(\sin\alpha)\,t}{\delta} \equiv \frac{\bar{z}}{\delta}\,, \tag{9.34}$$

where a prime refers to the rest frame. Thus

$$\frac{\partial}{\partial z'} = \delta\left(\frac{\partial}{\partial z}\right), \qquad k' = \delta k\,, \qquad \theta' = k' r_0 = \delta\theta\,. \tag{9.35}$$

The normalized generating function then transforms according to

$$G = R(\rho)\,e^{i(-\omega t + kz)} = R(\rho)\,e^{ik'z'} \equiv G', \tag{9.36}$$

when using expressions (9.34). Thus G' becomes time independent in the rest frame K'. Further

$$D = \bar{D}_\rho - \theta^2(\cos\alpha)^2 = \bar{D}_\rho - (\theta')^2 \equiv D', \qquad DG = D'G' \tag{9.37}$$

holds for the operators D and D' in K and K'.

For the electric and magnetic fields the Lorentz transformation becomes

$$\mathbf{E}' = \frac{1}{\delta}\,\mathbf{E} - \left(\frac{1}{\delta} - 1\right)(\hat{\mathbf{z}}\cdot\mathbf{E})\,\hat{\mathbf{z}} + \frac{1}{\delta}\,\mathbf{v}\times\mathbf{B}\,, \tag{9.38}$$

$$\mathbf{B}' = \frac{1}{\delta}\,\mathbf{B} - \left(\frac{1}{\delta} - 1\right)(\hat{\mathbf{z}}\cdot\mathbf{B})\,\hat{\mathbf{z}} - \frac{1}{\delta}\,\mathbf{v}\times\frac{\mathbf{E}}{c^2}\,, \tag{9.39}$$

where $\hat{\mathbf{z}} = (0,0,1)$. This results in the components

$$E'_r = -\,i\,G_0(\theta')^{-1}\,\frac{\partial}{\partial\rho}\left[(1-\rho^2 D')G'\right], \tag{9.40}$$

$$E'_\varphi = 0\,, \tag{9.41}$$

$$E'_z = G_0\,(1-\rho^2 D')\,G', \tag{9.42}$$

and

$$B'_r = -\,G_0 c^{-1}\,\rho^2 D'G', \tag{9.43}$$

$$B'_\varphi = 0\,, \tag{9.44}$$

$$B'_z = -\,i\,G_0\,(c\,\theta')^{-1}\left(\frac{\partial}{\partial\rho} + \frac{1}{\rho}\right)(\rho^2 D'G')\,. \tag{9.45}$$

Here it is observed that the axial components $E_z = E'_z$ and $B_z = B'_z$ are invariant during the Lorentz transformation, as given by Eqs. (9.38)–(9.39). The obtained components (9.40)–(9.45) can also be interpreted in the way that the components in K' are derived from those in K by replacing the wave number k by k' and the angle α by $\alpha' = 0$, i.e. by substituting the velocity vector (9.1) in K by

$$\mathbf{C}' = c\,(0, 1, 0)\,, \qquad (\alpha' = 0) \tag{9.46}$$

in K'. This supports the adopted form (9.1). In the rest frame K' the current density (2.8) has a component in the φ direction only, and it circulates around the axis of symmetry, thereby being connected with electric and magnetic fields which are purely poloidal, i.e. located in planes running through the same axis. This situation is similar to that of the "bound" steady equilibrium state of Chapter 5, with its static electric and magnetic fields.

§ 9.2 Axisymmetric wave packets

From a spectrum of normal modes with different wave numbers, a wave packet solution is now being formed which has finite radial and axial extensions and a narrow line width in wavelength space. Such a line width is consistent with experimental observations. We are free to rewrite the amplitude factor of the generating function (9.24) as

$$G_0 = g_0(\cos\alpha)^2. \tag{9.47}$$

The normal modes are superimposed to result in a wave packet having the amplitude

$$A_k = \left(\frac{k}{k_0^2}\right) e^{-z_0^2(k-k_0)^2} \tag{9.48}$$

in the interval dk and being centered around the wave number k_0. Further $2z_0$ represents the effective axial length of the packet. In the integration of the field components (9.26)–(9.31) the expression

$$P_\mu = \int_{-\infty}^{+\infty} k^\mu A_k\, e^{ik(z-vt)}\, dk\,, \qquad v = c\,(\sin\alpha) \tag{9.49}$$

is used, and the variables

$$p = z_0(k - k_0) + \frac{i\,\bar{z}}{2z_0}\,, \qquad \bar{z} = z - vt \tag{9.50}$$

are introduced. Then the integral (9.49) becomes

$$P_\mu = \left(\frac{k_0^\mu\sqrt{\pi}}{k_0 z_0}\right) \exp\left[-\Big(\frac{\bar{z}}{2z_0}\Big)^2 + ik_0\bar{z}\right] \cdot \left[1 + f\Big(\frac{\bar{z}}{z_0},\ \frac{1}{k_0 z_0}\Big)\right], \tag{9.51}$$

where f is a polynomial in terms of the quantities $\frac{\bar{z}}{z_0}$ and $\frac{1}{k_0 z_0}$.

The restriction to a narrow line width implies that the amplitude (9.48) drops to $\frac{1}{e}$ of its maximum value for a small deviation of k from the maximum at $k = k_0$. With $\Delta k = k - k_0 = \frac{1}{z_0}$ this implies that $\frac{\Delta k}{k_0} = \frac{1}{k_0 z_0} = \frac{\lambda_0}{2\pi z_0} \ll 1$, where $\lambda_0 = \frac{2\pi}{k_0}$ is the average wave length of the packet. Under this condition the contribution from f to the form (9.51) can be neglected with good approximation, as also being seen from a detailed evaluation of the integral (9.49). On the other hand, the wave packet model would also apply when the axial extension $2z_0$ is of the order of one wave length λ_0, but this leads to an extremely broad line width not being reconcilable with experiments.

With the notation

$$E_0 \equiv E_0(\bar{z}) = \left(\frac{g_0}{k_0 r_0}\right)\left(\frac{\sqrt{\pi}}{k_0 z_0}\right) \exp\left[-\left(\frac{\bar{z}}{2z_0}\right)^2 + i k_0 \bar{z}\right], \tag{9.52}$$

the spectral averages of the packet field components become

$$\bar{E}_r = -\,i\,E_0\left[R_5 + (\theta_0')^2\,R_2\right], \tag{9.53}$$

$$\bar{E}_\varphi = E_0\,\theta_0\,(\sin\alpha)(\cos\alpha)\left[R_3 - (\theta_0')^2\,R_1\right], \tag{9.54}$$

$$\bar{E}_z = E_0\,\theta_0\,(\cos\alpha)^2\left[R_4 + (\theta_0')^2\,R_1\right], \tag{9.55}$$

$$\bar{B}_r = -\frac{1}{c\,(\sin\alpha)}\,\bar{E}_\varphi\,, \tag{9.56}$$

$$\bar{B}_\varphi = \frac{1}{c}\,(\sin\alpha)\,\bar{E}_r\,, \tag{9.57}$$

$$\bar{B}_z = -\,i\,\frac{1}{c}\,\bar{E}_0\,(\cos\alpha)\left[R_8 - (\theta_0')^2\,R_7\right], \tag{9.58}$$

where $\theta_0 = k_0\,r_0$, $\theta_0' = \theta_0\,(\cos\alpha)$ and

$$R_1 = \rho^2 R\,, \qquad R_2 = \frac{d}{d\rho}R_1\,, \qquad R_3 = \rho^2 \bar{D}_\rho R\,, \tag{9.59}$$

$$R_4 = R - R_3\,, \qquad R_5 = \frac{d}{d\rho}R_4\,, \qquad R_6 = \bar{D}_\rho R_4\,, \tag{9.60}$$

$$R_7 = \left(\frac{d}{d\rho} + \frac{1}{\rho}\right)R_1\,, \qquad R_8 = \left(\frac{d}{d\rho} + \frac{1}{\rho}\right)R_3 \tag{9.61}$$

with the operator $\bar{D}_\rho$ given by Eq. (9.15).

It should be noticed that expressions (9.56)–(9.58) are approximate, on account of the restriction to a narrow line width. Therefore the

condition $\operatorname{div}\bar{\mathbf{B}} = 0$ is only satisfied approximately. In the limit of zero line width we would on the other hand be back to the exact form (9.29)–(9.31) for an elementary normal mode where $\operatorname{div}\mathbf{B} = 0$.

For the wave packet fields (9.53)–(9.58) the components $(\bar{E}_\varphi, \bar{E}_z, \bar{B}_r)$ are in phase with the generating function (9.24), whereas the components $(\bar{E}_r, \bar{B}_\varphi, \bar{B}_z)$ are ninety degrees out of phase with it. In the analysis which follows we choose a generating function which is symmetric with respect to the axial centre $\bar{z} = 0$ of the moving wave packet. Thus

$$G = R(\rho)\cos k\bar{z} \tag{9.62}$$

when the real parts of the forms (9.24), (9.49), and (9.52) are adopted. Then G and $(\bar{E}_\varphi, \bar{E}_z, \bar{B}_r)$ are symmetric and $(\bar{E}_r, \bar{B}_\varphi, \bar{B}_z)$ are antisymmetric functions of $\bar{z}$ with respect to the centre $\bar{z} = 0$.

§ 9.3 Spatially integrated field quantities

When elaborating a model for the individual photon, integrals have to be formed to obtain net values of the electric charge q, magnetic moment M, the total mass m which represents the total energy, and of the angular momentum (spin) s. Thereby the limits of $\bar{z}$ are $\pm\infty$, whereas those of ρ become unspecified until further notice. In this section general forms of the integrated field quantities will be deduced, then being followed by photon models which originate from special forms of the radial part of the generating function.

§ 9.3.1 Charge and magnetic moment

The integrated charge becomes

$$\begin{aligned} q &= \varepsilon_0 \int \operatorname{div}\bar{\mathbf{E}}\, dV = \\ &= 2\pi\varepsilon_0 \int \left\{ \frac{\partial}{\partial r}\left(r \int_{-\infty}^{+\infty} \bar{E}_r\, d\bar{z} \right) + r\left[\bar{E}_z\right]_{-\infty}^{+\infty} \right\} dr = 0\,, \end{aligned} \tag{9.63}$$

because $\bar{E}_r$ is antisymmetric and $\bar{E}_z$ symmetric with respect to $\bar{z}$.

The integrated magnetic moment is related to the component

$$j_\varphi = \bar{\rho}\, C_\varphi = \varepsilon_0 (\operatorname{div}\bar{\mathbf{E}})\, c\,(\cos\alpha) \tag{9.64}$$

of the space-charge current density. Thus

$$\begin{aligned} M &= \iint_{-\infty}^{+\infty} \bar{\rho}\, c\,(\cos\alpha)\pi r^2\, dr\, d\bar{z} = \\ &= \pi\varepsilon_0\, c\,(\cos\alpha) \int \left\{ r\, \frac{\partial}{\partial r}\left(r \int_{-\infty}^{+\infty} \bar{E}_r\, d\bar{z} \right) + r^2\left[\bar{E}_z\right]_{-\infty}^{+\infty} \right\} dr = 0 \end{aligned} \tag{9.65}$$

for the same symmetry reasons as those applying to the charge (9.63). It should be observed that, even if the net magnetic moment vanishes, the local magnetic field remains nonzero.

As in the case of the neutrino model of Chapter 7, the present photon model can have a structure with both positive and negative local contributions to the charge and the magnetic moment, but these end up to zero when being integrated over the total volume.

§ 9.3.2 Total mass

An equivalent total mass can be defined from the electromagnetic field energy, due to the energy relation by Einstein. Consequently we write

$$m = \frac{1}{c^2} \int w_f \, dV \tag{9.66}$$

as given by the field energy density of Eq. (3.25). Applying the condition (9.32) and using Eqs. (9.53)–(9.58), we then have

$$m \simeq 2\pi \, \frac{\varepsilon_0}{c^2} \int_{-\infty}^{+\infty} \int r \, \bar{E}_r^2 \, dr \, d\bar{z} \, . \tag{9.67}$$

When adopting the form (9.62) with an antisymmetric field $\bar{E}_r$, and introducing the integral[93]

$$J_z = \int_{-\infty}^{+\infty} (\sin k_0 \bar{z})^2 \, e^{-2(\bar{z}/2z_0)^2} d\bar{z} = z_0 \left(\frac{\pi}{2} \right)^{1/2} \tag{9.68}$$

in the limit $k_0 z_0 \gg 1$, the total mass finally becomes

$$m = a_0 W_m = \frac{h\nu_0}{c^2} \, , \qquad W_m = \int \rho \, R_5^2 \, d\rho \, , \tag{9.69}$$

where

$$a_0 = \varepsilon_0 \pi^{5/2} \sqrt{2} \, z_0 \left(\frac{g_0}{c k_0^2 z_0} \right)^2 \equiv 2 \, a_0^* \, g_0^2 \, . \tag{9.70}$$

For this wave packet the energy relations by Planck and Einstein also combine to

$$mc^2 = h\nu_0 \simeq \frac{h\,c}{\lambda_0} \, , \qquad \lambda_0 = \frac{2\pi}{k_0} \, , \tag{9.71}$$

where use has been made of the dispersion relation (9.22) applied to the wave packet as a whole, i.e.

$$\omega_0 = 2\pi\nu_0 \simeq k_0 \, c \, , \qquad \nu_0 = \frac{c}{\lambda_0} \, . \tag{9.72}$$

As shown earlier[18] in the case of a convergent radial part of the generating function (9.24), the final result of Eqs. (9.69)–(9.70) can also be obtained from the source energy density (3.26). This also comes out from a divergent part of the same function where the contributions to all integrals mainly originate from the region close to the axis of symmetry.

Here the slightly reduced phase and group velocity of Eq. (9.22) can be considered as being associated with a very small nonzero rest mass

$$m_0 = m\sqrt{1-\frac{v^2}{c^2}} = m\,(\cos\alpha)\,, \tag{9.73}$$

which will be further verified in the following §9.3.6. In the present model this rest mass, and its corresponding energy, constitute an integrating part of the total propagating wave packet configuration. In the analysis which follows, a formal separation of the contribution due to the rest mass from the total field and its energy does therefore not become necessary, and the wave packet can then be treated as one entity. In the two-frequency concept proposed by de Broglie, a separate frequency is related to this rest mass[18]. For small $\cos\alpha$, however, relation (9.71) with a single frequency becomes a satisfactory approximation.

§9.3.3 Angular momentum

Turning to the momentum balance governed by Eqs. (3.17)–(3.19), the local volume force of each normal mode becomes

$$\mathbf{f} = \bar{\rho}\,(\mathbf{E} + \mathbf{C}\times\mathbf{B})\,, \tag{9.74}$$

where

$$\frac{\bar{\rho}}{\varepsilon_0} = \frac{1}{r}\,\frac{\partial}{\partial r}\,(r\bar{E}_r) + \frac{\partial}{\partial z}\,\bar{E}_z\,. \tag{9.75}$$

From the solutions (9.26)–(9.31) the force (9.74) is seen to be of second order in $\cos\alpha$ and can be neglected in cylindrical geometry. It vanishes exactly in the limit of rectangular geometry[19]. Consequently, the conventional expressions[38]

$$\mathbf{s} = \mathbf{r}\times\frac{\mathbf{S}}{c^2}\,, \qquad \mathbf{S} = \bar{\mathbf{E}}\times\frac{\bar{\mathbf{B}}}{\mu_0} \tag{9.76}$$

apply for the density $\mathbf{s}$ of the angular momentum, where $\mathbf{r}$ is the radius vector from the origin and $\mathbf{S}$ is the Poynting vector. The density of angular momentum now becomes

$$s_z = \varepsilon_0 r\,(\bar{E}_z\bar{B}_r - \bar{E}_r\bar{B}_z) \simeq -\varepsilon_0 r\,\bar{E}_r\bar{B}_z\,, \tag{9.77}$$

when condition (9.32) applies and use is made of Eqs. (9.53), (9.55), (9.56), and (9.58). The total angular momentum is given by

$$s = \int s_z \, dV = -2\pi\varepsilon_0 \int_{-\infty}^{+\infty} \int r^2 \bar{E}_r \bar{B}_z \, dr \, d\bar{z} \,, \tag{9.78}$$

and it reduces to the final form

$$s = a_0 \, r_0 \, c \, (\cos\alpha) \, W_s = \frac{h}{2\pi} \,, \qquad W_s = -\int \rho^2 \, R_5 \, R_8 \, d\rho \tag{9.79}$$

for the model of a photon having the angular momentum of a boson.

Here it is noticed that, with the inclusion of a dimensionless profile factor, relations (9.79) and (9.69) indicate that the form of the angular momentum agrees with the simple picture of a mass which rotates at the velocity $c\,(\cos\alpha)$ around the axis at the distance r_0. It is further observed that the harmonic oscillations of the electromagnetic field can be taken into account by including an additional factor of $\frac{1}{2}$ in the coefficient a_0 of Eqs. (9.69) and (9.79), but it does not affect the results on the photon diameter obtained in the following Sections 9.3.4 and 9.3.5.

The components g_r, g_φ, and g_z of the momentum density (3.19) are further of second, first and zero order[19] in $\cos\alpha$. The solutions (9.26)–(9.31) thereby imply that the time averages of g_φ and g_z are nonzero, whereas those of g_r vanish.

The momentum concept $\mathbf{g}$ of the pure radiation field may be compared to the momentum operator $\mathbf{p} = -i\hbar\nabla$ which has been applied with success to a massive particle in the Schrödinger equation. However, when applying the same operator to the radiation field of an individual photon or of a light beam with limited cross-section, the results differ from those of $\mathbf{g}$, and are difficult to interpret physically for the components p_r and p_φ as shown elsewhere[19].

The result (9.79) and Eq. (9.73) show that a nonzero angular momentum requires a nonzero rest mass to exist, as represented by $\cos\alpha \neq 0$. Moreover, the factor $\cos\alpha$ in the expression (9.79) and Eq. (9.1) for the velocity vector $\mathbf{C}$ indicates that the angular momentum, as well as the nonzero rest mass, are associated with the component C_φ of circulation around the axis of symmetry.

The so far deduced relations also apply to a dense radially polarized beam of N photons per unit length, where expressions (9.69) and (9.78) both have to be multiplied by N to represent the total mass and angular momentum per unit length. The radius r_0 then becomes related to the effective macroscopic radius of the beam. We shall return to this question later in connection with the screw-shaped modes treated in §9.6.

§ 9.3.4 Wave packet with a convergent generating function

First a generating function will be considered which is finite at the axis $\rho = 0$, and which tends to zero at large ρ. These requirements are fulfilled by the two forms

$$R(\rho) = \rho^{\gamma}\, e^{-\rho} \tag{9.80}$$

and

$$R(\rho) = \rho^{-\gamma}\, e^{-1/\rho}, \tag{9.81}$$

where $\gamma > 0$. There are several arguments in favour of this choice, being similar to those forwarded in connection with the radial part of the generating function of the electron model of Chapters 5 and 6. In principle, the factors in front of the exponential parts would in a general case have to be replaced by series of positive or negative powers of ρ, but since we will here proceed to the limit of large γ, only one term becomes sufficient. The analysis is further limited to the form (9.80), because the corresponding end result becomes the same[17,18] as for the form (9.81). The latter turns into expression (9.80) when substituting ρ for $\frac{1}{\rho}$. Moreover, the exponential factor in Eq. (9.80) has been included to secure the general convergence of any moment with R at large ρ. In any case, the forthcoming final results will be found not to depend explicitly on this exponential factor.

In the evaluation of expressions (9.69) and (9.79) for W_m and W_s the Euler integral

$$J_{2\gamma-2} = \int_0^{\infty} \rho^{2\gamma-2}\, e^{-2\rho}\, d\rho = 2^{-(2\gamma+3)}\, \Gamma(2\gamma+1) \tag{9.82}$$

appears in terms of the gamma function $\Gamma(2\gamma+1)$. For $\gamma \gg 1$ only the dominant terms of the functions R_5 and R_8 of Eqs. (9.60) and (9.61) will prevail, $R_8 \simeq -R_5$, and the result becomes

$$W_m = \frac{W_s}{\gamma}\,. \tag{9.83}$$

The function (9.80) has a maximum at the radius

$$\hat{r} = \gamma\, r_0\,, \tag{9.84}$$

which becomes sharply defined at large γ, in analogy with an earlier obtained result[18]. Combination of Eqs. (9.69), (9.71), (9.79), (9.83), and (9.84) leads to an effective photon diameter

$$2\,\hat{r} = \frac{\lambda_0}{\pi\,(\cos\alpha)}\,. \tag{9.85}$$

The factor $\cos\alpha$ in Eq. (9.85) has dropped out by mistake in an earlier paper by the author[17]. The result (9.85) does not only apply to an individual photon of the effective radius $\hat{r}$, but can also stand for the corresponding radius of a radially polarized dense multiphoton beam of N photons per unit length.

Apart from the factor $\cos\alpha$, the diameter of Eq. (9.85) is similar to that reported in an earlier analysis by Hunter and Wadlinger[27]. The latter analysis is based on Maxwell's equations, with solutions for which a $\frac{1}{\rho}$ dependence is excluded, and where boundaries have been introduced within the vacuum region. These boundaries limit the ρ dependence of the field of their photon model to an elliptic cross section which has the diameter $\frac{\lambda}{\pi}$ and the axial dimension of a single wavelength λ.

§ 9.3.5 Wave packet with a divergent generating function

Turning now to the alternative of a radial part which *diverges* at the axis, the form

$$R(\rho) = \rho^{-\gamma}\, e^{-\rho}, \qquad \gamma > 0 \tag{9.86}$$

is taken into consideration, being identical with the form (6.1) for the electron model of Chapter 6. Here the question of substituting the first factor in Eq. (9.86) by a negative power series is similar to that already discussed in § 6.1. This motivates the choice of a single factor in front of the exponential factor of Eq. (9.86). The latter factor is again included, to secure the convergence at large ρ. When the radial variable increases monotonically, the function (9.86) decreases from large values, down to $R = e^{-1}$ at $\rho = 1$, and further to very small values when ρ becomes substantially larger than 1. Thus $\hat{r} = r_0$ can be taken as a characteristic radial dimension of the configuration.

To obtain *finite* values of the integrated total mass m and angular momentum s of Eqs. (9.69) and (9.79), a special procedure similar to that applied to the electron model is being applied. The lower limits of the integrals (9.69) and (9.79) are specified by

$$W_m = \int_{\rho_m}^{\infty} \rho R_5^2\, d\rho\,, \qquad W_s = -\int_{\rho_s}^{\infty} \rho^2 R_5 R_8\, d\rho\,, \tag{9.87}$$

where $\rho_m \ll 1$ and $\rho_s \ll 1$. Making the choice $\gamma \gg 1$, these integrals reduce to

$$W_m = \frac{1}{2}\,\gamma^5 \rho_m^{-2\gamma}\,, \qquad W_s = \frac{1}{2}\,\gamma^5 \rho_s^{-2\gamma+1}\,. \tag{9.88}$$

To secure finite values of m and s we must now permit the characteristic radius r_0 and the factor g_0 in Eqs. (9.47), (9.69), (9.70), and

(9.79) to "shrink" to very small but nonzero values, as the lower limits ρ_m and ρ_s approach zero. This is attained by introducing the relations

$$r_0 = c_r \cdot \varepsilon\,, \qquad c_r > 0\,, \tag{9.89}$$

$$g_0 = c_g \cdot \varepsilon^{\beta}, \qquad c_g > 0\,, \tag{9.90}$$

where $0 < \varepsilon \ll 1$, $\beta > 0$, c_r is a constant with the dimension of length, and c_g one with the dimension of electrostatic potential. The limit where $\varepsilon = 0$ is excluded, because this would correspond to the physically uninteresting case of a structureless geometry. Eqs. (9.69), (9.70), (9.71), (9.79), and (9.88) now combine to

$$m = a_0^* \gamma^5 c_g^2 \frac{\varepsilon^{2\beta}}{\rho_m^{2\gamma}} \simeq \frac{h}{\lambda_0 c}\,, \tag{9.91}$$

$$s = a_0^* \gamma^5 c_g^2 c_r c\,(\cos\alpha)\,\frac{\varepsilon^{2\beta+1}}{\rho_s^{2\gamma-1}} = \frac{h}{2\pi}\,, \tag{9.92}$$

where the average wave length λ_0 of the packet has been defined in §9.2. To obtain finite values of both m and s, it is then necessary to satisfy the conditions

$$\rho_m = \varepsilon^{\beta/\gamma}, \qquad \rho_s = \varepsilon^{(2\beta+1)/(2\gamma-1)}. \tag{9.93}$$

We are here free to choose $\beta = \gamma \gg 1$ by which

$$\rho_s \simeq \rho_m = \varepsilon \tag{9.94}$$

with good approximation. The lower limits of the integrals (9.87) and (9.88) then decrease linearly with ε and the radius r_0. This forms a "similar" set of geometrical configurations which thus have a shape being independent of ρ_m, ρ_s, and ε in the range of small ε.

The ratio of expressions (9.91) and (9.92) finally yields an effective photon diameter

$$2\hat{r} = \frac{\varepsilon \lambda_0}{\pi\,(\cos\alpha)}\,. \tag{9.95}$$

It should be observed that the wave packet diameters of Eqs. (9.95) and (9.85) both become independent of the particular values of the parameters γ and β. As compared to the relatively large photon diameter (9.85) obtained for a convergent generating function, the diameter (9.95) based on a divergent such function can shrink to very small dimensions. This is the case even when $\cos\alpha \ll 1$ provided that $\varepsilon \ll \cos\alpha$. Then the photon model becomes strongly "needle-shaped" in its transverse directions. This has no counterpart in the conventional axisymmetric solutions of §9.1.1, which in addition would consist of divergent integrated field quantities due to the contributions from large radial distances.

§9.3.6 Rest mass of the wave packet

The wave packets studied in §9.3.4 and §9.3.5 are deduced from radial parts (9.80) and (9.86), having large values of γ and where $\cos\alpha \ll 1$. The dominating field components of the normal modes (9.26)–(9.31) and (9.40)–(9.45) in the laboratory and rest frames, K and K', then become related by

$$E_r = cB_\varphi = \frac{E'_r}{\cos\alpha} = \frac{cB'_z}{\cos\alpha}\,. \tag{9.96}$$

A corresponding field energy density (3.25) is obtained for the superimposed normal modes which form the spectrum of a wave packet. For the latter there is a Lorentz contraction in the direction of propagation in the moving frame K, as defined by Eqs. (9.33) and (9.34). The total energies of the wave packets in the frames K and K' are then related by

$$mc^2 = \int w_f\, dV = \frac{1}{\cos\alpha}\int w'_f\, dV' = \frac{m_0\, c^2}{\cos\alpha}\,, \tag{9.97}$$

where m_0 is the rest mass, in accordance with Eq. (9.73).

This result has earlier been obtained in an alternative way[18], for a convergent radial part, and on the basis of the source energy density (3.26). Here relations (9.96) and (9.97) can also be recovered in terms of the average field components (9.53)–(9.61) in K and of the corresponding components[18] in K'.

§9.4 Features of present photon models

The present photon models have features being associated with a number of crucial questions that have been subject to extensive discussions in the current literature. Some fundamental properties of the photon models resulting from conventional theory and from the present approach are listed and compared in Fig. 9.1.

§9.4.1 The nonzero rest mass

The possible existence of a nonzero photon rest mass was first called attention to by Einstein[40], Bass and Schrödinger[41], and de Broglie and Vigier[31]. It includes such fundamental points as its relation to the Michelson-Morley experiment, and its so far undetermined absolute value.

The phase and group velocities of the present non-dispersive wave packets become slightly smaller than the velocity of light, as expressed by condition (9.32) and Eq. (9.22). Thereby the velocity constant c can

Property / Theory	Phase and group velocity	Rest mass	Axial field components	Field geometry	Poynting vector	Angular momentum
Conventional Theory div **E** = 0	c	Zero	Zero (transverse field)	Unlimited in space	Along axis	Zero
Present Theory div **E** ≠ 0	Slightly smaller than c	Nonzero but very small	Nonzero (helical field)	Limited in space	Helical; along and aroud axis	Nonzero

Figure 9.1: A comparison between the individual photon models of conventional theory and of the present approach.

be regarded as an asymptotic limit at infinite photon energy. A small deviation from this limit still permits the theory to be compatible with the Michelson-Morley experiments, as shown by the following consideration. The velocity of the earth in its orbit around the sun is about $10^{-4}\,c$. If this would also turn out to be the velocity with respect to a stationary "ether", and if massive photons would move at the velocity $v = c\,(\sin\alpha)$ in the same ether, then the velocity u of photons being measured at the earth's surface would become

$$u = \frac{v + w}{1 + \frac{vw}{c^2}}\,. \tag{9.98}$$

Here $w = \pm 10^{-4}\,c$ for the parallel or antiparallel directions of incoming light at the surface, as counted with respect to the orbital motion. With the condition (9.32) the departure from c of the recorded photon velocity would then be given by

$$1 - \frac{u}{c} \simeq \frac{1}{2}\,(\cos\alpha)^2 \left(1 \pm \frac{2w}{c}\right). \tag{9.99}$$

For the value $\cos\alpha \leqslant 10^{-4}$ corresponding to a photon rest mass $m_0 < 0.74 \times 10^{-39}$ kg, a change in the eight decimal of the recorded velocity would hardly become detectable. For a rest mass in the range $10^{-68} < m_0 < 10^{-45}$ kg considered by Evans and Vigier[4], this change even becomes much smaller. Moreover, when turning from a direction where $\frac{w}{c} = +10^{-4}$ to the opposite direction, the change in $1 - \frac{u}{c}$ becomes as small as about 10^{-12}. Consequently, there should not be observed any noticeable departure in recorded velocity and deviation from an

experiment of the Michelson-Morley type if the photon rest mass is changed from zero to about 10^{-39} kg $\simeq 10^{-9}\, m_e$ or less.

The Lorentz invariance in this theory is satisfied even if there is an axial velocity of propagation being slightly smaller than c. This is due to the velocity vector $\mathbf{C}$ which forms helical orbits, also having a small component which circulates around the axis of symmetry. With the condition $\gamma \gg 1$ and Eq. (9.32) the Poynting vector is also found from Eqs. (9.53)–(9.58) to become parallel with the velocity vector $\mathbf{C}$ in the first approximation.

The previous analysis shows that the physics in presence even of a very small rest mass becomes fundamentally different from that being based on a rest mass which is exactly equal to zero. In the latter case we are back from an EMS mode to a conventional axisymmetric EM mode with its divergent and physically unacceptable properties and lack of angular momentum. Since the results of the EMS mode hold only for a nonzero rest mass, the quantum conditions (9.71) for the total energy and (9.79) for the angular momentum become satisfied by a whole class of small values of $\cos\alpha$ and m_0.

As being pointed out by de Broglie and Vigier[31], such an indeterminableness of the photon rest mass appears at a first sight to be a serious objection to the underlying theory. The problem is that the derivations depend simply on the existence of the nonzero rest mass, but not on its magnitude. To this concept de Broglie and Vigier add other analogous examples that have been considered in theoretical physics, such as ferromagnetism and the possibility of indefinite precision in measuring Planck's constant. Additional examples are given in fluid mechanics and magnetohydrodynamics where there are fundamental changes in the fluid behaviour when making the transition from nonzero but very small values of the viscosity and the electrical resistivity to cases where these parameters are exactly equal to zero. Thus, the uncertainty in the absolute value of the nonzero photon rest mass does not necessarily imply that the corresponding theory is questionable. On the contrary, and as has been seen from the present analysis, such an unspecified rest mass rather becomes a strength of the theory. It namely makes variable ranges accessible of the effective radii, both for axisymmetric photon models and for corresponding light beams.

A number of possible methods for determining the photon rest mass have been proposed by several investigators, as described in a recent review[18]. These proposals concern such phenomena as the cosmical redshift, the cosmical background radiation, and the Goos-Hänchen and Sagnac effects. As found by de Broglie and Vigier[31,32] these two latter

effects require unconventional explanations, as being based on a small photon rest mass.

The present theory could in principle, and under certain circumstances, also permit the phase and group velocities to become substantially smaller than c, i.e. when $\cos\alpha$ approaches unity. Thereby the total energy being associated with Eqs. (9.71) and (9.73) would be shared to a larger extent by the rest mass. In a way such a situation could possibly be related to the recently observed slowing-down process of light[94], but it should then be kept in mind that such a process takes place when the light passes through a medium with a refractive index larger than that of the vacuum, and where light interacts with the medium.

§ 9.4.2 The integrated field quantities

The local electric charge density of the present theory can have either sign. In the models of § 9.3, the total integrated charge still vanishes according to Eq. (9.63). To obtain zero net charge it does therefore not become necessary to assert that the photon is its own antiphoton.

The total integrated magnetic moment vanishes as well due to Eq. (9.65). Nevertheless there is a nonzero local and helical magnetic field which has a component in the axial direction of propagation. This component is invariant to Lorentz transformations with respect to the same direction, and it thus exists as a time-independent component in the rest frame. These features are reconcilable but not identical with those of the theory by Evans and Vigier[4]. The helicity of the photon magnetic field in the laboratory frame has further been considered by Evans and by Dvoeglazov in the volume by Evans et al.[7]

As shown by Eq. (9.79) a nonzero angular momentum only becomes possible when there is a nonzero rest mass (9.73) with an associated factor $\cos\alpha$. In its turn, this factor is related to a nonzero axial magnetic field component of the helical field configuration. For a vanishing rest mass we would thus be back to the conventional case of § 9.1.1 where there is no axial magnetic field.

§ 9.4.3 The dualism of the particle and wave concepts

The obtained wave packet solutions are in some respects similar to the earlier wave-particle duality by de Broglie. Thus the total energy $h\nu = mc^2$ in the laboratory frame could be regarded to consist of the fraction $(m - m_0)\,c^2$ of a "free" pilot wave propagating along the axis, plus the fraction $m_0 c^2$ of a "bound" particle-like state of radiation which circulates around the same axis. The rest mass then merely represents

an integrating part of the total energy. Such a subdivision into a particle and an associated pilot wave is therefore not necessary in the present case where the wave packet behaves as an entity, having both particle and wave properties at the same time.

A de Broglie wave length $\lambda = \frac{h}{p_z}$ related to the axial relativistic momentum p_z can also be deduced from the present theory. Thereby there are contributions to the total energy associated with the two energy flows along and around the axis.

Turning to the effective photon diameter of these wave packet models, we first notice that a convergent generating function leads to an individual photon diameter (9.85) which in some cases is rather limited, but still does not become small enough to match atomic dimensions. As an example, an average wave length $\lambda_0 = 3 \times 10^{-7}$m and a factor $\cos\alpha = 10^{-4}$ which makes the velocity v deviate from c by 5×10^{-9} only, results in a diameter $2\hat{r} \simeq 10^{-3}$ m. On the other hand such a diameter could become reconcilable with that of a radially polarized dense multiphoton beam.

A divergent generating function can on the other hand result in a very small photon diameter (9.95) for sufficiently small ε, then having the size of atomic dimensions such as the Bohr radius. This becomes reconcilable with the ability of the photon to knock out an electron from an atom in the photoelectric effect. It is consistent with the proposed "needle radiation" of energy quanta with a directed momentum as obtained by Einstein[95]. Also here a proposal on two limits of the photon diameter can be forwarded, in analogy with §6.7.3 and applying to the part of the radiation which circulates around the axis of symmetry.

In the two-slit experiment by Tsuchiya et al.[22], a light source of low intensity was used to emit single photons at each instant. The photons could pass any of the two narrow slits of a small separation distance at a first screen S_1 shown in Fig. 9.2, and then impinge on a second screen S_2. Each single photon produces one dot-shaped mark at S_2, like that formed by a needle-shaped bullet. At the same time each single photon appears to have passed through both slits, and this results in an interference pattern at S_2. The pattern becomes visible in the form of a large number of marks which appear after some time when many photons have reached S_2.

From the quantum mechanical point of view and due to the uncertainty principle, it becomes impossible to determine through which slit the photon passes, i.e. without destroying the diffraction pattern[33]. This is due to the change of momentum which would occur on account of an applied detector.

Irrespective of whether the photon is represented as a plane wave or as an axisymmetric wave packet, it can in a first interpretation be imagined to become divided into two parts that pass each aperture, and then join each other to produce an interference at the screen S_2. The dark parts of the interference pattern at the same screen should be considered as regions of forbidden transitions, i.e. with zero quantum mechanical probability. Moreover, the photon has the energy $h\nu_0$ both at its source and at the end point P on the screen. The imagined division of the photon into two parts which move along the two trajectories in Fig. 9.2 would at a first sight be in conflict with the quantization of its energy. A way out of this problem can be found in terms of the Heisenberg uncertainty principle. A randomness in phase can thus be assumed to arise when the two photon parts are separated and later reunited. Since a photon of limited axial extensions includes wavetrains in the direction of propagation, the average uncertainty in phase is expected to be of the order of half a wavelength λ_0. At the surface of the screen S_2 this can in its turn be interpreted as an uncertainty $\Delta t \simeq \frac{\lambda_0}{2c} = \frac{1}{2\nu_0}$ in time. This finally leads to an uncertainty $\Delta E \simeq \frac{h}{2\pi\Delta t} = \frac{h\nu_0}{\pi}$ in energy. The latter uncertainty then comes out to be of the order of half the energy $h\nu_0$, thus being carried on the average by each imagined photon part.

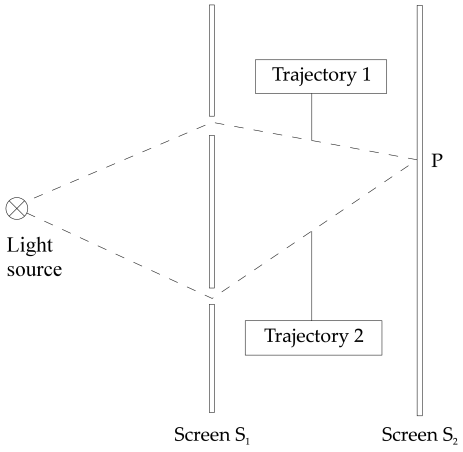

Figure 9.2: A two-slit experiment where an individual photon is emitted from a light source and appears to have passed through both slits of the Screen S_1, i.e. along both Trajectories 1 and 2 at the same time. The photon then ends up at the point P on the Screen S_2, in the form of a dot-shaped mark. When many photons have passed the system after each other, the resulting dot-shaped marks form an interference pattern on S_2. The separation distance between the slits is strongly exaggerated in the figure.

Recently Afshar et al.[96] have reported over a simultaneous determination of the wave and particle aspects of light in a two-slit "welcher-weg" experiment. Their results show that the single photon has particle and wave properties simultaneously. A particle-like photon thus passes

one of the pinholes, but an interference pattern can still be formed. Also this second interpretation appears to be consistent with the present theoretical model. The sampling can possibly be related to the long axial length of the wave packet and the ocurrence of a precursor at its front[24].

In the two-slit experiments the present needle-shaped wave packet model has an advantage over a plane wave model. The particle feature in the form of a very narrow needle-shaped transverse diameter makes the wave packet model reconcilable with the observed dot-shaped marks. At the same time the wave nature of the axisymmetric packet makes it possible for interference phenomena to occur, in the same way as for a plane wave. Two parts of such a wave packet which are 180° out of phase and meet at a point P on S_2 should namely also cancel each other by interference. This dualism and ability of interference becomes particularly obvious in the zero line width limit $\frac{1}{k_0 z_0} \to 0$ where the spectral distribution of Eq. (9.48) reduces to that of the elementary normal mode of §9.1.

The geometrical structure of the individual "localized" photon of the present theory is not in conflict with the concept of a quantum mechanical wave function. The latter represents the probability distribution of a photon before its position has been localized through a measurement.

§9.4.4 Possible applications to other bosons

The photon is the field quantum being responsible for the electromagnetic interaction. Likewise the weak field interaction acquires quanta, in the form of the W^+, W^-, and Z^0 bosons[21]. This raises the question whether an analogous Proca-type equation applied to the weak field case could result in axisymmetric solutions being similar to those deduced here for the electromagnetic field. This may provide the weak-field bosons with a nonzero rest mass, thereby arriving at a possible alternative to the Higgs particle concept.

§9.4.5 Proposed photon oscillations

The analysis performed so far may debouch into the idea that there exist different quantum states (modes) of the photon representing different solutions of the same basic equations. In a way this would become analogous to but not identical with the Copenhagen interpretation. Almost instantaneous transitions between these states also become imaginable. A similar situation has already been observed for neutrino oscillations which are associated with a nonzero neutrino rest mass. Consequently, it is here proposed that analogous "photon oscillations" can exist, by which rapid transitions between the various plane and axisymmetric

photon modes take place, under the constraints of total energy and angular momentum conservation. In this way the photon could behave differently in different physical situations. Such a preliminary proposal has, however, to be further investigated.

In a first attempt we outline some types of transition which could make it possible for the photon to interact on the atomic scale, such as in the photoelectric effect, as well as in other situations which require its energy to become spatially concentrated:

- A transition from the axisymmetric mode of §9.3.4 having a moderately large photon diameter to that of the "needle radiation" described in §9.3.5 is at least expected to face no difficulties with the conservation laws. A well-defined energy threshold is then preserved in the photoelectric interaction;
- A transition from an equivalent plane wave to any of the axisymmetric modes of Sections 9.3.4 and 9.3.5 is more complicated, since the plane wave has no angular momentum. For such a transition to become possible, it must occur as a three-mode event, similar to that of pair formation. The energy of the plane wave then has to be shared by two axisymmetric modes of either or both types given in the same sections, and the angular momenta of these modes must be antiparallel. To obtain a well-defined energy threshold, additional requirements have to be imposed. If there is only one mode of needle-shape involved, almost all the plane-wave energy has to be shared by this mode. But if there are instead two such modes, the energy should either be carried almost entirely by one of them, or both modes have to take part simultaneously in the energy transfer of the photoelectric interaction.

The proposed process of photon oscillations can become more specific in an example where a plane wave or a plane wave packet $(_p)$ is assumed suddenly to decay into two needle-shaped modes, $(_1)$ and $(_2)$, of the type deduced in §9.3.5. Here we limit ourselves to given values of the parameters $\cos\alpha$, ε of Eq. (9.89), and of the integrals (9.79) and (9.87). The φ components of the velocity vector (9.1) are now chosen to be antiparallel, as given by

$$C_{\varphi 1} = c\,(\cos\alpha) = -C_{\varphi 2}\,, \tag{9.100}$$

and being in accordance with the discussions at the beginning of §9.1. Energy conservation is then expressed by

$$h\nu_p = \frac{hc\varepsilon}{2\pi\,(\cos\alpha)}\left(\frac{1}{r_{01}} + \frac{1}{r_{02}}\right), \tag{9.101}$$

where use has been made of Eq. (9.95). Since the axial momentum is equal to $\frac{h\nu}{c}$ according to de Broglie, its balance becomes satisfied by Eq. (9.101) as well. For the balance of the angular momentum, the contributions from the two axisymmetric modes have to cancel each other. With relations (9.100) this leads to

$$h\nu_{01}r_{01} = h\nu_{02}r_{02}\,, \tag{9.102}$$

as obtained from combination of Eqs. (9.79) and (9.69). From the results (9.101) and (9.102) it is then seen that almost all the energy of the plane wave can be transferred to the needle-shaped mode $(_1)$, say, in the case of a very large ratio $\frac{r_{02}}{r_{01}}$. This then implies that mode $(_2)$ will possess a vanishingly small energy which is spread over a larger radius r_{02} in space, as compared to that of the mode $(_1)$.

The idea that the photon can exist in different states is also in a way related to the different possible forms of the electromagnetic energy density. Thus the field energy density (3.25) is evidently associated with the local energy in space of a propagating electromagnetic EM wave. On the other hand, when considering the axisymmetric state of an EMS wave packet, we can as well use the source energy density (3.26) when deducing the total mass.

§ 9.4.6 Thermodynamics of a photon gas

With a nonzero rest mass one would first expect a photon gas to have three degrees of freedom, i.e. two transverse and one longitudinal. Then Planck's radiation law would become altered by a factor of $\frac{3}{2}$, in contradiction with experience. A detailed analysis based on the Proca equation shows, however, that the part of the field being associated with the rest mass, the related angular momentum, and with the axial magnetic field component cannot be involved in a process of light absorption[4,6]. This is also made plausible by the axisymmetric wave packet model in which the axial part of the magnetic field behaves as a time-independent component in the rest frame, i.e. without having the features of a propagating wave. It is further observed that transverse photons cannot penetrate the walls of a cavity, whereas this becomes possible for longitudinal photons which do not contribute to the thermal equilibrium[41]. Consequently, Planck's law is recovered in all practical cases, also when there is a small nonzero photon rest mass[4,6].

The equations of state of the photon gas have further been considered by Mészáros[58] and Molnár[59] who found that Planck's distribution and the Wien and Rayleigh-Jeans laws cannot be invariant to adia-

batic changes of state which occur in an ensemble of photons. This dilemma is due to the fact that the changes of state cannot be adiabatic and isothermal at the same time. Probably the cause of the contradiction is a lack of longitudinal (axial) magnetic flux density in the original and standard treatments. These questions require further investigations.

§ 9.5 Light beams

Depending on the geometrical configuration to be investigated, and on the boundary and initial conditions to be imposed, the individual photon can in principle be treated as an equivalent plane wave or as an axisymmetric wave packet. When proceeding to the transition from a stream of individual photons of low density to a beam of high photon density, the analysis becomes straightforward when plane waves can be applied, but not when the beam is formed by a stream of axisymmetric wave packets. Being far from an easy issue, this latter case will be shortly discussed in the following subsections, in terms of crude tentative considerations.

§ 9.5.1 Density parameters

We consider a beam consisting of individual axisymmetric photon wave packets of narrow line width, and where the macroscopic breadth of the beam is much larger than the effective radius $\hat{r}$ of an individual packet. With the volume density n_p of photons, the mean transverse distance between the packet centra becomes

$$d = \left(\frac{1}{n_p} \right)^{1/3} . \tag{9.103}$$

The energy $h\nu_0$ of each photon then results in an energy flux per unit area

$$\psi_p = n_p \, v \, h \, \nu_0 \simeq \frac{n_p \, h \, c^2}{\lambda_0} \tag{9.104}$$

according to Eqs. (9.32), (9.71), and (9.72). In this connection the ratio

$$\theta_\perp = \frac{d}{2\hat{r}} \tag{9.105}$$

between the mean separation distance and the effective photon diameter will be of special interest. Introducing the results (9.85) or (9.95) this ratio has the alternative values

$$\theta_\perp = \pi \left(\frac{h \, c^2}{\psi_p \, \lambda_0^4} \right)^{1/3} \cdot \; (\cos \alpha) \left\{ \begin{array}{c} 1 \\ 1/\varepsilon \end{array} \right\} , \tag{9.106}$$

where the upper factor refers to Eq. (9.85) and the lower to Eq. (9.95). Multiphoton states[27] are not considered here, but could somewhat modify the analysis.

Since $\hat{r}$ is a rather sharply defined radius according to the previous deductions, there is a critical value $\theta_{\perp c} \simeq 1$ of the ratio (9.103) for a beginning transverse packet overlapping, as given by

$$(\psi_p \lambda_0^4)\, \frac{\theta_{\perp c}}{(\cos\alpha)^3} \cdot \left\{ \begin{array}{c} 1 \\ \varepsilon^3 \end{array} \right\} \simeq \pi^3 h c^2 \simeq 1.85 \times 10^{-15} \left[\mathrm{W \cdot m^2}\right]. \qquad (9.107)$$

There is in principle also a longitudinal (axial) overlapping of consecutive wave packets situated on exactly the same axis. Such packets can match their phases and combine into more elongated wave trains having a more narrow line width. This would have no additional consequences on the beam formation and does not require further consideration.

Transverse packet overlapping implies on the other hand that the individual photon fields would interfere with each other. The axisymmetric solutions of an individual wave packet then break down, and the analysis of Sections 9.1–9.4 in no longer applicable.

§ 9.5.2 Energy flux preservation

The quantization and preservation of the beam energy flux has to be imposed as a necessity.

In the case of transverse field overlapping a tentative approach is then proposed, by assuming that the deficit of beam energy due to a cancellation of the axisymmetric EMS wavepacket fields by interference is compensated by the energy contribution from a simultaneously appearing plane wave of the EM or EMS type. This assumption also preserves a wave system which has phase and group velocities in the direction of the beam, i.e. with wave fronts being perpendicular to the direction of propagation. Consequently an ansatz

$$\psi_p = \psi_{EMS} + \psi_{PL} \qquad (9.108)$$

is made where ψ_{EMS} and ψ_{PL} are the contributions to the total energy flux from the individual axisymmetric EMS fields and from the plane wave. In the regime $\theta_\perp \gg \theta_{\perp c}$ of negligible overlapping we then have $\psi_p = \psi_{EMS}$, whereas the regime $\theta_\perp \ll \theta_{\perp c}$ of strong overlapping leads to the limit $\psi_p = \psi_{PL}$.

In the tentative approach of Eq. (9.108) there arises an additional question about the preservation of angular momentum. In a low-density

beam with no overlapping the photon wave packets all carry their own spin. A high-density beam which has been converted into a plane wave system would on the other hand have no angular momentum, as long as the wave has infinite transverse extensions. The angular momentum of a beam with a finite transverse cross-section can on the other hand still be preserved. This is due to the transverse derivatives which exist at the boundaries of the beam, and which contribute to an angular momentum[23,97]. The angular momenta which would have existed for the individual photons within the volume of the beam are then imagined to become substituted by the momentum generated at the bounding surface. Such a situation somewhat resembles that of gyrating charged particles in a magnetized and bounded plasma body. There the diamagnetic contributions from all the freely gyrating particles within the plasma volume cancel each other, and become substituted by a diamagnetism produced by an electric current which circulates along the plasma boundary.

Thus, a light beam with a spatially limited cross-section and an angular momentum can in principle be described by the present revised theory[19], in analogy with the deductions of § 9.3.3 which apply to the individual photon. Then a rectangular frame becomes appropriate to the study of a linearly or elliptically polarized beam core. Such a study applies as well to the limit of an individual photon with a linearly polarized core and with an internal structure. But it does not deal with the entangled quantum states of two interacting photons. Also in this case conventional theory merely leads to a vanishing angular momentum.

§ 9.5.3 Applications to present wave packet models

A convergent generating function results in an effective photon diameter (9.85) which becomes rather limited in some cases. As an example, a wave length $\lambda_0 = 3 \times 10^{-7}$m and a factor $\cos\alpha = 10^{-4}$ result in a diameter $2\hat{r} \simeq 10^{-3}$m. In a corresponding photon beam where the intensity exceeds about $2 \times 10^{-4}\,\mathrm{W/m^2}$, adjacent wave packets would then overlap according to Eq. (9.106).

In the case of a divergent generating function, however, the photon diameter (9.95) with $\varepsilon \ll \cos\alpha$ for needle radiation should become quite small. The critical value for the energy flux (9.104) then becomes considerably higher than in the former case (9.85) of a convergent generating function. Adjacent wave packets then have a much larger parameter range within which they do not overlap, and where the beam consists of a stream of individual axisymmetric wave packets.

§9.6 Modes with a periodic angular dependence

As described in a review article by Battersby[98], a number of new results have recently been reported on twisted light beams in which the energy travels in a corkscrew-shaped path, spiralling around the beam's central axis. In the experimental set-ups being used, a single helix beam geometry can be achieved, as well as helix forms of increasing multiplicity, all with an orbital angular momentum. It has also been observed that such a corkscrew laser beam creates a ring of light with a dark centre of its cross-section. The question has further been raised whether even a single photon with an angular momentum can become "twisted". Such a feature is supported by an investigation by Mair and collaborators[99]. These discoveries are expected to become important by introducing new and more efficient methods into the field of communication, and by providing microscopic laser "spanners" and "motors" which form new tools in microbiology. A pulse of twisted light, or even a single twisted photon, can hold a lot of information, because there are many more states (modes) to choose from than those being available in the case of conventional light.

In this treatise it is first shown that light beams or individual photons, having limited transverse dimensions in space and a nonzero angular momentum, cannot be described in terms of conventional theory based on Maxwell's equations. In its turn, this leads to an analysis based on the present extended(revised) electromagnetic theory which results in beam and photon models possessing an angular momentum, a limited transverse spatial extension, and several other main features of twisted light.

In finishing this chapter, we shall consider such modes which are not strictly axisymmetric but also depend periodically on the angular coordinate φ of a cylindrical frame (r, φ, z). Thus the electric field is assumed to have the form

$$\mathbf{E} = \hat{\mathbf{E}}(\rho)\, e^{i(-\omega t + \bar{m}\varphi + kz)} \equiv \hat{\mathbf{E}}(\rho)\, e^{i\theta_m}, \qquad \rho = \frac{r}{r_0}\,. \tag{9.109}$$

The form (9.109) represents the general case of cylindrical waves to be treated here, and like the strictly axisymmetric case of §9.1 it will lead to nearly radially polarized electric field solutions. Thus elliptically polarized dense plane-wave beams are not included in this concept. Here the phase factor θ_m represents screw-shaped(twisted) modes at a given time t. The parameter $\bar{m}$ is a positive or negative integer, the various values of which represent different states of twisted photons or light beams. For a single corkscrew-shaped beam with $\bar{m} = \pm 1$, the axial

distance between the crests becomes equal to the wave length $\lambda = \frac{2\pi}{k}$. We further assume the velocity vector still to have the form (9.1). With the operator (9.2) the basic equation (4.2) and the associated relation (4.3) then become

$$\left(D_1 - \frac{1}{r^2} + \frac{1}{r^2}\frac{\partial^2}{\partial\varphi^2}\right) E_r - \frac{2}{r^2}\frac{\partial}{\partial\varphi} E_\varphi = \frac{\partial}{\partial r}(\operatorname{div}\mathbf{E}), \tag{9.110}$$

$$\left(D_1 - \frac{1}{r^2} + \frac{1}{r^2}\frac{\partial^2}{\partial\varphi^2}\right) E_\varphi + \frac{2}{r^2}\frac{\partial}{\partial\varphi} E_r = \\ = \left[\frac{1}{r}\frac{\partial}{\partial\varphi} + \frac{1}{c}(\cos\alpha)\frac{\partial}{\partial t}\right](\operatorname{div}\mathbf{E}), \tag{9.111}$$

$$\left(D_1 + \frac{1}{r^2}\frac{\partial^2}{\partial\varphi^2}\right) E_z = \left[\frac{\partial}{\partial z} + \frac{1}{c}(\sin\alpha)\frac{\partial}{\partial t}\right](\operatorname{div}\mathbf{E}), \tag{9.112}$$

and

$$\left[\frac{\partial}{\partial t} + c(\cos\alpha)\frac{1}{r}\frac{\partial}{\partial\varphi} + c(\sin\alpha)\frac{\partial}{\partial z}\right](\operatorname{div}\mathbf{E}) = 0, \tag{9.113}$$

where

$$\operatorname{div}\mathbf{E} = \left(\frac{\partial}{\partial r} + \frac{1}{r}\right) E_r + \frac{1}{r}\frac{\partial}{\partial\varphi} E_\varphi + \frac{\partial}{\partial z} E_z. \tag{9.114}$$

In this connection the momentum equation (3.16) also has to be considered, with the resulting volume force

$$\mathbf{f} = \bar{\rho}(\mathbf{E} + \mathbf{C}\times\mathbf{B}). \tag{9.115}$$

Here the Poynting vector of Eq. (3.19) has the φ component

$$S_\varphi = \frac{E_z B_r - E_r B_z}{\mu_0} \tag{9.116}$$

to be taken into account when considering the density (9.76) of angular momentum.

Relation (9.113), which is obtained from taking the divergence of the basic equation (3.6), can be used as a suitable divider of possible options in this analysis:

- When $\operatorname{div}\mathbf{E} = 0$ there is a conventional EM mode;
- When $\operatorname{div}\mathbf{E} \neq 0$ there are three types of extended EMS modes. As the first we recover the mode with $\frac{\partial}{\partial\varphi} = 0$ being treated in the previous Sections 9.1–9.4. The second is a mode with $\cos\alpha = 0$ and no rest mass. The third is represented by the general case of Eqs. (9.110)–(9.113).

With the phase factor of Eq. (9.109) the basic equations (9.110)–(9.112) reduce to the system

$$\left(\frac{\bar{m}^2}{r^2}+k^2-\frac{\omega^2}{c^2}\right)E_r+\frac{\bar{m}}{r}\left(\frac{\partial}{\partial r}+\frac{1}{r}\right)(iE_\varphi)+k\,\frac{\partial}{\partial r}(iE_z)=0\,, \quad (9.117)$$

$$\left[\frac{\bar{m}}{r}\left(\frac{\partial}{\partial r}-\frac{1}{r}\right)-\frac{\omega}{c}\,(\cos\alpha)\left(\frac{\partial}{\partial r}+\frac{1}{r}\right)\right]E_r+$$
$$+\left[\frac{\partial^2}{\partial r^2}+\frac{1}{r}\frac{\partial}{\partial r}-\frac{1}{r^2}-k^2+\frac{\omega^2}{c^2}-\frac{\omega}{c}\,(\cos\alpha)\,\frac{\bar{m}}{r}\right](iE_\varphi)+$$
$$+k\left[\frac{\bar{m}}{r}-\frac{\omega}{c}\,(\cos\alpha)\right](iE_z)=0\,, \quad (9.118)$$

$$\left[k-\frac{\omega}{c}\,(\sin\alpha)\right]\left[\left(\frac{\partial}{\partial r}+\frac{1}{r}\right)E_r+\frac{\bar{m}}{r}\,(iE_\varphi)\right]+$$
$$+\left\{\frac{\partial^2}{\partial r^2}+\frac{1}{r}\frac{\partial}{\partial r}-\frac{\bar{m}^2}{r^2}+\frac{\omega}{c}\left[\frac{\omega}{c}-k\,(\sin\alpha)\right]\right\}(iE_z)=0\,, \quad (9.119)$$

and Eq. (9.113) turns into

$$\left[\omega-k\,c\,(\sin\alpha)-\frac{\bar{m}}{r}\,c\,(\cos\alpha)\right](\mathrm{div}\,\mathbf{E})=0\,. \quad (9.120)$$

§ 9.6.1 The conventional EM mode

In the case of the conventional EM mode where $\mathrm{div}\,\mathbf{E}$ and $\mathbf{C}$ vanish and there is no photon rest mass, we have $\omega = kc$ and Eqs. (9.109)–(9.113) reduce to the set

$$\left[\frac{\partial^2}{\partial\rho^2}+\frac{1}{\rho}\frac{\partial}{\partial\rho}-\frac{1}{\rho^2}(1+\bar{m}^2)\right](E_r, iE_\varphi)-\frac{2\bar{m}}{\rho^2}\,(iE_\varphi, E_r)=0\,, \quad (9.121)$$

$$\left[\frac{\partial^2}{\partial\rho^2}+\frac{1}{\rho}\frac{\partial}{\partial\rho}-\frac{\bar{m}^2}{\rho^2}\right]E_z=0\,. \quad (9.122)$$

There are relations being analogous to Eqs. (9.121)–(9.122) for the magnetic field $\mathbf{B}$ in this case, but not in the general case where $\mathrm{div}\,\mathbf{E}\neq 0$. The conventional condition $\mathrm{div}\,\mathbf{E}=0$ yields

$$-i\,k\,r_0\,E_z=\frac{1}{\rho}\frac{\partial}{\partial\rho}\,(\rho\,E_r)+\frac{\bar{m}}{\rho}\,(iE_\varphi)\,. \quad (9.123)$$

In the z direction Eq. (9.122) gives the general solution for $\bar{m}\neq 0$ having the form

$$E_z=(c_{1z}\,\rho^{\bar{m}}+c_{2z}\,\rho^{-\bar{m}})\,e^{i\theta_m}, \quad (9.124)$$

and in the transverse direction Eqs. (9.121) combine to

$$E_r = \left[c_{1r}\, \rho^{1\pm\bar{m}} + c_{2r}\, \rho^{-(1\pm\bar{m})} \right] e^{i\theta_m} = \pm i E_\varphi \,, \quad (1 \pm \bar{m} \neq 0) \quad (9.125)$$

when $1 \pm \bar{m} \neq 0$. Here it is observed that $\bar{m} = 0$ brings us back to the case already discussed in § 9.1.1, as given by Eqs. (9.16) and (9.17). When on the other hand $1 \pm \bar{m} = 0$ the solution becomes

$$E_r = \left[c_{1r_0} + c_{2r_0} \ln\rho \right] e^{i\theta_m} = \pm i E_\varphi \,, \qquad (1 \pm \bar{m} = 0) \,. \qquad (9.126)$$

However, all the general solutions (9.124)–(9.126) are either divergent at the origin or at large distances from it. It is further seen from Eq. (9.115) that the volume forces vanish in the conventional limit. The axial component of the angular momentum per unit volume is then given by

$$s_z = \frac{(\mathbf{r} \times \mathbf{S})_z}{c^2} = \varepsilon_0\, r\, (E_z B_r - E_r B_z) \,, \qquad (9.127)$$

where $\mathbf{r}$ is the radius vector from the origin. Thus, a nonzero angular momentum can only arise for nonzero field components (E_r, E_z) and (B_r, B_z). But such components always become divergent in space, and this is not acceptable from the physical point of view. Moreover, and what again becomes a serious additional constraint as in the case of Eq. (9.17), the electric field divergence has to vanish for all $(\rho, \bar{m}, k)$, such as for an arbitrary spectrum of a wave packet. This makes the component E_z disappear, in the same way as B_z. Then the Poynting vector has only a component in the direction of propagation, and there is again no spin with respect to the z axis. The same result has also been obtained by Stratton[24] in the limit $\omega = \pm kc$.

Consequently, a photon model based on the conventional screw-shaped mode, and on an arbitrary value of the parameter (9.11), would also lead to the unacceptable result of infinite field energy. This can only be avoided in a wave guide where there is a limiting wall.

§ 9.6.2 An extended EMS mode with vanishing rest mass

When $\cos\alpha = 0$ and $\operatorname{div}\mathbf{E} \neq 0$ the solution of Eq. (9.113) has the form of a dispersion relation $\omega = kc$ which corresponds to a vanishing rest mass. Eq. (9.110) then reduces to

$$E_r = -\frac{1}{\bar{m}} \left(\rho\, \frac{\partial}{\partial\rho} + 1 \right) (iE_\varphi) - i\, \frac{k r_0}{\bar{m}^2}\, \rho^2\, \frac{\partial}{\partial\rho}\, E_z \,. \qquad (9.128)$$

This expression for E_r can be substituted into Eq. (9.111) to result in Eq. (9.122) for E_z. The same equation is also obtained from relation

(9.112) when $\sin\alpha = 1$ and the dispersion relation $\omega = kc$ is satisfied. This shows that Eqs. (9.110)–(9.112) are no longer independent of each other.

Eq. (9.122) yields solutions (9.124) which are divergent, and we are now free to limit ourselves to the case $E_z \equiv 0$. It is then seen from Eq. (9.128) that iE_φ can be considered as an arbitrary generating function which determines E_r, thereby satisfying Eqs. (9.110)–(9.112). Moreover, when inserting E_r from Eq. (9.128) into Eq. (3.7), the axial magnetic field component becomes

$$B_z = i\,\frac{\rho}{\bar{m}\,c}\,\frac{\partial}{\partial\rho}\,E_z \tag{9.129}$$

and thus vanishes when $E_z \equiv 0$. From Eqs. (3.7) we further obtain $cB_r = -E_\varphi$ and $cB_\varphi = E_r$, and this shows that the force (9.115) vanishes. The angular momentum will then also vanish according to Eqs. (9.116) and (9.76).

A particular example can be given in choosing a convergent and limited configuration in space, as given by

$$iE_\varphi = E_0\,\rho^\alpha\left[e^{-\beta\rho}\right]e^{i\theta_m} \tag{9.130}$$

with positive values of α and β. Eq. (9.128) then yields

$$-\frac{\bar{m}\,E_r}{iE_\varphi} = \alpha + 1 - \beta\,\rho\,. \tag{9.131}$$

The function (9.130) has a maximum at the radius $\rho = \hat{\rho} = \frac{\alpha}{\beta}$ for which the amplitude ratio $\left|\frac{E_r}{E_\varphi}\right| = 1$ when $\bar{m} = \pm 1$. Near this relatively flat maximum the resulting electric field then becomes somewhat like a "linearly polarized" wave. The configuration of Eq. (9.130) can further be limited to a narrow region around the z axis, by choosing a sufficiently large β.

A spectrum of this elementary mode with a vanishing spin can finally be made to form a wave packet of finite axial length. The corresponding total energy and mass can then be obtained from the energy density (3.25), and be quantized in terms of the frequency $\nu_0 = \frac{c}{\lambda_0}$ in the case of a narrow line width.

§9.6.3 The general type of screw-shaped EMS mode

In the general case of Eqs. (9.110)–(9.113) the formalism appears to be in a more complicated state. Thus an exact solution has so far neither been found in terms of a generating function including all the three electric

field components, nor without such a function. This also applies to a situation where there is a nonzero radial component C_r of the velocity vector, and to attempts in solving Eq. (9.113) by means of the method of characteristic curves.

To proceed further there is a first approximation and iteration available from the case of a small but nonzero photon rest mass, as expressed by the condition (9.32) and a related approximate dispersion relation (9.22), then being obtained from Eq. (9.120). With $\delta \equiv \cos\alpha$ this implies that

$$k^2 - \frac{\omega^2}{c^2} \simeq k^2(\cos\alpha)^2 \equiv k^2\delta^2. \tag{9.132}$$

Then Eqs. (9.117)–(9.119) become

$$\left(\frac{\bar{m}^2}{r^2} + k^2\delta^2\right) E_r + \frac{\bar{m}}{r}\left(\frac{\partial}{\partial r} + \frac{1}{r}\right)(iE_\varphi) + k\,\frac{\partial}{\partial r}(iE_z) = 0\,, \tag{9.133}$$

$$\begin{aligned}\left[\frac{\bar{m}}{r}\left(\frac{\partial}{\partial r} - \frac{1}{r}\right) - k\,\delta\left(1 - \frac{1}{2}\,\delta^2\right)\left(\frac{\partial}{\partial r} + \frac{1}{r}\right)\right] E_r + \\ + \left[\frac{\partial^2}{\partial r^2} + \frac{1}{r}\,\frac{\partial}{\partial r} - \frac{1}{r^2} - k^2\delta^2 - \frac{\bar{m}}{r}\,k\,\delta\left(1 - \frac{1}{2}\delta^2\right)\right](iE_\varphi) + \\ + k\left[\frac{\bar{m}}{r} - k\,\delta\left(1 - \frac{1}{2}\,\delta^2\right)\right](iE_z) = 0\,,\end{aligned} \tag{9.134}$$

$$k\,\delta^2\left[\left(\frac{\partial}{\partial r} + \frac{1}{r}\right) E_r + \frac{\bar{m}}{r}(iE_\varphi)\right] + \left(\frac{\partial^2}{\partial r^2} + \frac{1}{r}\,\frac{\partial}{\partial r} - \frac{\bar{m}^2}{r^2}\right)(iE_z) = 0\,. \tag{9.135}$$

The lowest order approximation of small δ is now studied for these equations. Thereby a negligible axial component E_z becomes reconcilable with a magnitude being of the order of δ^2 as compared to the components E_r and E_φ. As will be seen later, the same approximation will not rule out the influence of an axial magnetic field component B_z.

We first turn to Eq. (9.133) which is multiplied by the factor $(\frac{\bar{m}}{r})^2 - \delta^2$, to result in

$$E_r \simeq -\frac{r}{\bar{m}}\left[1 - k^2\delta^2\left(\frac{r}{\bar{m}}\right)^2\right]\left(\frac{\partial}{\partial r} + \frac{1}{r}\right)(iE_\varphi) \tag{9.136}$$

in a first approximation. When inserting this relation into Eq. (9.134) the latter is found to become identically satisfied for small δ. Finally, Eq. (9.135) also becomes approximately satisfied for $E_z \simeq 0$ and small δ.

With the result (9.136) and $E_z \simeq 0$, the component iE_φ can be used as a generating function F which determines the total electric field

through Eq. (9.136). Thus we write

$$iE_\varphi = F = G_0 G\,, \qquad G = R(\rho)\, e^{i\theta_m}, \tag{9.137}$$

where G_0 is a characteristic amplitude, and G a dimensionless part with $\rho = \frac{r}{r_0}$. Contrary to the conventional case of §9.6.1 there now remains a degree of freedom in choosing the function $R(\rho)$ such as to become physically acceptable throughout the entire space.

The normal modes are now superimposed to form a wave packet of finite axial length, in analogy with §9.2. The packet is assumed to have the spectral amplitude

$$\tilde{A}_k = \left(\frac{1}{k_0}\right) e^{-z_0^2 (k-k_0)^2} \tag{9.138}$$

in the interval dk, and being centered around the wave number $k_0 = \frac{2\pi}{\lambda_0}$ defined by the main wavelength λ_0. Further $2z_0$ represents the effective axial length of the packet. We introduce the axial coordinate

$$\bar{z} = z - v\,t\,, \qquad v = c\,(\sin\alpha)\,, \tag{9.139}$$

which follows the propagating packet, and consider the integral

$$\int_{-\infty}^{+\infty} \tilde{A}_k\, e^{ik\bar{z}}\, dk = \frac{\sqrt{\pi}}{k_0 z_0} \exp\left[-\left(\frac{\bar{z}}{2z_0}\right)^2 + ik_0\bar{z}\right]. \tag{9.140}$$

The analysis has also to be restricted to a narrow line width to agree with experimental observations, and this leads to the condition $k_0 z_0 \gg 1$.

To lowest order the wave packet electric field components now become

$$i\bar{E}_\varphi = E_0\, R(\rho)(\sin\bar{m}\varphi)\,, \tag{9.141}$$

$$\bar{E}_r = -E_0 \left[1 - k_0^2\,\delta^2 \left(\frac{\rho r_0}{\bar{m}}\right)^2\right] \frac{\rho}{\bar{m}} \left(\frac{\partial}{\partial\rho} + \frac{1}{\rho}\right) R(\rho)(\sin\bar{m}\varphi)\,, \tag{9.142}$$

where

$$E_0 = a_0 \exp\left[-\left(\frac{\bar{z}}{2z_0}\right)^2 + ik_0\bar{z}\right], \qquad a_0 = \frac{\sqrt{\pi}\,G_0}{k_0 z_0}\,, \tag{9.143}$$

and we have chosen the $\sin\bar{m}\varphi$ part of the function $\exp(i\bar{m}\varphi)$. The corresponding magnetic field becomes

$$\bar{\mathbf{B}} = \left[i\,\frac{k_0}{\omega}\,(i\bar{E}_\varphi)\,,\ \ \frac{k_0}{\omega}\,\bar{E}_r\,,\ \ \frac{\bar{m}}{\omega r_0 \rho}\,\bar{E}_r + \frac{1}{\omega r_0 \rho}\,\frac{\partial}{\partial\rho}\,(i\bar{E}_\varphi\rho)\right]. \tag{9.144}$$

Here the axial magnetic field component is seen from a combination with Eq. (9.142) to reduce to

$$\bar{B}_z = -k_0^2\,\delta^2 E_0\,\frac{r_0}{\omega}\,\frac{1}{\bar{m}^2}\,\rho^2\left(\frac{\partial}{\partial\rho}+\frac{1}{\rho}\right)R(\sin\bar{m}\varphi)\,. \tag{9.145}$$

In the analysis which follows we choose a function

$$E_0(\bar{z}) = a_0\exp\left[-\left(\frac{\bar{z}}{2z_0}\right)^2\right](\sin k_0\bar{z})\,, \tag{9.146}$$

which is antisymmetric with respect to the axial centre $\bar{z}=0$ of the moving wave packet. This implies that also $\bar{E}_r$ and $i\bar{E}_\varphi$ of Eqs. (9.141) and (9.142) become antisymmetric with respect to $\bar{z}$.

The integrated(net) electric charge is given by

$$\begin{aligned} q = \varepsilon_0\int(\operatorname{div}\mathbf{E})\,dV = \varepsilon_0\,r_0\int_0^{2\pi}\!\!\int_0^{\infty}\left[\frac{\partial}{\partial\rho}\left(\rho\int_{-\infty}^{+\infty}\bar{E}_r\,d\bar{z}\right)+\right. \\ \left.+\,\bar{m}\int_{-\infty}^{+\infty}(i\bar{E}_\varphi)\,d\bar{z}\right]d\rho\,d\varphi = 0\,. \end{aligned} \tag{9.147}$$

This result holds even before carrying out the integration with respect to ρ and φ, because q disappears on account of the antisymmetry of $\bar{E}_r$ and $i\bar{E}_\varphi$. A disappearing total charge would also result from the obtained surface integral due to Gauss' theorem, provided that the field quantities vanish at the origin and at infinity. Since we shall later also treat a function R which is divergent at the origin, however, the result $q=0$ will here be based on the antisymmetry just being mentioned.

The integrated magnetic moment further becomes

$$\begin{aligned} M &= \varepsilon_0\int_{-\infty}^{+\infty}\int_0^{2\pi}\left[\int_0^{\infty}(\operatorname{div}\mathbf{E})\,c\,(\cos\alpha)\,\pi r^2\,dr\right]d\varphi\,d\bar{z} = \\ &= \pi\,\varepsilon_0\,c\,(\cos\alpha)\,r_0^2\int_0^{2\pi}\!\!\int_0^{\infty}\left[\rho\,\frac{\partial}{\partial\rho}\left(\rho\int_{-\infty}^{+\infty}\bar{E}_r\,d\bar{z}\right)+\right. \\ &\left.+\,\bar{m}\,\rho\int_{-\infty}^{+\infty}(i\bar{E}_\varphi)\,d\bar{z}\right]d\rho\,d\varphi = 0 \end{aligned} \tag{9.148}$$

for the same symmetry reasons as those applying to the total charge.

In the local energy equation (3.20) we consider the first term of the right-hand member. With the present approximation where $\bar{E}_z$ is neglected and $C_\varphi = c\cdot\delta$ is small, the contribution from this term becomes negligible as compared to the second term. Consequently the energy

density can be written as given by the form (3.25). The main contributions to w_f then originate from the components (E_r, E_φ, B_r, B_φ). Here the periodic dependence and the phase differences have to be taken into account when performing an integration over a period of oscillation and over the volume elements. With the field components given by Eqs. (9.141)–(9.144), the average local energy density of the packet can be written as

$$\bar{w} = \frac{1}{2}\,\varepsilon_0\,(\bar{E}_r^2 + \bar{E}_\varphi^2) \tag{9.149}$$

in the present approximation. From expressions (9.146) and the integral

$$\int_{-\infty}^{+\infty} E_0^2\,d\bar{z} = \left(\frac{\sqrt{\pi}\,G_0}{k_0 z_0}\right)^2 \int_{-\infty}^{+\infty} (\sin k_0\bar{z})^2\,e^{-2(\bar{z}/2z_0)^2}\,d\bar{z} \simeq \simeq G_0^2\,\frac{\pi^{3/2}}{k_0^2 z_0\sqrt{2}} \tag{9.150}$$

for a small line width, we then obtain an integrated total mass

$$m = \frac{1}{c^2}\int \bar{w}\,dV = \frac{1}{c^2}\,A_0\,r_0^2\,W_m \tag{9.151}$$

with

$$A_0 = \pi^{5/2}\,\varepsilon_0\,G_0^2\,\frac{z_0}{k_0^2 z_0^2\sqrt{8}}\,, \tag{9.152}$$

$$W_m = \int_{\rho_m}^{\infty} \rho\left\{\left[\left(\rho\,\frac{\partial}{\partial\rho} + 1\right)R\right]^2 + R^2\right\}\,d\rho\,. \tag{9.153}$$

Here $\rho_m = 0$ and $\rho_m \neq 0$ for the options of convergent and divergent forms at the origin $\rho = 0$ of the function R.

Considering the momentum equation (3.16) we introduce the field

$$\mathbf{E}' = \mathbf{E} + \mathbf{C}\times\mathbf{B}\,. \tag{9.154}$$

In the present approximation Eq. (9.144) then combines with Eq. (9.154) to the field components

$$\bar{E}_r' = \bar{B}_z c\,(\cos\alpha)\,, \tag{9.155}$$

$$\bar{E}_\varphi' = 0\,, \tag{9.156}$$

$$\bar{E}_z' = \bar{E}_\varphi(\cos\alpha)\,. \tag{9.157}$$

Thus $\bar{E}_r'$ is of the order δ^3 and can readily be neglected, $\bar{E}_\varphi'$ vanishes, and $\bar{E}_z'$ is of first order in δ. Concerning the axial force component $\bar{\rho}E_z'$

of Eq. (3.16) it is further observed that it includes the factors div $\mathbf{E}$ and E_φ which vary as $\sin \bar{m}\varphi$ and $\cos \bar{m}\varphi$ due to Eqs. (9.110)–(9.112) and (9.114). Integration of the axial force from $\varphi = 0$ to $\varphi = 2\pi$ then yields a vanishing net result. Only the electromagnetic momentum density (3.19) thus remains to be considered for the wave packet in its entirety. The related angular momentum density is then given by the conventional expression (9.76). In the present approximation it reduces to

$$\bar{\mathbf{s}} \simeq \varepsilon_0 \left[0, \quad r \frac{k_0}{\omega} (\bar{E}_r^2 + \bar{E}_\varphi^2), \quad -r \bar{E}_r \bar{B}_z \right] \tag{9.158}$$

since $|\bar{B}_r|$ is proportional to $|i\bar{E}_\varphi|$ according to Eq. (9.114), and $\left|\frac{\bar{E}_r}{i\bar{E}_\varphi}\right| \gg 1$ as shown later here when having specified the radial function $R(\rho)$.

The axial spin component $\bar{s}_z$ is of particular interest to this study. Its volume integral becomes

$$s \equiv \int \bar{s}_z \, dV = -\frac{1}{\bar{m}^3} \frac{k_0}{c} A_0 r_0^4 \delta^2 W_s \,, \tag{9.159}$$

where

$$W_s = \int_{\rho_s}^{\infty} \rho^3 \left[\left(\rho \frac{\partial}{\partial \rho} + 1 \right) R \right]^2 d\rho \,. \tag{9.160}$$

In analogy with the integral (9.153) the lower limits are here $\rho_s = 0$ and $\rho_s \neq 0$ for convergent and divergent forms of R. The result (9.159) shows that there are two possible spin directions, depending upon the sign of $\bar{m}$.

In the present helical configuration the Poynting vector thus has one component in the direction of propagation, and one in the direction around the z axis, as obtained in the present approximation.

The results (9.151) and (9.159) are now applied, either to a dense light beam which includes a large number N of photons per unit length, or to an individual and free photon ($N = 1$). In the case of a dense beam it is further assumed that the average distance d between the photons is smaller than the effective transverse diameter $2\hat{r}$ of an individual photon. In this case the photon fields overlap each other. These conditions will be further discussed in the following sections.

Using the energy concepts by Einstein and Planck, Eqs. (9.151) and (9.159) now lead to the quantum conditions

$$mc^2 = A_0 r_0^2 W_m = \frac{Nhc}{\lambda_0} \,, \tag{9.161}$$

$$|s| = \frac{1}{|\bar{m}|^3} \frac{2\pi}{c\lambda_0} A_0 r_0^4 \delta^2 W_s = \frac{Nh}{2\pi} \tag{9.162}$$

for photons in the capacity of boson particles. Combination of Eqs. (9.161) and (9.162) results in

$$2r_0 = \frac{\lambda_0}{\pi\delta}\,|\bar{m}|^{3/2}\left(\frac{W_m}{W_s}\right)^{1/2} \tag{9.163}$$

both for a dense beam and for an individual photon, under the conditions just being specified.

To proceed further with the analysis, the radial part $R(\rho)$ of the generating function and corresponding integrals have now to be specified. This concerns two cases, namely when R is convergent all over space, and when R diverges at the origin, in analogy with the earlier analysis of Sections 9.3.4 and 9.3.5. One option is to adopt a radial part R which is finite at the origin $\rho = 0$ and which vanishes at large ρ. These requirements are met by

$$R = \rho^\gamma\, e^{-\rho}, \qquad \rho = \frac{r}{r_0}\,, \tag{9.164}$$

where $\gamma \gg 1$. As in §9.3.4 the final result then becomes independent of γ. The form (9.164) has a rather sharp maximum at $\rho = \hat{\rho} = \gamma$, and

$$\hat{r} = \gamma\, r_0 \tag{9.165}$$

can therefore be taken as an effective radius of the radial configuration.

To work out expressions (9.153) and (9.160) the Euler integral

$$\int_0^\infty \rho^n\, e^{-2\rho}\, d\rho = \frac{n!}{2^{n+1}} \tag{9.166}$$

is being used. After some algebra and with γ as an integer, the result becomes

$$\frac{W_s}{W_m} = \gamma^2 \tag{9.167}$$

for $\gamma \gg 1$. Inserted into Eq. (9.163) this yields an effective diameter

$$2\hat{r} = \frac{\lambda_0}{\pi\,\delta\,|\bar{m}|^{-3/2}}\,, \tag{9.168}$$

which is independent of γ.

With the function (9.164) and expressions (9.141) and (9.142) the relative magnitude of the electric field components further becomes

$$\left|\frac{\bar{E}_r}{i\bar{E}_\varphi}\right| \sim |\,\gamma + 1 - \rho\,| \gg 1\,, \tag{9.169}$$

when $\rho \ll \gamma$ and $\gamma \gg 1$. A corresponding beam or an individual photon would then become nearly radially polarized within the main parts of

its volume. Moreover, insertion of E_r from expressioin (9.133) into Eq. (9.135) yields a relation which shows that E_φ and E_z are of the same order of the radial parameter γ. Thus $\left|\frac{E_r}{iE_z}\right| \gg 1$ which justifies the approximation $E_z = 0$ of the present analysis.

Possible models for a dense beam or for an individual photon are now discussed on the basis of the result (9.168). When first considering an individual photon, this can be illustrated by the range $\delta \leqslant 10^{-4}$ for solutions which are reconcilable with experiments of the Michelson-Morley type. In the case of visible light of a single corkscrew shape with $\bar{m} = 1$ and the wave length $\lambda_0 = 3 \times 10^{-7}$ m, say, the photon diameter would become $2\hat{r} \geqslant 10^{-3}$ m. This diameter is much larger than atomic dimensions. Second, for such a photon diameter determined by Eq. (9.168), the critical limit of transverse photon field overlapping and interference would correspond to an energy flow per unit area

$$\psi_p \leqslant \frac{\pi^3 h c^2 \delta^3}{\lambda_0^4} \simeq 1.85 \times 10^{-15} \frac{\delta^3}{\lambda_0^4} \quad [\mathrm{W/m^2}] \tag{9.170}$$

according to Eq. (9.107). With the data of the previous numerical example this results in a maximum energy flux $\psi_p \simeq 2$ W/m^2 for the photon fields not to overlap. In many cases of practical interest, the diameter (9.168) could therefore apply to models of dense photon beams.

In the case of such beams it is finally observed that the energy density (9.149) determined by Eqs. (9.141), (9.142) and (9.164) leads to a radial distribution of intensity which forms a ring-shaped region with an annular radius of the order of the radius $\hat{r}$ given by Eq. (9.168).

The vanishing field strengths at the axis $\rho = 0$ of such a ring-shaped distribution thereby support the use of the approximate dispersion relation (9.22), because there are then negligible contributions to the field intensity from regions near the axis.

Turning finally to the alternative of a radial part of the generating function which is divergent at the axis $\rho = 0$, the form

$$R(\rho) = \rho^{-\gamma} e^{-\rho} \tag{9.171}$$

is taken into consideration where $\gamma > 0$. The question of substituting the factor $\rho^{-\gamma}$ by a series of negative powers of ρ is similar to that already discussed on the form (9.164). As in §9.3.5, $\hat{r} = r_0$ can here be taken as an effective radial dimension of the configuration. This makes, however, the approximation (9.132) of the basic equation (9.120) even more questionable than in the former convergent case. Therefore the analysis based on the form (9.171) which now follows should only be

taken as a first hint of the behaviour due to a divergent radial part of the generating function.

To obtain finite values of the integrated mass and angular momentum, a procedure being analogous to that of §9.3.5 is applied as follows. The lower limits $\rho_m \ll 1$ and $\rho_s \ll 1$ of the integrals (9.153) and (9.160) are thus taken to be nonzero. Adopting the condition $\gamma \gg 1$, and retaining only the dominant terms of highest negative power of ρ in these integrals, the result becomes

$$W_m = \frac{1}{2}\,\gamma\,\rho_m^{-2\gamma+2}, \tag{9.172}$$

$$W_s = \frac{1}{2}\,\gamma\,\rho_s^{-2\gamma+4}. \tag{9.173}$$

We further "shrink" the characteristic radius r_0 and the amplitude factor G_0 of Eq. (9.137) by introducing the relations

$$r_0 = c_r \cdot \varepsilon\,, \qquad c_r > 0\,, \tag{9.174}$$

$$G_0 = c_G \cdot \varepsilon^{\beta}, \qquad c_G > 0\,, \qquad \beta > 0\,, \tag{9.175}$$

where $0 < \varepsilon \ll 1$ is a corresponding smallness parameter. Then

$$mc^2 = A_0^* c_r^2 c_G^2 \gamma\,\frac{\varepsilon^{2\beta+2}}{\rho_m^{2\gamma-2}} = \frac{Nhc}{\lambda_0}\,, \tag{9.176}$$

$$|s| = A_0^* c_r^4 c_G^2 \gamma\delta^2\,\frac{2\pi}{c\lambda_0}\,\frac{1}{|\bar{m}^3|}\,\frac{\varepsilon^{2\beta+4}}{\rho_s^{2\gamma-4}} = \frac{Nh}{2\pi}\,, \tag{9.177}$$

where $A_0^* = \frac{A_0}{2G_0^2}$. For finite values of mc^2 and $|s|$ it is thus required that

$$\rho_m = \varepsilon^{(2\beta+2)/(2\gamma-2)}, \qquad \rho_s = \varepsilon^{(2\beta+4)/(2\gamma-4)}. \tag{9.178}$$

This becomes possible for $\beta = \gamma \gg 1$ where

$$\rho_m \simeq \rho_s \simeq \varepsilon\,, \tag{9.179}$$

and there is a set of configurations with preserved geometrical shape within a range of small ε.

Combination of expressions (9.163), (9.172), (9.173), and (9.178) finally yields

$$W_m = \varepsilon^2 W_s \tag{9.180}$$

and an effective transverse diameter

$$2\hat{r} = \frac{\varepsilon\lambda_0}{\pi\,\delta\,|\bar{m}|^{-3/2}}\,. \tag{9.181}$$

With the function (9.171) and expressions (9.141) and (9.142) the divergent case now gives

$$\left|\frac{\bar{E}_r}{i\bar{E}_\varphi}\right| \sim |\,\gamma - 1 + \rho\,| \gg 1 \tag{9.182}$$

for all ρ when $\gamma \gg 1$. Also here, as in the case (9.164), we obtain $\left|\frac{E_r}{iE_z}\right| \gg 1$. A corresponding individual photon or beam then becomes almost radially polarized.

The result (9.181) leads to far smaller effective diameters than that of Eq. (9.168) for a convergent function R. It would also introduce a factor $\frac{1}{\varepsilon^3}$ into expression (9.170) for the critical energy flux with respect to individual photon overlapping. A dense beam of overlapped photon fields would then require the critical flux to be much larger.

To investigate the possibility of describing an individual photon ($N = 1$) of small effective diameter (9.181) within the frame of the present approximation (9.22) of the dispersion relation, the ratio

$$F_m = \frac{|\,\frac{\bar{m}}{r}\,c\,(\cos\alpha)|}{|\,k_0\,c\,(\sin\alpha)|} \simeq \frac{|\bar{m}|\delta\lambda_0}{2\pi\rho\,\hat{r}} \tag{9.183}$$

has now to be considered. In combination with Eq. (9.181) we obtain

$$F_m = \frac{|\bar{m}|^{5/2}\,\delta^2}{\rho\,\varepsilon}\,. \tag{9.184}$$

According to Eqs. (9.171) and (9.179) the main contributions to the present needle-shaped field configuration originate from the range $\rho \geqslant \varepsilon$ near $\rho = \varepsilon$ in the integrals (9.153) and (9.160). In a first approximation it is then required that $F_m(\rho = \varepsilon) \equiv F_{m0} \ll 1$. By further introducing a constant ratio

$$\frac{\varepsilon}{\delta} = C_0 = const, \tag{9.185}$$

expressions (9.181) and (9.184) can be written as

$$2\,\hat{r} = \frac{C_0\lambda_0}{\pi|\bar{m}|^{-3/2}}\,, \tag{9.186}$$

$$F_{m0} = \frac{|\bar{m}|^{5/2}}{C_0^2}\,. \tag{9.187}$$

These relations are thus conditions for the approximate dispersion relation to become applicable at relevant effective diameters of the configuration to be studied. As an example we choose $\bar{m} = 1$, $\lambda_0 = 3 \times 10^{-7}$m, and $F_{m0} = 10^{-2}$, say, from which $C_0 = 10$ and $2\,\hat{r} = 10^{-6}$ m. This value

is much smaller than that obtained from the convergent model. It exceeds on the other hand atomic dimensions by a substantial factor, this being due to the limit of validity of the approximation imposed on the dispersion relation (9.22). The result (9.186) can in any case be taken as an indication in the direction towards a strongly needle-shaped individual photon configuration. Such a geometry at atomic dimensions could possibly become realizable in an exact analysis of the basic equations without approximations, but a corresponding treatment remains to be performed.

For dense light beams of a comparatively small cross-section, condition (9.187) appears to become rather well satisfied. With an example of $\bar{m}=1,\ \lambda_0=3\times10^{-7}$ m, $F_{m0}=10^{-6}$ and $C_0=10^3$ one would obtain $2\hat{r}=10^{-4}$ m.

§9.6.4 Summary on the modes with a periodic angular dependence

The features of the periodic modes being investigated in this subchapter are now summarized as follows:

- The conventional EM mode propagates at the full velocity c, and has no rest mass. The solutions obtained from Maxwell's equations are, however, not reconcilable with the recently observed screw-shaped twisted light phenomena, because these solutions are lacking of an angular momentum (spin) and cannot be confined to a limited region of space;
- The extended EMS mode with a vanishing rest mass also propagates at the full velocity c. It only includes transverse field components which become "linearly polarized" within a narrow radial range at the point of maximum field strength when $\bar{m}=\pm1$. This mode can be based on a generating function which leads to solutions that are convergent in the radial direction, and can form a wave packet of narrow line width. However, there is a vanishing angular momentum;
- No exact solution has so far been found in the general case of a spatially limited mode with a nonzero angular momentum. Through Eq. (9.120) such a solution requires a narrow ring-shaped radial profile of arbitrary size to be formed, somewhat as observed in recent experiments[98]. A superposition of modes with somewhat different values of δ would broaden the profile. Solutions based on the approximation of a small but nonzero photon rest mass appear on the other hand to be reconcilable with the observed features of

twisted light. These solutions are corkscrew-shaped and include a series of modes of increasing geometrical complexity. All the modes possess an angular momentum(spin), have a limited extension in space, and propagate at a velocity being only slightly smaller than c. The theory is further applicable both to models of dense photon beams and to individual photons. Beam models have been obtained where the intensity forms a ring-shaped cross-section. The solutions based on a divergent generating function give rise to individual photon models of needle-shaped geometry, but are not compatible with Eq. (9.120). Within the limits of validity of the approximations made in the present analysis it is thus not clear whether the effective diameter of the individual model can become as small as to approach atomic dimensions. Such an approach is on the other hand possible for axisymmetric modes with $\bar{m} = 0$, as shown earlier in § 9.3.5;

- A nonzero parameter $\bar{m}$ does not make a general and exact solution of Eq. (9.120) possible. A special self-consistent solution is on the other hand available, by replacing the radial variable r by a constant average radius being proportional to $\frac{1}{k\delta}$, as in relation (9.168). This leads to a similar final result except for a different constant factor of order unity, and with phase and group velocities still being less than c.

§ 9.6.5 Discussion on the concept of field polarization

In the case of conventional plane electromagnetic waves, the concept of electric and magnetic field polarization becomes well defined and experimentally confirmed[97]. This also applies to the related geometry of light beams. Then there are no field components in the direction of the wave normal. The transverse field components are further homogeneous in planes being perpendicular to the wave normal, and they can become linearly, elliptically or circularly polarized. Thereby both an angular momentum and a rest mass are non-existing.

When turning to a three-dimensional mode geometry having transverse field derivatives, the concept of field polarization becomes less clear, and can even be called in question. This also applies to experimental investigations, such as those with Nicols prism and similar devices. Some reasons for this uncertainty are here illustrated by the following points:

- The axisymmetric mode of Eqs. (9.26)–(9.31) has a main radially polarized electric field component, and an associated magnetic

field component in the φ direction;

- Also the screw-shaped modes of §9.6.3. have a more complex geometry than a simple linearly polarized plane EM wave;
- The field geometry of the needle-shaped wave packets being analysed is strongly inhomogeneous in space, both in respect to the amplitudes of the field components and to the directions of the resulting total electric and magnetic fields;
- The transverse length scale of the needle-shaped geometry can become comparable to and even smaller than the average wave length of the wave packets to be considered;
- There are nonzero electric and magnetic field components in the axial direction of propagation;
- The interaction of a needle-shaped EMS wave packet with Nicols prism is not clear at this stage, because the underlying theory does not apply to waves in solid matter, and the packet has a field geometry being far from that of a polarized plane wave.

On the other hand, special models have been elaborated[19] of individual photons and of beams having limited spatial extensions and a nonzero angular momentum. In these models there is a homogeneous core with a linearly or elliptically polarized convetional EM wave, in a first approximation being matched to an EMS wave in the inhomogeneous boundary region. The slight phase mismatch which then arises between the two waves can further be removed be replacing the EM wave in the core by a similar plane EMS wave, being related to a velocity vector of the form (8.17). The contribution to the spin from the plane EMS core wave is in this case negligible as compared to that from the boundary region.

In this connection it may be of interest to extend the experiments by Tsuchiya et al.[22] on individual photons by placing Nicol prisms in the pathways of Fig. 9.2. At this stage it is not clear what could come out of such an investigation.

Also the proposed concept of photon oscillations, and the possible transition of plane waves into needle-shaped modes as described in §9.4.5, may enter into this complex of questions and problems.

Chapter 10

SUPERLUMINOSITY

The possible existence of objects traveling faster than the velocity c of light, but at a limited speed, has a long history which can be traced back to the early 1900s, as described in reviews by Recami[100,101], Barut et al.[102], and Cardone and Mignani[103] among others. The physics of superluminal phenomena was regarded until the mid 1990s by most physicists as "a waste of time", or worse. First after a number of new observations and experimental facts, mainly being found since 1991, the interest in superluminal processes has been revived, even if these processes are still subject to controversial discussions. This chapter is devoted to a brief description of some main points in the research on superluminosity.

§ 10.1 Tachyon theory

The problem of faster-than-light particles was first reconsidered by Bilaniuk et al.[104], and G. Feinberg later called these objects tachyons. The Italian school headed by E. Recami generalized special relativity to superluminal inertial frames[100] and introduced the term "extended relativity". The latter concept was based on the two postulates of the principle of relativity and of the homogeneity of spacetime and isotropy of space. Thereby the vacuum speed c of light is generalized to become a two-side limit, in the sense that one can approach it either from below or from above. The two basic postulates imply that the metric tensor is invariant for subluminal velocities, and also invariant except for its sign in the case of superluminal velocities. In two dimensions the corresponding generalized Lorentz transformation by Recami and Mignani then becomes[100]

$$x'_0 = \pm \frac{x_0 - \bar{\beta} x}{\sqrt{|1 - \bar{\beta}^2|}} \,, \tag{10.1}$$

$$x' = \pm \frac{x - \bar{\beta} x_0}{\sqrt{|1 - \bar{\beta}^2|}} \,, \tag{10.2}$$

where $\bar{\beta} = \frac{u}{c}$ and $-\infty < u < +\infty$. Superluminal Lorentz transformations in four dimensions are somewhat more complicated, because

they involve imaginary quantities in the components of the four-vectors being transverse to the direction of relative motion.

In the theory based on extended relativity, the space-like dispersion relation for tachyons further becomes

$$E_t^2 - p_t^2 c^2 = -m_{t_0}^2 c^4 \tag{10.3}$$

with E_t, p_t, and m_{t_0} as the energy, momentum, and rest mass of the tachyon[100]. Here $m_{t_0}^2 < 0$ is interpreted as an imaginary mass.

The central concepts of tachyon theory can also be made to emerge from the present theory. Thus, the condition $\mathbf{C}^2 = c^2$ of Lorentz invariance given by the second of Eqs. (3.3) is not only satisfied by velocity vectors of the form (9.1) in the subluminal case, but also by vectors of the form

$$\mathbf{C} = c\,(0,\ i\sinh\alpha,\ \cosh\alpha) = c\,(0,\ C_\varphi,\ C_z) \tag{10.4}$$

in a superluminal case. For propagating normal modes varying as $\exp\big[i\,(-\omega t + kz)\big]$, Eq. (4.3) for an EMS-like tachyon mode then yields the dispersion relation

$$\omega = k\,C_z = k\,u\,, \qquad u = c\,(\cosh\alpha) \tag{10.5}$$

which replaces relation (9.22), and where $u > c$ for $\alpha > 0$.

We further introduce the total (positive) energy of a tachyon wave packet having an average frequency ν_0, and obtain in analogy with Eq. (9.71)

$$h\nu_0 = m_t\,c^2 > 0 \tag{10.6}$$

with a corresponding positive total mass m_t. When applying the result (10.5) to expression (9.73) for the total mass of the tachyon and its rest mass, the latter becomes

$$m_{t_0} = i\,(\sinh\alpha)\,m_t\,. \tag{10.7}$$

This rest mass therefore becomes imaginary, in accordance with current tachyon theory.

Comparison between expressions (10.4) and (9.1) indicates that $\cos\alpha$ has to be replaced by $i(\sinh\alpha)$, and $\sin\alpha$ by $\cosh\alpha$, to convert the earlier deduced subluminal results of Chapter 9 into a corresponding axisymmetric tachyon superluminal wave-packet theory. Care is then necessary in not confusing the imaginary unit used to indicate the phase in time with the same unit applied in the velocity expression (10.4). Eqs. (9.85) and (9.95) yield imaginary transverse tachyon diameters. The physical interpretation of an imaginary photon rest mass and diameter is not clear at this stage.

The question can finally be raised whether a superluminal behaviour does imply violation of Einstein causality due to which no information can be transmitted faster than light. An answer to this may be found in extended relativity. It includes the statement that any object moving backward in time, and carrying negative energy, must be interpreted as its antiobject with positive energy moving forward in time[105].

§ 10.2 Observations and experiments

Recent astronomical observations and experiments have given results which may be interpreted as a support to superluminal phenomena, but definite conclusions on these phenomena are still missing in several cases. Here the following examples can be mentioned[103]:

- Faster-than-light expansions were first reported in 1971 for the quasars 3C279 and 3C273. Since then superluminal motions have been claimed to be observed in many quasars and in galactic nuclei. The main problem in the interpretation of these data is related to the fact that they critically depend on the distance from the earth of the observed source. This has therefore given rise to a number of debates. Superluminal motions have also been reported for objects in our galaxy ("microquasars") where the estimated distances are less uncertain. However, at present one is unable to give a definite answer to the question whether these expansions are superluminal or not;
- The solar neutrino deficit is explained on the basis of neutrino oscillations which only can occur if the neutrinos are massive. One possible explanation which has been forwarded is that neutrinos are tachyons which carry a nonzero imaginary rest mass. Another explanation is due to the steady-state neutrino models of Chapter 7 which include a nonzero rest mass, and correspond to a subluminal state when being in motion;
- Particle tunneling through a potential barrier has been studied in several experiments, and been subject to an extensive theoretical analysis[106]. On theoretical grounds one expects photon tunneling to take place at superluminal speed[103]. This is what has also appeared to be observed since 1992 by some experimental research groups. In particular, Nimtz et al.[107] performed an experiment where a wavepacket was used to transmit Mozart's Symphony No.40 at a speed of $4.7\,c$ through a tunnel formed by a barrier of 114 mm length. But there is a difficulty in the interpretation of tunneling experiments, because no group velocity can be defined

in the barrier traversal that is associated with evanescent waves. In a critical review Olkhovsky and Recami[106] have further discussed the theoretical deductions of tunneling times. They have found that the speeds inside the barrier can assume arbitrarily large values, as long as one deals with nonrelativistic quantum physics. These very large speeds could, however, disappear in a self-consistent relativistic quantum theoretical treatment;

- Propagation of electromagnetic waves in media with anomalous dispersion results in group velocities that can take superluminal, infinite, and even negative values. To understand this behaviour, there is an accepted and widespread belief that the very concept of group velocity breaks down in this case. However, in 1970 it was shown that a propagating pulse remains essentially undistorted even in regions of anomalous dispersion, and that its velocity is just the group velocity which can become faster than c, as well as negative;
- Superluminal phenomena have also been reported which have their grounds in the solutions of the field equations. The "X waves" are X-shaped in a plane passing through the propagation axis. They can travel at a group velocity larger than c, in an isotropic and homogeneous medium. The evidence for such waves was found in Tartu in 1997, within the optical domain[108]. Tachyonic particles have been predicted by extended relativity to appear exactly as X waves;
- A special study in terms of the currently used Lienard-Wiechert potentials has been performed by Walker[109] on the electromagnetic field generated by an oscillating electric dipole. The instantaneous phase and group velocities were calculated in the near-field of the dipole, in terms of their conventional definitions. Upon creation the waves were then found to travel with infinite speed, and then rapidly to reduce their speed towards the value c after having propagated about one wavelength away from the source. An interesting extension of this result would consist of studies on the speed of propagation of waves generated by an analogous but pulsed system.

Chapter 11

NONLOCALITY

Another class of electromagnetic phenomena beyond the concepts of conventional theory is characterized by nonlocality, in the form of instantaneous long-range interaction. Also these phenomena have recently attracted an increasing interest, and have become the object of extensive and partly controversial discussions.

§ 11.1 General questions

Nonlocal interaction has features in common with quantum mechanics in which a wave function connects all parts of coordinate space into one single entity. It may then be questioned whether nonlocal interaction at a distance gets into conflict with causality. Cufaro-Petroni et al.[110] have shown that this does not have to be the case, and that the Einstein causality criteria can still be satisfied. There are additional quantum mechanical arguments in favour of long-range interaction, such as that of the Aharonov-Bohm effect[111], and those raised in connection with the Einstein-Podolsky-Rosen (EPR) thought experiment[112].

As already argued by Faraday and Newton, and further stressed by Chubykalo and Smirnov-Rueda[53] and Pope[113] among others, instantaneous long-range interaction can take place not instead of but along with the short-range interaction in classical field theory. The two concepts of action at a distance with infinite speed and the short-range interaction of finite speed c have therefore not to become antithetical. As a consequence, c does not merely have to be interpreted as a velocity, but as a space-time constant having the dimension of velocity.

§ 11.2 The electromagnetic case

It has been pointed out by Dirac[63] that, as long as we are dealing only with transverse waves, Coulomb interaction cannot be included. There must then also arise longitudinal interactions between pairs of charged particles. Argyris and Ciubotariu[114] further notify that the unquantized longitudinal-scalar part of the electromagnetic field yields the Coulomb potential, and that transverse photons transport energy whereas longitudinal (virtual) photons do not carry energy away. Thus, there is direct interaction between a transverse photon and the gravitation field

of a black hole, but not with a longitudinal photon. The Coulomb field is therefore able to cross the event horizon of a black hole.

In their considerations on the field generated by a single moving charged particle, Chubykalo and Smirnov-Rueda[53–55] have claimed the Lienard-Wiechert potentials to be incomplete, by not being able to describe long-range instantaneous Coulomb interaction. This question is still under discussion[10].

A further analysis on long-range interaction has been performed in which the Proca-type field equation is subdivided into two parts[53–55]. The first part manifests the instantaneous and longitudinal aspects of the electromagnetic nature, as represented by functions $f\,[\mathbf{R}(t)]$ of an implicit time dependence. For a single charge system this would lead to the form $\mathbf{R}(t) = \mathbf{r} - \mathbf{r}_q(t)$, where $\mathbf{r}$ is a fixed vector from the point of observation to the origin, and $\mathbf{r}_q(t)$ is the position of the moving charge. The implicit time dependence then implies that all explicit time derivatives are left out from the part of the basic equations which belongs to the instantaneous interaction. The second part, given by functions $\mathbf{g}\,(\mathbf{r}, t)$ where the explicit time derivatives are retained, is connected with propagating transverse EM waves. This proposed subdivision can at a first sight be commented on, from two different points of view:

- The charges and currents are the sources of the electromagnetic field, and they emit signals which reach a field point after a certain transit time. When the time variation of the same sources becomes slow enough for the transit time of an EM wave to be very short, then the velocity of light would appear as infinite, and the terms with explicit time derivatives in Eq. (2.1) can be neglected with good approximation. As a result of this, it would not become possible to distinguish such wave propagation from a real instantaneous interaction based on an implicit time dependence where the explicit time derivatives are exactly equal to zero;
- There are, however, a number of arguments that appear to support the existence of long-range instantaneous interaction as described in § 11.1, as well as the interesting idea of subdividing the Proca-type equation. Further supporting arguments are based on the longitudinal wave concept itself[7], and on observations of the universe[113]. Instantaneous interaction, represented by longitudinal components, can thus be interpreted as a classical equivalent of nonlocal quantum interaction[53].

The proposed subdivision of the basic equations into long-range and short-range parts can also be applied to the present extended field equa-

tions (3.6)–(3.10). The steady solution of the electron model deduced in Chapter 6 then gives rise to a static Coulomb field of Eq. (3.10).

In the following §11.4 an example is given where an S wave results in instantaneous interaction when being combined with a curl-free magnetic vector potential.

§11.3 The gravitational case

There are similarities between electromagnetism and gravitation that could have some bearing on the investigations of long-range interaction. Thus, there is a resemblance between the Coulomb and Newton potentials[114]. A holistic view of these two fields would imply that action at a distance can possibly occur in a similar way for gravitation[7]. This is supported by the general principle that there exists no screen against gravitational forces acting between distant massive sources[45]. According to such a standpoint the velocity and acceleration of a source of gravity would be felt by the target body in much less that the light-time between them.

In celestial mechanics the Newtonian potential is usually treated as being due to instantaneous interaction, i.e. without having the character of a retarded potential related to gravitons which propagate at a finite velocity. As long as the mutual speeds of celestial bodies are much smaller than that of light, it becomes difficult to decide from orbit observations whether the corresponding interactions are of an instantaneous nature or not.

Recently, in the year 2003, two American astronomers have performed measurements of the speed of gravity, thereby concluding that gravity travels at the speed c of light. This result has been subjected to some criticism, and the discussion is still going on. It should be clear that both photons and gravitons can give rise to short-range interactions of the electromagnetic and gravitational fields, and where these interactions lead to propagation at a finite velocity c in the sense of Einstein. This may, however, not exclude a possible and simultaneous existence of a second long-range branch of gravitational instantaneous interaction, being similar to the electromagnetic action at a distance just being discussed in this context.

§11.4 Space-charge wave in a curl-free magnetic vector potential

To an increasing extent it has been realized that the electromagnetic four-potential $A_\mu = \left(\mathbf{A}, \frac{i\phi}{c}\right)$ does not only serve the purpose of a mathe-

matical intermediary in deducing the electric and magnetic field strengths, but also has a direct physical meaning of its own. Even on the U(1) unitary matrix level of Maxwell's equations the related potentials can be interpreted physically, as was the intent of Maxwell and Faraday. On the level of the O(3) rotation matrix group the same potentials are always physical[11].

One theoretical and experimental confirmation of this is due to the Aharonov-Bohm effect[110,116] according to which there is a shift of the interference pattern in an electron two-slit experiment when a long straight coil with an internal steady magnetic field is placed between the slits, such as in a configuration being similar to that of Fig. 9.1. The electrons then move in a magnetically and electrically field-free region, but are still affected by the curl-free magnetic vector potential generated by the coil in the space outside of it. According to Chubykalo and Smirnov-Rueda[53,55] among others the Aharonov-Bohm effect indicates in an indirect way that there can exist a nonlocal and instantaneous long-range interaction in electromagnetism.

Here an application related to the Aharonov-Bohm geometry will be analysed, but in a time-dependent state. We will study a combination of the longitudinal purely electric space-charge S wave of § 4.2 with a curl-free magnetic vector potential. This yields a solution which only appears to be satisfied in a case of instantaneous interaction at a distance, but the physical relevance of such a case is at this stage open for further discussions.

§ 11.4.1 Basic equations without a magnetic field

Starting from Eqs. (3.6)–(3.10), we now consider an S wave. Then the two terms of the right-hand member of Eq. (3.6) balance each other, i.e. the displacement current is cancelled by the space-charge current (3.3), and there is no resulting magnetic field. In such a case the magnetic vector potential has the form

$$\mathbf{A} = \nabla\psi\,, \tag{11.1}$$

and the electric field becomes

$$\mathbf{E} = -\nabla\phi^*\,, \qquad \phi^* = \phi + \frac{\partial\psi}{\partial t}\,, \tag{11.2}$$

according to Eq. (3.9). Consequently the basic equations for the S wave reduce to

$$\left(\mathbf{C}\,\mathrm{div} + \frac{\partial}{\partial t}\right)\nabla\phi^* = 0 \tag{11.3}$$

since Eq. (3.7) becomes automatically satisfied.

§11.4.2 Space-charge wave in cylindrical geometry

To study the joint effects of the curl-free vector potential and the S wave, a simple time-dependent case is now chosen where there is cylindrical geometry of the Aharonov-Bohm type. The long straight coil has its axis at $r=0$ and is extended along the z direction of a cylindrical frame (r,φ,z). The coil cross section has the radius R_0. In the interior of the coil there is a time-dependent homogeneous magnetic field $B(t)$ being directed along z. The corresponding total magnetic flux becomes

$$\Phi(t)=\pi R_0^2 B(t)\,. \tag{11.4}$$

In the external vacuum space $r>R_0$ we further make the ansatz of an S wave according to Eq. (11.3). There is no magnetic field in the vacuum region outside of the coil, as described in §11.4.1.

For a path encircling the z axis at distances $r>R_0$, the integral of the vector potential (11.1) becomes

$$\oint \mathbf{A}\cdot d\mathbf{s}=\Phi(t)=\int_0^{2\pi}\frac{1}{r}\,\frac{\partial\psi}{\partial\varphi}\,r\,d\varphi\,, \tag{11.5}$$

which yields

$$\psi=\frac{\varphi}{2\pi}\,\Phi(t) \tag{11.6}$$

in analogy with an example on the Aharonov-Bohm effect treated by Ryder[21]. Here it is observed that ψ becomes a multivalued function of φ in a non-simply connected vacuum region. Thereby the theorem by Stokes has to be applied with care, but the line integral of $\mathbf{A}$ around a circle in the φ direction still becomes nonzero. It is now possible to write

$$\nabla\phi^*=\left[\,\frac{\partial\phi}{\partial r}\,,\ \frac{1}{2\pi r}\,\frac{d\Phi}{dt}\,,\ 0\,\right] \tag{11.7}$$

and

$$\operatorname{div}\nabla\phi^*=\frac{1}{r}\,\frac{\partial}{\partial r}\left(r\,\frac{\partial\phi}{\partial r}\right). \tag{11.8}$$

To satisfy Eq. (11.3), the velocity vector $\mathbf{C}$ must have components both in the r and the φ directions, i.e.

$$\mathbf{C}=\mathbf{c}\,(\sin\alpha,\ \cos\alpha,\ \mathbf{0})\,. \tag{11.9}$$

Then Eq. (11.3) leads to the system

$$c\,(\sin\alpha)\,\frac{\partial}{\partial r}\left(r\,\frac{\partial\phi}{\partial r}\right)+\frac{\partial}{\partial t}\left(r\,\frac{\partial\phi}{\partial r}\right)=0\,, \tag{11.10}$$

$$c\,(\cos\alpha)\,\frac{\partial}{\partial r}\left(r\,\frac{\partial\phi}{\partial r}\right)+\frac{1}{2\pi}\,\frac{d^2\Phi}{dt^2}=0\,. \tag{11.11}$$

Here the two cases $\Phi \equiv 0$ and $\Phi \neq 0$ will be considered.

When $\Phi \equiv 0$ the system (11.10)–(11.11) reduces to that of an earlier treated purely longitudinal electric space-charge wave[18,115]. Then Eq. (11.11) is satisfied by $\cos\alpha = 0$, $\mathbf{C} = (c, 0, 0)$, $\mathrm{div}\,\mathbf{C} \neq 0$, and Eq. (11.10) yields $\mathbf{E} = (E, 0, 0)$ where

$$E = -\frac{\partial \phi}{\partial r} = \frac{1}{r} f(r - ct) \tag{11.12}$$

for propagation in the positive r direction at the speed c of light. The corresponding wave equation (11.10) is similar to but not identical with that of sound waves in a compressible medium[117]. The wave equations for these two phenomena have the same form for plane waves only. In spherical geometry[117] there is a solution being similar to that of Eq. (11.12), but with the factor $\frac{1}{r^2}$ ahead of $f(r - ct)$.

When $\Phi \neq 0$ there is an entirely new situation. To find the solution of Eqs. (11.10)–(11.11) an ansatz

$$r \frac{\partial \phi}{\partial r} = c \cdot f\left(t - \frac{r}{c}\right) \tag{11.13}$$

is now examined. It results in a charge density (3.10) given by

$$\bar{\rho} = \frac{\varepsilon_0 f'}{r}\,, \tag{11.14}$$

where a prime denotes derivation with respect to $t - \frac{r}{c}$. When f and its derivatives are finite, the density (11.4) also becomes finite. With

$$\sin\alpha = 1 - \varepsilon\,, \qquad \cos\alpha \simeq (2\varepsilon)^{1/2}, \qquad 0 < \varepsilon \ll 1\,, \tag{11.15}$$

there is a velocity (11.9) being mainly oriented along the radial direction and circulating slowly around the z axis. Eqs. (11.10) and (11.11) then become

$$c\varepsilon f' = 0\,, \tag{11.16}$$

$$c\,(2\varepsilon)^{1/2} f' = \frac{1}{2\pi} \frac{d^2\Phi}{dt^2}\,. \tag{11.17}$$

To satisfy this system for all (r, t), and for finite values of f' and $\frac{d^2\Phi}{dt^2}$, the following procedure has to be adopted. For a constant and finite value of c it is readily seen that there are no solutions. Therefore the velocity c has to be ascribed a new unconventional interpretation. In order to prevent the left-hand member of Eq. (11.17) from vanishing with ε, the constant c has now to tend to infinity, such as to satisfy the condition

$$c \cdot \varepsilon^{1/2} = c_0\,, \tag{11.18}$$

where c_0 is a finite constant. With this condition inserted into Eq. (11.16), the result becomes

$$\frac{c_0^2 f'}{c} = 0\,. \tag{11.19}$$

In its turn, this relation can only be satisfied in the limit of an infinite value of c. As a final consequence Eq. (11.17) takes the form

$$\frac{1}{2\sqrt{2}\,\pi c_0}\,\frac{d^2\Phi}{dt^2} = f'\left(t - \frac{r}{c}\right) \to f'(t)\,, \qquad (c \to \infty) \tag{11.20}$$

where all members become functions of t only. The characteristic length $L_c = |\,f \cdot (\partial f/\partial r)^{-1}|$ and the characteristic time $t_c = |\,f \cdot (\partial f/\partial t)^{-1}|$ are then related through $\frac{t_c}{L_c} = \frac{1}{c} \to 0$.

Consequently, this analysis indicates that the underlying equations can only be satisfied in the limit of instantaneous interaction at a distance. Then the Lorentz condition (2.4) reduces to that of the Coulomb gauge, and the divergence of $\mathbf{A}$ vanishes in agreement with Eq. (11.6). The S wave signal of the curl-free and time-dependent magnetic coil field is thus expected to arrive instantaneously at a point far from the origin. The problem of detecting such an S-wave is, however, by no means simple, nor is it even clear at this stage if such a signal can exist.

As obtained from an analysis by Angelidis[118], the concept of instantaneous interaction does not become reconcilable with special relativity which is based on a finite velocity c of propagation. The result (11.20) can therefore also be understood as an example and a confirmation of such an interpretation.

§ 11.5 Questions on energy and signal propagation

Conventional transverse electromagnetic waves and their radiation field are known to propagate at a finite velocity of light. Thereby the energy density of the field decreases as $\frac{1}{r^2}$ at large distances from the source. This is also expected from the point of energy conservation for a flux of undamped waves, because the corresponding surface in spherical geometry increases as r^2.

The elementary longitudinal S wave in cylindrical geometry of the case $\Phi \equiv 0$ represented by Eq. (11.12) also propagates at the constant velocity c, but its energy density $\frac{\varepsilon_0 E^2}{2}$ decreases as $\frac{1}{r^2}$. Since the corresponding surface in cylindrical geometry only increases as r, the energy of this wave is not expected to become conserved. This argument against energy transportation by such a purely longitudinal wave agrees with the statement by Argyris and Ciubotariu[114] on longitudinal (virtual) photons.

Turning now to instantaneous long-range interaction, a propagation of energy at an infinite speed generally appears to become questionable. Instead the associated field can be considered to be "rigidly" connected with its sources all over space. It would then form a non-localized system, having the character of one single entity, like a quantum mechanical wave function. Thus, it would not include a localized small-scale wave motion which transports a localized energy density. But one also has to face the question whether information can be transmitted and received in practice by instantaneous interaction, without including a contemporary transfer of energy.

Due to the similarity of the Coulomb and Newton potentials, the possible concept of instantaneous gravitational interaction would also become faced with the same questions as those concerning the electromagnetic field.

We finally ponder upon an imagined configuration in which the generalized S wave of Sections 11.4.2 and 11.4.3 is applied to a toroidal (ring-shaped) coil. Such a geometry can be interpreted as a dipole-like transmitter of the electric field and the curl-free magnetic vector potential. The ring-shaped time-dependent internal magnetic field within the coil then generates an external curl-free potential due to the S wave, in the same way as the electric current along a ring-shaped conductor generates a magnetic field. The resulting magnetic vector potential in the space outside of the coil then has the same spatial distribution as the magnetic field from a circular loop. At the axis of symmetry $\nabla\psi$ then decreases as $\frac{1}{r^3}$ at large r. With $\mathbf{E} = -\nabla\frac{\partial\psi}{\partial t}$ this leads to the same $\frac{1}{r^3}$ dependence of the electric field in spherical geometry as for the steady Coulomb field. Consequently, also this case of instantaneous interaction does not become reconcilable with propagation of an energy density, and it has to be further investigated.

The concepts treated in this chapter, at the beginning of § 2.1, and in connection with the Aharonov-Bohm effect, are somewhat related to the search for tapping the zero-point energy of the vacuum fluctuations, as being discussed by Puthoff and collaborators[119,120], and by Bearden and collaborators[121] among others. Such approaches are at present subject to a number of controversial discussions. The main points to be faced with in this connection concern the way in which energy can be extracted from a state which at least on the average represents the lowest energy level, the question how much of the zero point energy can at most be gained in practice, and how this has to be realized from the technical point of view.

Chapter 12

SUMMARY OF OBTAINED MAIN RESULTS

§ 12.1 General conclusions

The main results which are specific to the present theoretical approach can now be summarized. These are expected to contribute to an increasing understanding of a number of fundamental physical phenomena, and they also predict new features of the electromagnetic field to exist. It should be noticed here that the recently presented theories by Kaivarainen[122] and Tauber[123] have some parts in common with this approach, such as the concept of a nonzero electric field divergence in the vacuum state, models of the leptons with an internal vortex-like structure, and a small but nonzero photon rest mass.

Maxwell's equations with a vanishing electric field divergence in the vacuum have been used as a guideline and basis in the development of quantum electrodynamics (QED)[33,73,74]. Therefore QED is expected also to be subject to the typical shortcomings of conventional electromagnetic theory. The revised electromagnetics described here, with its nonzero electric field divergence, provides a way of eliminating these shortcomings in a first step of extended quantum electrodynamics ("EQED"). The present theory is thus based on the hypothesis of a vacuum state which does not merely consist of empty space but can become electrically polarized, to give rise to a local electric space charge density and a related nonzero electric field divergence. On account of this, and of the condition on Lorentz invariance, an additional space-charge current density arises as a matter of necessity. It occurs along with the conventional displacement current in the resulting extended field equations. Maxwell's equations thus become a special class of this approach. The nonzero electric field divergence introduces an additional degree of freedom, and this leads to a number of new electromagnetic properties. From the analysis performed in the previous chapters, it is thereby seen that the present theory has features and leads to results which in several respects become directly or indirectly supported by experimental observations.

So far quantum field theories have all incorporated Lorentz invariance in their basic structure, but its breaking has recently become subject of several investigations[124]. Whatever the true origin of a possible

Lorentz breaking may be, the fact that it has not yet been observed means it must be small at the energy scales corresponding to known standard-model physics.

The present theory also has the important feature of being gauge invariant, due to the form of the space-charge current density. This invariance does not necessarily hold for other forms of the four-current in a Proca-type field equation.

The present theory leads to some results of a general character, of which the following should be mentioned:

- The extended equations make it possible for electromagnetic steady states to exist in the vacuum;
- New types of wave modes arise, such as a longitudinal purely electric space-charge (S) wave, and a nontransverse electromagnetic space-charge (EMS) wave.

§ 12.2 Steady electromagnetic states

Conventional theory excludes steady electromagnetic states in the vacuum. The present theory includes on the other hand electrically charged steady states which result in a model of charged leptons such as the electron:

- For a particle-shaped configuration to possess a nonzero net electric charge, its characteristic radius has to shrink to that of a point-charge-like geometry, in agreement with experiments;
- Despite of the success of the conventional renormalization procedure, a more satisfactory way from the physical point of view is needed in respect to the infinite self-energy problem of a point charge. This problem is removed by the present theory which provides a more surveyable alternative, by compensating the divergence of the generating function through a shrinking characteristic radius and thereby leading to finite integrated field quantities;
- The Lorentz invariance of the electron radius is formally satisfied in the present theory, by allowing the same radius to shrink to that of a point charge. The obtained solutions can on the other hand also be applied to the physically relevant case of a very small but nonzero radius of a configuration having an internal structure;
- The ratio q^* between the deduced net electric charge and the experimentally determined elementary charge has been subject to a variational analysis. Thereby the lowest values of q^* are found

to be distributed over a flat plateau-like parameter region, with q^* ranging from a minimum of 0.97 to a highest value of 1.01;

- A steady equilibrium of the average radial forces can under certain conditions be established, such as to prevent the electron from "exploding" under the action of its electric self-charge. This becomes possible for the point-charge-like model, at parameter values of the plateau region which correspond to $q^* \simeq 0.99$. The remaining degrees of freedom being available in the parameter ranges of the plateau have then been used up by the condition of a radially balanced equilibrium;
- That there is only a small deviation of q^* from unity can, in itself, be interpreted as an experimental support of the present theory. This is particularly the case as the deduced result has been obtained from two independent aspects, namely the minimization of the charge by a variational analysis, and the determination of the charge from the requirement of a radial balance of forces;
- The deduced charge thus deviates only by about one percent from the measured elementary charge. To remove this small deviation, some additional quantum mechanical corrections have been proposed. Provided that such corrections become relevant, the elementary charge would no longer remain as an independent constant of nature, but can be derived from the present theory in terms of the velocity of light, Planck's constant, and the permittivity of vacuum;
- The results of the present analysis can also be taken as an indirect support and deduction of the correct Landé factor, as well as of the adopted quantum condition for the magnetic flux;
- The question can finally be raised whether the basic ideas of the present theory may also be applied to establish models of the quarks. It has then to be noticed that no free quarks have so far been observed, and that the quarks form configurations within the interior of the baryons where they interact with each other and are kept in place by the strong force. This does, however, not explain why the quarks do not "explode" due to their self-charges.

There also exist steady states having a zero net electric charge and forming possible models for the neutrino:

- A small but nonzero rest mass is in conformity with the analysis;
- The equilibrium state includes an angular momentum, but no net magnetic moment;

- Long mean free paths are predicted for neutrinos in their interaction with solid matter, possibly being in agreement with observed data.

§ 12.3 Electromagnetic wave phenomena

Conventional theory is based on a vanishing electric field divergence. In the cases of plane and spherical waves far from their source, as well as of axisymmetric and screw-shaped wave modes, there are then no electric and magnetic field components in the direction of propagation. The integrated energy also becomes divergent when being extended all over the vacuum space. The Poynting vector possesses a component in this direction only, and there is no angular momentum(spin). This feature should also prevail in a fully quantized analysis. According to Schiff[33] and Heitler[23] the Poynting vector namely forms as well the basis for the quantized field momentum. The electromagnetic field strengths are then expressed in terms of quantum mechanical wave expansions. Thereby also quantum electrodynamics in the vacuum is based on Maxwell's equations in empty space, having a vanishing electric field divergence[33]. The deduced axisymmetric EMS wave modes lead on the other hand to models of the individual photon, in the form of wave-packets with a narrow line width and having the following features:

- For the photon to possess a nonzero angular momentum (spin) in the capacity of a boson particle, the axisymmetric field geometry has to become helical, as well as the Poynting vector;
- This helical structure is associated with a nonzero rest mass, and it has field components also in the longitudinal (axial) direction of propagation;
- The nonzero rest mass can become small enough not to get into conflict with experiments of the Michelson-Morley type, thereby still preserving a helical field structure;
- There are wave-packet solutions with a very small characteristic transverse radius. These have the form of "needle radiation" which becomes a necessary concept for the explanation of the photoelectric effect where a photon interacts with a single electron in an atom, and of the dot-shaped marks observed at a screen in double-slit experiments;
- The axisymmetric wave-packet models behave as one single entity, having particle and wave properties at the same time. This dualism, with its associated needle geometry and interference ability,

becomes particularly obvious in the limit of zero line width, i.e. in the form of the elementary normal mode of a long string-like photon;

- In terms of the present EMS modes, models can also be elaborated which have the characteristic features of radially or linearly polarized as well as screw-shaped light, both in the form of dense multiphoton beams and of individual photon models;
- It is proposed that the various plane and axisymmetric wave modes represent different quantum states of the photon, and that rapid transitions can take place between these states, in the form of "photon oscillations" and under the conditions of energy and momentum conservation. In this way a plane wave may decay into two needle-shaped wave packets of which one carries almost the entire energy.

It is finally observed that the nonzero electric field divergence gives rise to a large new effect in the radial force balance of the present electron model, whereas the same divergence becomes related to a small effect but being of decisive importance to the photon model and its angular momentum (spin).

There should exist more applications of the present theory, both of a steady-state and of a dynamic nature, which have not been treated in this book. Possible examples are given by the quark states with bound charges and other types of steady modes, as well as by dynamic states including oscillating membrane-like and body-like configurations being somewhat in analogy with the string concept.

The nonzero electric charge density in the vacuum also introduces a somewhat modified aspect on the unification problem of gravity and electromagnetism. As long as there are conventional Coulomb and gravitational interactions between the electric charges and between the masses of the volume elements, such as those treated in this book, the former interactions will by far exceed those of the latter. Exceptions from this would be black holes and the early state of the Big Bang when there is still an electrically quasi-neutral state of moderately large charge density but having an excessively large mass density.

Bibliography

1. Feynman R. P. Lectures on Physics: Mainly Electromagnetism and Matter. Addison-Wesley, Reading, MA, 1964, p. 28–1.
2. Lakhtakia A. (Ed.) Essays on the Formal Aspects of Electromagnetic Theory. World Scientific, Singapore, 1993.
3. Sachs M. Relativity in Our Time. Taylor and Francis, 1993; in *Modern Nonlinear Optics*, Part 1, Second Edition, *Advances in Chemical Physics*, vol. 119, Edited by M. W. Evans, I. Prigogine, and S. A. Rice, John Wiley and Sons, Inc., New York, 2001, p. 667.
4. Evans M. and Vigier J.-P. The Enigmatic Photon. Kluwer, Dordrecht, vol. 1, 1994 and vol. 2, 1995.
5. Barett T. and Grimes D. M. (Eds.) Advanced Electromagnetics. World Scientific, Singapore, 1995.
6. Evans M. W., Vigier J.-P., Roy S., and Jeffers S. The Enigmatic Photon. Kluwer, Dordrecht, vol. 3, 1996.
7. Evans M. W., Vigier J.-P., Roy S., and Hunter G. (Eds.) The Enigmatic Photon. Kluwer, Dordrecht, vol. 4, 1998, pp. 1 and 33; Evans M. W. *Found.Phys. Lett.*, 2003, v. 16, 367.
8. Hunter G., Jeffers S., and Vigier J-P. (Eds.) Causality and Locality in Modern Physics. Kluwer, Dordrecht, 1998.
9. Lehnert B. and Roy S. Extended Electromagnetic Theory. World Scientific, Singapore, 1998.
10. Dvoeglazov V. V. (Ed.) Contemporary Fundamental Physics. Nova Science Publishers, Huntington, New York, 2000.
11. Evans M. W., Prigogine I., and Rice S. A. (Eds.) Modern Nonlinear Optics. Parts 1–3, Second Edition, *Advances in Chemical Physics*, vol. 119, John Wiley and Sons, Inc., New York, 2001, p. 250.
12. Amoroso R. L., Hunter G., Kafatos M., and Vigier J.-P. (Eds.) Gravitation and Cosmology: From the Hubble Radius to the Planck Scale. Kluwer, Dordrecht, 2002.
13. Lehnert B. Report TRITA-EPP-79-13. Electron and Plasma Physics, Royal Institute of Technology, Stockholm, 1979.
14. Lehnert B. *Spec. Sci. Technol.*, 1986, vol. 9, 177; 1988, vol. 11, 49; 1994, vol. 17, 259 and 267.
15. Lehnert B. *Optik*, 1995, vol. 99, 113.
16. Lehnert B. *Physica Scripta*, 1999, vol. T82, 89.
17. Lehnert B. In: *Contemporary Fundamental Physics*, V. V. Dvoeglazov (Ed.), Nova Science Publ., Huntington, New York, 2000, vol. 2, p. 3.

18. Lehnert B. In: *Modern Nonlinear Optics*, Part 2, Second Edition, *Advances in Chemical Physics*, vol. 119, Edited by M. W. Evans, I. Prigogine, and S. A. Rice, John Wiley and Sons, Inc., New York, 2001, p. 1.
19. Lehnert B. *Physica Scripta*, 2002, vol. 66, 105; 2005, vol. 72, 359; 2006, vol. 74, 139; *Progress in Physics*, 2006, vol. 2, 78; 2006, vol. 3, 43; 2007, vol. 1, 27.
20. Lehnert B. In: *Gravitation and Cosmology: From the Hubble Radius to the Planck Scale*, Edited by R. L. Amoroso, G. Hunter, M. Kafatos, and J.-P. Vigier, Kluwer, Dordrecht, 2002, p. 125.
21. Ryder L. H. Quantum Field Theory. Cambridge Univ.Press, 1996, Ch. 2.8, Ch. 10; p. 406; Ch. 1; Ch. 3.4; also Edition of 1987.
22. Tsuchiya Y., Inuzuka E., Kurono T., and Hosoda M. *Adv. Electron Phys.*, 1985, vol.64A, 21.
23. Heitler W. The Quantum Theory of Radiation. Third Edition, Clarendon Press, Oxford, 1954, p. 401; p. 409; p. 58.
24. Stratton J. A. Electromagnetic Theory. First Edition, McGraw-Hill Book Comp., Inc., New York and London, 1941, Ch. VI, Sec. 6.7; Sec. 1.10, Ch. II and Sec. 1.23, 5.15.2 and 9.4–9.8; Sec. 2.5; Sec. 2.19; Sec. 2.8 and 2.14; Sec. 8.5 and 3.9.
25. Jackson J. D. Classical Electrodynamics. John Wiley and Sons, Inc., New York-London-Sydney, 1962, Ch. 6, p. 201, Ch. 17, p. 589.
26. Thomson J. J. *Nature*, 1936, vol. 137, 232.
27. Hunter G. and Wadlinger R. L. P. *Physics Essays*, 1989, vol. 2, 154; with an experimental report by F. Engler.
28. Donev S. In: *Photon: Old Problems in Light of New Ideas*, Edited by V. V. Dvoeglazov, Nova Science Publishers, Huntington, New York, 2000, p. 32.
29. Hütt R. *Optik*, 1987, vol. 78, 12.
30. Mazet A., Imbert C., and Huard S. *C. R. Acad. Sci.*, Ser. B, 1971, vol. 273, 592.
31. de Broglie L. and Vigier J.-P. *Phys. Rev. Lett.*, 1972, vol. 28, 1001.
32. Vigier J.-P. *Physics Letters A*, 1997, vol. 234, 75.
33. Schiff L. I. Quantum Mechanics. McGraw-Hill Book Comp., Inc., New York-Toronto-London, 1949, Ch. IV; Ch. I; Ch. XIV.
34. Casimir H. B. G. *Proc. K. Ned. Akad. Wet.*, 1948, vol. 51, 793.
35. Lamoreaux S. K. *Phys. Rev. Letters*, 1997, vol. 78, 5.
36. Richtmyer F. K. and Kennard E. H. Introduction to Modern Physics. McGraw-Hill Book Comp., Inc., New York and London, 1947, p. 600.
37. Dirac P. A. M. *Proc. Roy. Soc.*, 1928, vol. 117, 610 and 1928, vol. 118, 351.
38. Morse P. M. and Feshbach H. Methods of Theoretical Physics. McGraw-Hill Book Comp., Inc., New York 1953, Part I, p. 260 and 331; Part II, p. 1320.

39. Sherwin C. W. Introduction to Quantum Mechanics. Holt, Rinehart and Winston, New York, 1960, Ch. II.
40. Einstein A. *Ann. Phys.* (Leipzig), 1905, vol. 7, 132 and 1917, vol. 18, 121.
41. Bass L. and Schrödinger E. *Proc. Roy. Soc. A*, 1955, vol. 232, 1.
42. Evans M. W. *Physica B*, 1992, vol. 182, 227 and 237.
43. Bartlett D. F. and Corle T. R. *Phys. Rev. Lett.*, 1985, vol. 55, 99.
44. Harmuth H. F. *IEEE Trans.*, 1986, EMC-28(4), 250, 259 and 267.
45. Vigier J.-P. *IEEE Trans. on Plasma Science*, 1990, vol. 18, 64.
46. Haisch B. and Rueda A. In: *Causality and Locality in Modern Physics*, Edited by G. Hunter, S. Jeffers, and J.-P. Vigier, Kluwer, Dordrecht, 1998, p. 171.
47. Roy M. and Roy S. In: *The Present State of Quantum Theory of Light*, Edited by J.-P. Vigier, S. Roy, S. Jeffers, and G. Hunter, Kluwer, Dordrecht, 1996.
48. Kar G., Sinha M., and Roy S. *Int. Journal of Theoretical Physics*, 1993, vol. 32, 593.
49. Roy S., Kar G., and Roy M. *Int. Journal of Theoretical Physics*, 1996, vol. 35, 579.
50. Hertz H. *Wied. Ann.*, 1890, vol. 41, 369.
51. Hertz H. *Ges. Werke*, 1894, vol. 2, 256.
52. Hertz H. Electric Waves. Transl. by D. E. Jones, Dover, New York 1962.
53. Chubykalo A. E. and Smirnov-Rueda R. In: *The Enigmatic Photon*, vol. 4, Edited by M. W. Evans, J.-P. Vigier, S. Roy, and G. Hunter, Kluwer, Dordrecht, 1998, p. 261.
54. Chubykalo A. E. and Smirnov-Rueda R. *Modern Physics Letters A*, 1997, vol. 12, 1.
55. Chubykalo A. E. and Smirnov-Rueda R. *Physical Review E*, 1996, vol. 53, 5373.
56. Anastasovski P. K., Bearden T. E., Ciubotariu C., Coffey W. T., Crowell L. B., Evans G. J., Evans M. W., Flower R., Jeffers S., Labounsky A., Lehnert B., Mészáros M., Molnár P. R., Vigier J.-P., and Roy S. *Found. Phys. Lett.*, 2000, vol. 13, 179.
57. Feldman G. and Mathews P. T. *Phys. Rev.*, 1963, vol. 130, 1633.
58. Mészáros M. In: *The Enigmatic Photon*, vol. 4, Edited by M. W. Evans, J.-P. Vigier, S. Roy, and G. Hunter, Kluwer, Dordrect, 1998, p. 147.
59. Molnár P. R., Borbély T., and Fajszi B. In: *The Enigmatic Photon*, vol. 4, Edited by M. W. Evans, J.-P. Vigier, S. Roy, and G. Hunter, Kluwer, Dordrecht, 1998, p. 205.
60. Imeda K. *Prog. Theor. Phys.*, 1950, vol. 5, 133.
61. Ohmura T. *Prog. Theor. Phys.*, 1956, vol. 16, 684, 685.
62. Múnera H. A. In: *Modern Nonlinear Optics*, Part 3, Second Edition, *Advances in Chemical Physics*, vol. 119, Edited by M. W. Evans, I. Prigogine, and S. A. Rice, John Wiley and Sons, Inc., New York, 2001, p. 335.

63. Dirac P. A. M. Directions in Physics. Wiley-Interscience, New York, 1978.
64. Particle Data Group. *Phys. Rev. D*, 1994, vol. 50, Part I.
65. Ignatiev A. Yu. and Joshi G. C. *Phys. Rev. D*, 1996, vol. 63, 984.
66. Isrealit M. *Found. Phys.*, 1989, vol. 19, 35.
67. Sachs M. General Relativity and Matter. D. Reidel Publ. Comp., Dordrecht, 1982.
68. Sachs M. In: *Modern Nonlinear Optics*, Part 1, Second Edition, *Advances in Chemical Physics*, vol. 119, Edited by M. W. Evans, I. Prigogine, and S. A. Rice, John Wiley and Sons, Inc., New York, 2001, p. 677.
69. Sarfatti J. In: *Gravitation and Cosmology: From the Hubble Radius to the Planck Scale*, Edited by R. L. Amoroso, G. Hunter, M. Kafatos, and J.-P. Vigier, Kluwer, Dordrecht, 2002, p. 419.
70. Goldstein H. Classical Mechanics. Addison-Wesley Publ. Comp., Reading, Mass., 1957, Ch. 11–5.
71. Soad D., Horwitz L. P., and Arshansky R. I. *Found. Phys.*, 1989, vol. 19, 1126.
72. Land M. C., Shnerb N., and Horwitz L. P. *J. Math. Phys.*, 1995, vol. 36, 3263.
73. Gersten A. Preprints CERN-TH.4687/87 and CERN-TH.4688, Geneva: CERN, 1987.
74. Gersten A. *Found. Phys. Lett.*, 1999, vol. 12, 291.
75. Dvoeglazov V. V. In: *The Enigmatic Photon*, vol. 4, Edited by M. W. Evans, J.-P. Vigier, S. Roy, and G. Hunter, Kluwer, Dordrecht, 1998, p. 305.
76. Dvoeglazov V. V. *J. Phys. A: Math. Gen.*, 2000, vol. 33, 5011.
77. Bruce S. *Nuovo Cimento B*, 1995, vol. 110, 115.
78. Dvoeglazov V. V. *Nuovo Cimento B*, 1997, vol. 112, 847.
79. Leighton R. B. Principles of Modern Physics. McGraw-Hill Book Comp., New York-Toronto-London, 1959, Ch. 20.
80. Lehnert B. Report TRITA-EPP-89-05. Electron and Plasma Physics, Royal Institute of Technology, Stockholm, 1989.
81. Nambu Y. The Confinement of Quarks. *Scientific American*, July 1976, p. 48.
82. Schwinger J. *Phys. Rev.*, 1949, vol. 76, 790; Feynman R. QED: The Strange Theory of Light and Matter. Penguin, London, 1990.
83. Lehnert B. and Scheffel J. *Physica Scripta*, 2002, vol. 65, 200; Lehnert B. *Physica Scripta*, 2004, vol. T113, 41.
84. Cohen E. R. and Taylor B. N. *Physics Today*, BG 7, August 1998.
85. Lehnert B. Reports TRITA-ALF-2003-05, 2003, and TRITA-ALF-2004-01, 2004, Fusion Plasma Physics, Royal Institute of Technology, Stockholm.

86. Weber J. General Relatitivity and Gravitational Waves. Interscience Publ., New York, 1961, Ch. 5.4.
87. Scheffel J. Unpublished numerical analysis, 1996, 2001, 2003.
88. Johnson K. A. The Bag Model of Quark Confinement. *Scientific American*, July 1979, p. 100.
89. Lehnert B. In: *Dirac Equation, Neutrinos and Beyond*, Edited by V. V. Dvoeglazov, the Ukrainian Journal *Electromagnetic Phenomena*, 2003, vol. 3, no. 1(9), 35.
90. Snellman H. *Physica Scripta*, 2001, vol. T93, 9.
91. Close F., Marten M., and Sutton H. The Particle Explosion. Oxford University Press, New York-Tokyo-Melbourne, 1987, p. 143.
92. Bethe H. A. Elementary Nuclear Theory. John Wiley and Sons, Inc., New York, 1947, Ch. II.
93. Spiegel M. R. Mathematical Handbook of Formulas and Tables. Schaum's Outline Series, McGraw-Hill Book Comp., New York, 1968, p. 98.
94. Vestergaard Hau L., Harris S. E., Dutton Z., and Behroozi C. H. *Nature*, 1999, vol. 397, 594.
95. Einstein A. On the Quantum Theory of Radiation (1917). In: *Sources of Quantum Mechanics*, B. L. van der Waerden (Editor), Amsterdam, 1967.
96. Afshar S. S., Flores E., McDonald K. F., and Knoesel E. *Foundations of Physics*, 2007, vol. 37, 295.
97. Ditchburn R. W. Light. Academic Press, London, New York, San Francisco, 1976, Third Edition, Sec. 17.24.
98. Battersby S. *New Scientist*, 12 June 2004, p. 37.
99. Mair A., Vaziri A., Weihs G., and Zeilinger A. *Nature*, 2001, vol. 412, 313.
100. Recami E. *Riv. Nuovo Cimento*, 1986, vol. 9, 1.
101. Recami E. In: *Causality and Locality in Modern Physics*, Edited by G. Hunter, S. Jeffers, and J.-P. Vigier, Kluwer, Dordrecht, 1998, p. 113.
102. Barut O. A., Maccarone G. D., and Recami E. *Il Nuovo Cimento*, 1982, vol. 71A, 509.
103. Cardone F. and Mignani R. In: *Modern Nonlinear Optics*, Part 3, Second Edition, *Advances in Chemical Physics*, vol. 119, Edited by M. W. Evans, I. Prigogine, and S. A. Rice, John Wiley and Sons, Inc., New York, 2001, p. 683.
104. Bilaniuk O. M., Deshpande V. K., and Sudarshan E. C. G. *Am. Journ. Phys.*, 1962, vol. 30, 718.
105. Recami E. and Mignani R. *Riv. Nuovo Cimento*, 1974, vol. 4, 209.
106. Olkhovsky V. S. and Recami E. *Physics Reports* (Review Section of *Physics Letters*), 1992, vol. 214, 339.

107. Nimtz G., Enders A., and Spieker H. In: *Wave and Particle in Light and Matter*, A. van der Merwe and A. Garuccio (Eds.), Proc. Trani Workshop (Italy, Sept. 1992), Plenum, New York, 1992.
108. Saari P. and Reivelt K. *Phys. Rev. Lett.*, 1997, vol. 79, 4135.
109. Walker W. D. In: *Gravitation and Cosmology: From the Hubble Radius to the Planck Scale*, Edited by R. L. Amoroso, G. Hunter, M. Kafatos, and J.-P. Vigier, Kluwer, Dordrecht, 2002, p. 189.
110. Cufaro-Petroni N., Dewdney C., Holland P. R., Kyprianidis A., and Vigier J.-P. *Foundations of Physics*, 1987, vol. 17, 759.
111. Aharonov Y. and Bohm D. *Phys. Rev.*, 1959, vol. 115, 485.
112. Cufaro-Petroni N., Droz-Vincent P., and Vigier J.-P. *Lettre al Nuovo Cimento*, 1981, vol. 31, 415.
113. Pope N. V. In: *Causality and Locality in Modern Physics*, Edited by G. Hunter, S. Jeffers, and J.-P. Vigier, Kluwer, Dordrecht, 1998, p. 187.
114. Argyris J. and Ciubotariu C. In: *Causality and Locality in Modern Physics*, Edited by G. Hunter, S. Jeffers, and J.-P. Vigier, Kluwer, Dordrecht, 1998, p. 143.
115. Kafatos M. In: *Causality and Locality in Modern Physics*, Edited by G. Hunter, S. Jeffers, and J.-P. Vigier, Kluwer, Dordrecht, 1998, p. 29.
116. Chambers R. G. *Phys. Rev. Letters*, 1960, vol. 5, 3.
117. Lehnert B. *Found. Phys. Lett.*, 2002, vol. 15, 95.
118. Angelidis T. Private communication, 2003.
119. Puthoff H. E. *Phys. Rev. D*, 1987, vol. 35, 3266; *Phys. Rev. A*, 1989, vol. 39, 2333.
120. Haisch B., Rueda A., and Puthoff H. E. *Phys. Rev. A*, 1994, vol. 49, 678.
121. Bearden T. E. Energy from the Vacuum. Cheniere Press, Santa Barbara, California, 2002.
122. Kaivarainen A. Bivacuum Mediated Electromagnetic and Gravitational Interactions. In: *Frontiers in Quantum Physics Research*, Edited by F. Columbus and V. Krasnoholvets, Nova Science Publishers, Inc., 2004, pp. 83–128.
123. Tauber H. *Physics Essays*, 2003, vol. 16, 200.
124. Pospelov M. and Romalis M. Lorentz Invariance of Trial. *Physics Today*, July 2004, p. 40.

Author Index

Subject Index

Bo Lehnert. A Revised Electromagnetic Theory with Fundamental Applications. Svenska fysikarkivet, 2008, 158 pages.
ISBN 978-91-85917-00-6

Summary: There are important areas within which the conventional electromagnetic theory of Maxwell's equations and its combination with quantum mechanics does not provide fully adequate descriptions of physical reality. As earlier pointed out by Feynman, these difficulties are not removed by and are not directly associated with quantum mechanics. Instead the analysis has to become modified in the form of revised quantum electrodynamics, for instance as described in this book by a Lorentz and gauge invariant theory. The latter is based on a nonzero electric charge density and electric field divergence in the vacuum state, as supported by the quantum mechanical vacuum fluctuations of the zero-point energy. This theory leads to new solutions of a number of fundamental problems, with their applications to leptons and photon physics. They include a model of the electron with its point-charge-like nature, the associated self-energy, the radial force balance in presence of its self-charge, and the quantized minimum value of the free elementary charge. Further there are applications on the individual photon and on light beams, in respect to the angular momentum, the spatially limited geometry with an associated needle-like radiation, and the wave-particle nature in the photoelectric effect and in two-slit experiments.

Bo Lehnert. En reviderad elektromagnetisk teori med fundamentala tillämpningar. Svenska fysikarkivet, 2008, 158 sidor.
ISBN 978-91-85917-00-6

Sammandrag: Det finns betydelsefulla områden inom vilka de Maxwellska ekvationernas konventionella elektromagnetiska teori och dess kombination med kvantmekanik inte tillhandahåller fullt adekvata beskrivningar av fysikalisk verklighet. Såsom tidigare påpekats av Feynman, undanröjes dessa svårigheter inte och är inte direkt förbundna med kvantmekaniken. Analysen måste i stället modifieras i form av reviderad kvantelektrodynamik, till exempel så som beskrives i denna bok av en Lorentz- och gaugeinvariant teori. Den senare är baserad på en från noll skild elektrisk laddningstäthet och elektrisk fältdivergens i vakuumtillståndet, med stöd av de kvantmekaniska vakuumfluktuationerna hos nollpunktsenergin. Denna teori leder till nya lösningar för ett antal fundamentala problem jämte deras tillämpningar på leptoner och fotonfysik. De innefattar en modell av elektronen med dess punktladdningsliknande natur, den åtföljande egenenergin, radiella kraftbalansen i närvaro av dess egen laddning, och det kvantiserade minimivärdet hos den fria elementarladdningen. Vidare innefattas tillämpningar på den individuella fotonen och på ljusstrålar, med avseende på impulsmomentet, den rumsligt begränsade geometrin med tillhörande nålliknande strålning, samt våg-partikelnaturen hos fotoelektriska effekten och tvåspaltexperiment.

Bo Lehnert was born in Stockholm, Sweden, in 1926. He received his M.Sc. degree at the Royal Institute of Technology in Stockholm, 1950, and studied plasma physics at Professor Hannes Alfvén's department. Lehnert was a guest researcher at the department of Professor Subrahmanyan Chandrasekhar, Yerkes Observatory, USA, 1953–1954, and received his PhD (Tekn. Dr.) in electrodynamics at the Royal Institute of Technology in 1955. He became full professor (personal chair) at the Swedish Atomic Research Council in 1968, and was a member of the International Fusion Research Council of the International Atomic Energy Agency in Vienna, 1970–1991. During 1980–1990 he served as head of the Swedish Fusion Research Unit being associated with the Euratom Research Programme in Brussels. Lehnert's main fields of interest have been magnetohydrodynamics, cosmical plasma physics, controlled thermonuclear fusion, and electromagnetic field theory, as reported in more than 200 publications in international journals. Professor Lehnert is a member of the Royal Swedish Academies of Sciences and Engineering Sciences, and of the Electromagnetics Academy, Cambridge, Mass., USA.

Bo Lehnert föddes i Stockholm, Sverige, år 1926. Han avlade sin civilingenjörsexamen vid Kungl. Tekniska Högskolan i Stockholm år 1950, samt studerade plasmafysik vid Professor Hannes Alfvéns institution. Lehnert var gästforskare vid Professor Subrahmanyan Chandrasekhars institution vid Yerkes Observatory, USA, 1953–1954, och erhöll sin Teknologie Doktorsexamen vid Kungl. Tekniska Högskolan år 1955. Han tilldelades en professur (personlig forskartjänst) vid Statens Råd för Atomforskning år 1968, och var ledamot av International Fusion Research Council vid International Atomic Energy Agency i Wien 1970–1991. Under åren 1980–1990 tjänstgjorde han som chef för den Svenska Fusionsforskningsenheten som tillordnats Euratoms forskningsprogram i Bryssel. Lehnerts huvudsakliga verksamhetsområden har varit magnetohydrodynamik, kosmisk plasmafysik, kontrollerad termonukleär fusion, och elektromagnetisk fältteori, såsom rapporterats i mer är 200 publikationer i internationella tidskrifter. Professor Lehnert är ledamot av Kungl. Vetenskapsakademien och Kungl. Ingenjörsvetenskapsakademien, samt av Electromagnetics Academy, Cambridge, Mass., USA.

ISBN 978-91-85917-00-6

9 789185 917006 >

LEHNERT • A REVISED ELECTROMAGNETIC THEORY